Progress in Polymer Science xxx (2018) xxx–xxx

Contents lists available at ScienceDirect

Progress in Polymer Science

journal homepage: www.elsevier.com/locate/ppolysci

Star-shaped and branched polylactides: Synthesis, characterization, and properties

Adam Michalski, Marek Brzezinski, Grzegorz Lapienis*, Tadeusz Biela*

Centre of Molecular and Macromolecular Studies, Polish Academy of Sciences, Sienkiewicza 112, 90-363, Lodz, Poland

ARTICLE INFO

Article history:
Received 10 April 2018
Received in revised form 25 October 2018
Accepted 26 October 2018
Available online xxx

Keywords:
Star-shaped PLAs
Branched PLAs
Stereocomplexes
Biodegradable polymers

ABSTRACT

The syntheses, properties and selected applications of star-shaped polymers with arms composed of homo- or copolymers of polylactide (PLA) is reviewed. The star-shaped (including miktoarm stars), dendritic, and branched polymers with a specified or varying numbers of arms were synthesized depending on the applied core molecule. Examples of a large number of various structures of star-shaped PLA polymers are precisely described. The growing interest in the synthesis of star-shaped and branched PLAs is primarily motivated by their potential applications in the biomedical and pharmaceutical areas. Therefore, the thermal, rheological, and mechanical properties, as well as various applications, of PLA stars as, for example, drug carriers, medical materials, and components of hydrogels, are also reported.

Abbreviations: 5HDON, 5-hydroxymethyl-1,4-dioxane-2-on; AFM, atomic force microscopy; ATRP, atom transfer radical polymerization; BFG, Bovine Fibrinogen; BHB, 2,2-bis(hydroxymethyl)butyric acid; bisMPA, 2,2-bis(hydroxymethyl)propionic acid; Boltorn H20, hyperbranched polymer (16 hydroxyl groups and Mw = 2100 g/mol); Boltorn H40, hyperbranched polymer (64 hydroxyl groups and Mw = 5100 g/mol); BOX, 2, 2′-bis(2-oxazoline); Bpy, bipyridine; BSA, bovine serum albumin; CA, cholic acid; CCS, cross-linked star (polymer); β-CD, β-cyclodextrin; CE, chain-extender; CGC, critical gel concentration; ε-CL, ε-caprolactone; CMC, critical micelle concentration; CNTs, carbon nanotubes; Dh, hydrodynamic diameter; DB, degree of branching; dbm, dibenzoylmethane; DBU, 1,8-diazabicyclo[5.4.0]-undec-7-ene; DCC, *N*,*N*′-dicyclohexyl carbodiimide; DCP, bis(1-methyl-1-phenylethyl) peroxide; DiI, 3,3′-dioctadecylindocarbocyanine; DLS, dynamic light scattering; DLSPs, dendrimer-like star polymers; DMAEMA, 2-(dimethylamino)ethyl methacrylate; DMAP, 4-dimethylaminopyridine; DOX·HCl, doxorubicin hydrochloride; DP, degree of polymerization; DPE, dipentaerythritol; DPTS, 4-(dimethylamino)pyridinium p-toluenesulfonate; DSC, differential scanning calorimetry; DTMP, di(trimethylolpropane); DTX, docetaxel; EHMOX, 3-ethyl-3-hydroxymethyl-oxetane; EO, ethylene oxide; ESMP, electroactive shape memory polymer; f, number of arms; g, branching index; G′, the storage modulus; G″, the loss modulus; GMA, glycidyl methacrylate; HBM, hyperbranched D-mannan; hbPEI, hyperbranched polyethylenimine; hbPGA, hyperbranched polyglycerols; HEP, heparin; HMDI, hexamethylene diisocyanate; HMMOX, 3-hydroxymethyl-3-methyl-oxetane; IND, indomethacin; IPNs, interpenetrating networks; LA, lactide (lactic acid); D,D-LA, D,D-lactide; DL-LA, D,L-lactide; L,L-LA, L,L-lactide; LCB, long-chain branched (long-chain branching); LC–CC, liquid chromatography at the critical point of adsorption; Mn, number-average molar mass; Mw, mass-average molar mass; MALDI-TOF, matrix assisted laser desorption/ionization time of flight; MALS, multi angle light scattering; ML, D,L-mevalonolactone; MPEG, methyl ether of poly(ethylene glycol); mPEI, multi-branched polyethyleneimine; MTX, methotrexate; MWCNTs, multiwalled carbon nanotubes; NAS, *N*-acryloxysuccinimide; NIPAAm, *N*-isopropylacrylamide; NMR, nuclear magnetic resonance; NPs, nanoparticles; PAA, poly(acrylic acid); PAMAM, poly(amidoamine); PBA, poly(butyl acrylate); PBOZ, 1,4-phenylene-bis-oxazoline; PBS, phosphate buffered saline; PCL, poly(ε-caprolactone); PCOE, poly(cis-cyclooctene); PDI, perylene diimide; PDLA, poly(D-lactide); PDLLA, poly(D,L-lactide); PDMAEMA, poly(2-(*N*,*N*-dimethylamino)ethyl methacrylate); PEEP, poly(ethyl ethylene phosphate); PEG, poly(ethylene glycol); PEGDMA, poly(ethylene glycol) dimethacrylate; PEI, poly(ethylene imine); PETA, pentaerythritol triacrylate; PG, polyglycerol; PGA, polyglycolide; PGAMA, poly(gluconamidoethyl methacrylate); PGE, pentaerythritol polyglycidyl ether; PGL, polyglycidol; PHB, poly(3-hydroxybutyrate); PHIC, poly(*n*-hexyl isocyanate); PLA, polylactide; PLGA, poly(D,L-lactide-*co*-glycolide); PLLA, poly(L-lactide); PLLG, poly(L-lactide-*co*-glycolide); PMDA, pyromellitic dianhydride; PMDETA, *N*,*N*,*N*′,*N*″,*N*″-pentamethyldiethylenetriamine; PMPC, poly(2-methacryloyloxyethyl phosphorylcholine); PNIPAAm, poly(*N*-isopropylacrylamide); POSS, polyhedral oligomeric silsesquioxane; PPEGA, poly(polyethylene glycol acrylate); PS, polystyrene; PTMC, poly(trimethylene carbonate); PTMEG, poly(tetramethylene ether); PULG, polyesterurethane network; Rg, radius of gyration; Rh, hydrodynamic radius; RAFT, reversible addition-fragmentation transfer; RALS, right angle light scattering; RIF, rifampicin; ROMP, ring-opening metathesis polymerization; ROP, ring opening polymerization; sc-PLA, stereocomplex PLA; SEC, size exclusion chromatography; sHPB, star-shaped hydroxylated polybutadiene; SMP, shape memory polymer; $Sn(Oct)_2$, stannous octoate; sPLA, star-shaped PLA; Tc, crystallization temperature; Td, decomposition temperature; Tg, glass transition temperature; Tm, melting temperature; TAIC, triallyl isocyanurate; TAM, triallyl trimesate; TBD, 1,5,7-triazabicyclo[4.4.0]dec-5-ene; TDI, 2,4-tolylene diisocyanate; TEM, transmission electron microscopy; TG, thermogravimetry; TGIC, triglycidyl isocyanurate; THF, tetrahydrofuran; TMC, trimethylene carbonate; TMP, 1,1,1-tris(hydroxymethyl)propane; TMPTA, trimethylolpropane triacrylate; TPGS, D-α-tocopheryl polyethylene glycol 1000 succinate; TPP-T, triphenylphosphonium trifluoromethanesulfonate; Tween 80, polyoxyethylene (20) sorbitan monolaurate (polyethylene glycol sorbitan monooleate); UV, ultraviolet; WAXD, wide-angle X-ray diffractometry; Xc, degree of crystallinity; XRD, X-ray diffraction.

* Corresponding authors.
E-mail addresses: lapienis@cbmm.lodz.pl (G. Lapienis), tadek@cbmm.lodz.pl (T. Biela).

https://doi.org/10.1016/j.progpolymsci.2018.10.004
0079-6700/

Contents

1. Introduction

Polylactide (PLA) is one of the most important biodegradable polymers. PLA has attracted considerable attention as a candidate for non-petroleum-based biodegradable polymeric materials because PLA is a biocompatible polymer with thermal plasticity, a semicrystalline nature with good processing properties and mechanical properties similar to those of polystyrene [1]. PLA is one of the most promising candidates capable of replacing petrochemical polymers [2,3], but it has inherent brittleness and low toughness, which restrict the range of applications [3]. PLA can be used in industrial, biomedical, pharmaceutical, and environmental applications [4], and also in other fields, such as agriculture, food applications, packaging, and furnishings [5–8]. It is widely used in many processing applications, including cast and blown films, as well as thermoforming, extrusion, and injection mouldings [9]. In addition, PLA has a wide range of applications in medical fields, such as sutures, screws for bone fractures, and drug delivery systems because of its good biocompatibility, high mechanical strength, and excellent shaping and moulding properties. PLA belongs to the family of aliphatic polyesters derived from α-hydroxy acids. The building block of PLA, lactic acid (2-hydroxy propionic acid), can exist in optically active D- or L-enantiomers. The petrochemical synthesis yields an optically inactive 50:50 mixture of D- and L-forms of lactic acid, whereas the bacterial fermentation-derived lactic acid exists almost exclusively in the L-form [10–12]. The structures of three stereoisomeric forms, L,L-lactide, D,D-lactide, and meso-lactide (D,L-lactide), are shown in Fig. 1. PLA is usually obtained via the ring opening polymerization (ROP) of lactides or the polycondensation of lactic acid [7,13]. Depending on the proportion of the enantiomers, PLA with variable material properties can be

Please cite this article in press as: Michalski A, et al. Star-shaped and branched polylactides: Synthesis, characterization, and properties. Prog Polym Sci (2018), https://doi.org/10.1016/j.progpolymsci.2018.10.004

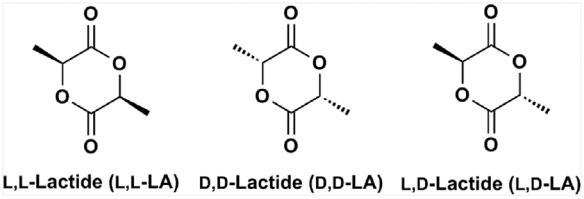

Fig. 1. Structures of L,L-lactide (L,L-LA), D,D-lactide (D,D-LA), D,L-lactide (D,L-LA).

obtained. This approach enables the production of a wide spectrum of PLA polymers to match performance requirements [14].

PLA is also filling the gap for bioplastics, and it is used to overcome the shortage of non-renewable resources and to help decrease the amount of non-recyclable waste produced. A plastic is biobased when it is partly or entirely derived from natural resources, including starch, cellulose, fatty acids, sugars, and proteins. PLA can be broken down into H_2O, CO_2, CH_4, and other low molar mass products and compost by means of light, heat, bacterial activity, and moisture; therefore, it is biodegradable and a safe biocompatible polymer for our environment [10,15,16].

To enhance or modify mechanical/hydrolytic stability and thermal degradation resistance of PLA materials a variety of branched molecular architectures has been proposed, e.g., long-chain branched, grafted, star-shaped, dendritic, and cross-linked [17–26]. In addition, blending, copolymerization, cross-linking, chain-extension or stereocomplexation were also used for further improvement of PLA properties [27].

Recently, an increased interest in star-shaped PLA materials has been observed due to their highly desirable rheological, mechanical and biomedical properties that are inaccessible in the case of linear polymers. Star polymers are branched, multi-armed polymeric materials in which the branches radiate from a central core. The first example of a star PLA macromolecule was reported in 1989 [28]. However, the marked rise in interest with respect to star-shaped PLAs and other macromolecular PLA frameworks is due to their unique properties compared with those of the linear homopolymers. Star-shaped PLAs have attracted significant attention in multiple fields of chemistry, biochemistry, and engineering. Star-shaped polyesters contain more chain ends than their linear counterparts of equal molar mass, and in consequence, the higher number of terminal groups induces improvements in solubility and differences in hydrodynamic volume [29,30].

Excellent reviews were devoted to the synthesis, characterization, properties, and applications of star polymers [31–34]. Star-shaped/branched PLA polymers were mentioned in several review papers devoted to the synthesis, characterization, and properties of these materials [25,27,29,35–41]. However, a detailed survey of star-shaped PLA polymers has not been published to date.

Substantially more review papers were devoted to the description of linear PLA (e.g., their synthesis, properties, and applications) [4,5,42–44]. PLA copolymers and the effect of copolymer ratio and end capping on their properties were also studied [45].

In this review, recent progress in the synthesis of star-shaped and branched polymers having PLA components, as well as some applications, is presented. Apart from the discussed synthetic methods of the star, branched, cross-linked PLA polymers, and the formation of stereocomplexes, the properties (namely, thermal, crystallization and mechanical) and applications of these polymers in comparison with their linear analogs are described. The different methods applied to the improvement of PLA properties and the analysis of star/branched structures are discussed as well. In the most of the investigations, the overlapping effects derived from branched structures and some other effects (e.g. end groups) on PLA properties were analyzed. The pure effects of branching architecture on physicochemical properties using linear 2-arm and 4-arm star poly(L-lactide)s were studied by Tsuji et al., with using the wide range of molar mass polymers, reducing in this way the effects other than branching [46].

Recently, very good reviews on graft and comb PLA polymers were published [27,38,39,47]. Therefore, we do not discuss these types of PLA structures in our paper.

2. Types of star/branched polymers

According to the IUPAC-recommended nomenclature [48–50], branched macromolecules are divided into the following groups:

- *Star polymers*: characterized by the presence of one single point of branching, from which linear chains originate. The functionality of this point is referred to as the number of arms (linear chains) departing from it. Star polymers are prepared either through a convergent ("arm-first", "arm-in") or divergent ("core-first", "arm-out") approach (Fig. 2). The independent synthesis of the arms ("arm-first") enables their better characterization, but steric hindrance may make functionalization of the core far from quantitative, above all when the arms are many and/or have a large molecular weight. A star polymer is defined as miktoarm (or μ-star) when certain arms are chemically different from others [36].

- *Graft polymers*: when the side chains of any architecture are connected to a main chain that differs in chemical composition. Graft polymers are prepared by coupling pre-formed side chains onto the main chain (grafting on also referred to as grafting to), (co)polymerizing appropriate macromonomers (grafting through) or producing side chains *in situ* via initiation from the pendent groups of the main chain (grafting from) [36].

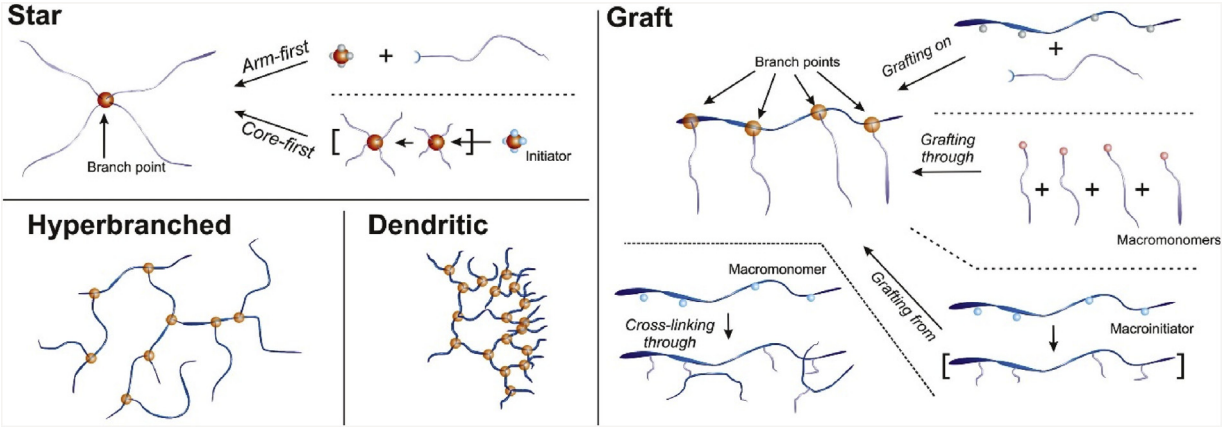

Fig. 2. Summary of the most common branch polymer architectures [36], Copyright 2018. Reproduced with permission from Elsevier Ltd.

Please cite this article in press as: Michalski A, et al. Star-shaped and branched polylactides: Synthesis, characterization, and properties. Prog Polym Sci (2018), https://doi.org/10.1016/j.progpolymsci.2018.10.004

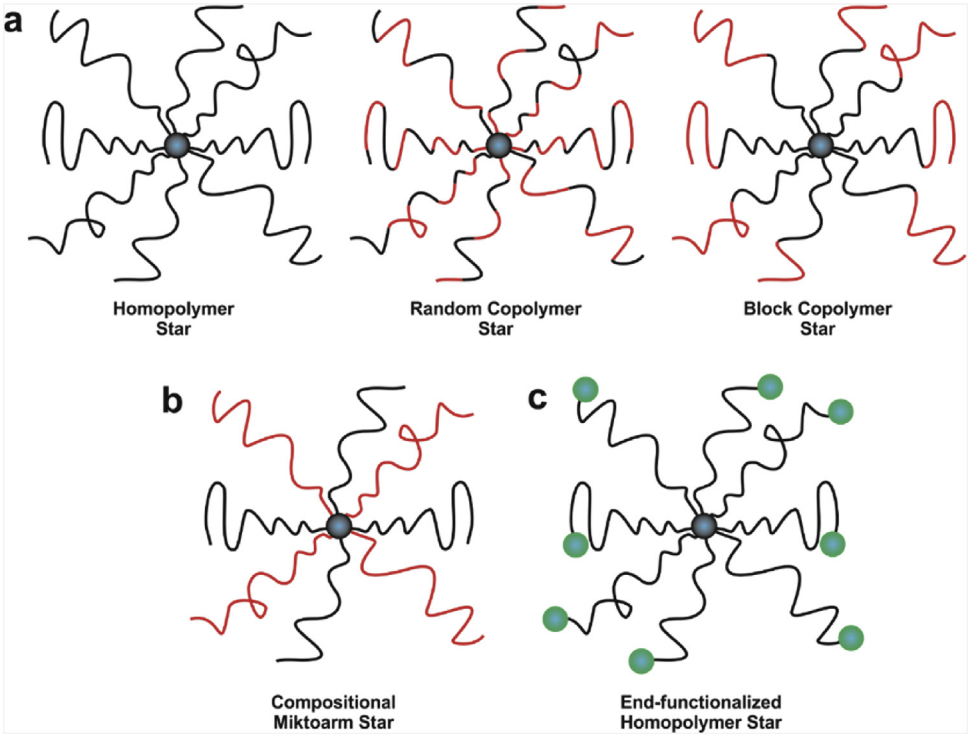

Fig. 3. Illustration of various types of star polymers classified by (a) composition and sequence distribution of the arm polymer, (b) difference in arm species, and (c) functional placement [32].

- *Comb polymers*: when regularly or irregularly spaced linear side chains depart from branch points on the main chain. Comb polymers are therefore a special case of graft macromolecules (more commonly obtained via grafting through) [36].

- *Dendritic and hyperbranched polymers*: in both cases, the macromolecule presents a nested structure of branch points that has a regular and cascade-like architecture for dendritic polymers and is randomly organized for hyperbranched polymers, which have a statistically identical number of sub-chains in any direction [36].

Star polymers are composed of a central branching point (a core) and linear "arms" from homopolymers and copolymers with different monomer composition and sequence distribution. In addition, the synthesis of miktoarm stars having chemically different arms linked to the core was also reported. This variety of different star polymer structures are depicted in Fig. 3 [32].

Star-shaped polymers, block polymers, hyperbranched and dendritic polymers [51–57] have been attracting significant attention because of their various functions and properties resulting from their special three-dimensional structures. Among these characteristics, increasing importance is attached to star-shaped polymers. These polymers have low melt viscosities, different thermal and mechanical properties, and improved physical processability, as their properties are more influenced by arm length than the total molar mass [29,58,59].

3. Synthesis of star-shaped PLA

There are two main methods for the synthesis of star-shaped polymers, namely, "arm first" and "core first" approaches. The method most commonly used for star-shaped polymers synthesis is based on the "core-first" approach, in which a multifunctional reagent (the core) plays the role of the co-initiator. Therefore, star-shaped polylactides are mainly synthesized by the ring-opening polymerization of lactide (LA) with stannous octoate $(SnOct)_2$) and a polyol forming the actual initiator. The syntheses of star-shaped PLA with a multifunctional core are performed usually in the bulk (130–200 °C) (cf. Tables 1–4, 7 and 8), as well as in solvents, e.g., THF [60], DMF [61,62], m-xylene [63–65], toluene [66–68], methylene chloride [69–71], chlorobenzene [72], chloroform [18], DMSO [73] and C_6D_6 [74].

In general, the number of arms in the polymer corresponds to the number of functional groups in the initiator. The position of the hydroxyl group in the core and the ratio of monomer to the polyol decide if all the hydroxyl groups serve to initiate the growth of the PLA chain. In general, primary hydroxyl groups are effective in initiating the polymerization, and the number of arms is increased by increasing the ratio of monomer to initiator [75–77]. A prerequisite for effective initiation activity is the solubility of the initiator in the polymerization mixture.

By employing multifunctional initiators, different molecular architectures can be obtained. Thus, in Tables 1–4, the structures of star-shaped polymers with a specified number of arms from 3 to 32 are presented. The stars with a higher number of arms (up to 160) [78] are shown as polymers with branched and/or dendritic cores (cf. Tables 7 and 8).

Different polyol cores used for the synthesis of star-shaped PLA are shown in Figs. 4 and 5.

To date, the synthesis and physical properties of star-shaped poly(L-lactide) (PLLA) have been intensively investigated by various research groups [8,64,79–82].

3.1. Studies on the formation of star-shaped PLA polymers

The ring-opening polymerization (ROP) of cyclic esters and their mechanisms of ionic and coordination processes were broadly previously described [13,83]. In the presence of stannous octoate $Sn(Oct)_2$, LA polymerizes according to a coordination–insertion mechanism [1,13,83].

Please cite this article in press as: Michalski A, et al. Star-shaped and branched polylactides: Synthesis, characterization, and properties. Prog Polym Sci (2018), https://doi.org/10.1016/j.progpolymsci.2018.10.004

Table 1
Star polymers with a specified number of PLLA arms.

star				
f [a)]	core	PLLA end groups[b)]	catalyst[c)]	Ref.
3	THMB[d)]	-OH (3490)	Sn	[126]
3	TMP[e)]	-OH (4200-7300)	Sn	[91]
3	TMP[e)]	-OH (2300-74 000)	Sn	[214]
3	TMP[e)]	-OH (10 400-38 500)	Sn	[263]
3	TMP[e)]	-OH (3300-23 000)	$Bi(OAc)_3$	[17]
3	TMP[e)]	-OH (4600)	NHCs	[458]
3	TMP[e)]	-UPy[f)] (14 600-75 500)	Sn	[163,165]
3	glycerol	-OH (4000-67 000)	Sn	[303]
3	glycerol	-OH (7300-54 100)	Sn	[81]
3	glycerol	-OH (9000-130 000)	Sn	[305]
3	glycerol	-OH	Sn	[459]
3	glycerol	-OH (9000-40 000)	Sn/TPhT	[193]
3	glycerol	-OH (2800-33 600)	Sn	[64]
3	glycerol	-OH, -COOH, $-NH_2$, -Cl (18 800-21 200)	Sn	[30]
3	THME[g)]	-OH (16 500)	imidazolium salt	[460]
3	3Bn-DPE[h)]	-OH (7700-11 800)	Sn	[213]
3	3Bn-DPE[h)]	-OH and –Pyr[i)] (11 000)	Sn	[134]
3	APD[j)]	-OH (800-57 000)	Sn	[194]
3	triethanolamine	-OH (46 800)	$(bisBTP)_2Cu$	[67]
3	AESO[k)]	-OH (45 600)	TBD	[461]
3	castor oil	-OH (2020-5010)	TfA	[71]
4	pentaerythritol	-OH (13 250)	Sn	[90]
4	pentaerythritol	-OH (460-96 800)	Sn	[75]
4	pentaerythritol	-OH (82 000-201 000)	Sn	[85]
4	pentaerythritol	-OH, -COOH, $-NH_2$, -Cl (31 700-33 700)	Sn	[30]
4	pentaerythritol	-OH (13 250)	Sn	[80]
4	pentaerythritol	-OH (5920)	Sn	[342]
4	pentaerythritol	-OH and -furanyl (6900)	(*a-f*)	[156]
4	pentaerythritol	-OH (2500-9400)	CaH_2	[86,124, 316]
4	pentaerythritol	-OH (4200-7300)	Sn	[91]
4	pentaerythritol	-OH (38 000-320 000)	Sn	[462]
4	pentaerythritol	-OH (7600-40 200)	DMAP	[69]
4	pentaerythritol	-OH (3800-33 200)	DMAP	[61]
4	pentaerythritol	-OH (3300-23 000)	$Bi(OAc)_3$	[17]
4	pentaerythritol	-OH (3000-32 800)	$Bi(OAc)_3$/Sn	[104]
4	pentaerythritol	-OH (14 000-84 000)	Sn	[365]
4	pentaerythritol	-OH (19 400)	Sn	[8]
4	pentaerythritol	-OH and M[l)] (1630-4790)	Sn	[139]
4	pentaerythritol	-OH (350-860)	Sn	[72,317, 463]
4	pentaerythritol	-OH (2700-55 000)	Sn	[9]
4	pentaerythritol	-OH (89 000)	Sn	[232]
4	pentaerythritol	-heparin (10 600)	Sn	[438]
4	pentaerythritol	-OH (3500-17 000)	L	[102]
4	pentaerythritol	-maleimide (arm: n = 5, 10, 15)	Sn	[322]
4	pentaerythritol	-OH (arm: n = 6, 16, 48)	PPY	[464]
4	pentaerythritol	-OH (5700)	NHCs	[458]
4	pentaerythritol ethoxylate	-OH (7600-77 100)	SPI	[18]
4	ZnP[m)]	-OH (73 000)	Sn	[455]
4	APDH[n)]	-OH (610-11 800)	Sn	[194]
4	2Bn-DPE[h)]	-OH (9800-10 400)	Sn	[213]
4	2Bn-DPE[h)]	-OH and –Pyr[i)] (15 230)	Sn	[134]
4	erythritol	-OH (2800-33 600)	Sn	[64]
4	erythritol	-OH (7300-14 500)	Sn	[409]
4	DTMP[o)]	-OH (2300-74 000)	Sn	[214]
4	TfP[p)]	-OH (10 700-39 800)	Sn	[333]
4	THMPP[q)]	-OH (13 900)	DMAP	[170]
4	MTHMPP[r)]	-OH (19 800)	$[(DAIP)_2Ca]_2$	[465]
5	1Bn-DPE[h)]	-OH (2300-74 000)	Sn	[213]
5	1Bn-DPE[h)]	-OH and –Pyr[i)] (12 590, 16 920)	Sn	[134]
6	dipentaerythritol	-OH (8600-8700)	Sn salen salan	[109]
6	dipentaerythritol	-OH (2300-74 000)	Sn	[214]
6	dipentaerythritol	-OH (5500-29 000)	Sn	[90]
6	dipentaerythritol	-OH (88 000)	Sn	[297]
6	dipentaerythritol	-OH and –Pyr[i)] (16 260, 18 670)	Sn	[134]
6	dipentaerythritol	-OH (8450)	Sn	[342]
6	dipentaerythritol	-OH (6200-27 700)	Sn	[302]
6	dipentaerythritol	-OH (5530-29 060)	Sn	[80]
6	dipentaerythritol	-OH (7600-40 200)	DMAP	[69]

Please cite this article in press as: Michalski A, et al. Star-shaped and branched polylactides: Synthesis, characterization, and properties. Prog Polym Sci (2018), https://doi.org/10.1016/j.progpolymsci.2018.10.004

Table 1 (*Continued*)

star				
f [a)]	core	PLLA end groups[b)]	catalyst[c)]	Ref.
6	dipentaerythritol	-OH (5300-35 100)	Sn	[340]
6	dipentaerythritol	-OH ($M_{n\,theor.}$ ~ 40 000)	Sn	[448]
6	dipentaerythritol	-OH (4200-7300)	Sn	[91]
6	dipentaerythritol	-OH and -COOH (15 000-20 000)	Sn	[121]
6	dipentaerythritol	OH and -COOH (10 000)	Sn	[122]
6	dipentaerythritol	-OH and -COOH (2300-9900)	$Ca(OH)_2$	[124]
6	dipentaerythritol	-OH (47 500-66 800)	Sn	[466]
6	dipentaerythritol	-OH (13 100-15 800)	Sn	[213]
6	dipentaerythritol	-OH (67 000)	Sb_2O_3	[116]
6	inositol	-OH (12 000)	Sn	[150]
6	inositol	-OH (11 000-34 000)	Sn	[436]
6	inositol	-OH (11 000-34 000)	L	[102]
6	HHMB[s)]	-OH (8900)	Sn	[342]
6	HfP[t)]	-OH (13 600-53 700)	Sn	[333]
6	myoinositol	-OH (2900-88 500)	$Bi(OAc)_3$/Sn	[104]
6	polyglycerine-06	-OH (82 000-201 000)	Sn	[85]
6	sorbitol	-OH (2800-33 600)	Sn	[64]
6	sorbitol	-OH (1000-10 000)	Sn/TPhT	[198]
6	sorbitol	-OH (16 900-37 000)	Sn	[440]
6	sorbitol	-OH and -furanyl (6920)	(*a-f*)	[156]
6	xylitol	-OH (2800-33 600)	Sn	[64]
6	xylitol	-OH (1800-7600)	Sn	[349]
6	HHMPCTP[u)]	-OH (7100-25 270)	Sn	[52]
8	polyglycerine-06	-OH (4000-34 300)	L	[102]
8	Q8M8H[v)]	-OH (8700-20 500)	Sn/hydrosilylation	[34]
10	polyglycerine-06	-OH (82 000-201 000)	Sn	[85]
13	HMEX[w)]	-OH (125 000)	Sn	[297]
22	polyglycerine-20	-OH (10 800-30 300)	L	[102]

[a)] *f*: number of arms.
[b)] in brackets M_n (g/mol) of star polymer or number of LA units in arms.
[c)] polymers were obtained by "*core-first*" method; *a-f* (in parenthesis) denotes "*arm-first*" method; descriptions of used catalyst:
Sn: stannous octoate (tin(II) octoate, stannous 2-ethylhexanoate), $Sn(Oct)_2$.
$Bi(OAc)_3$: bismuth(III) acetate.
NHCs: N-heterocyclic carbenes.
TPhT: tetraphenyltin.
$(bisBTP)_2Cu$: copper catalysts supported by bis-BTP ligands (BTP = N,O-bidentate benzotriazole phenoxide).
TBD: 1,5,7-triazabicyclo-[4.4.0]dec-5-ene.
TfA: trifluoromethanesulfonic acid.
DMAP: 4-dimethylaminopyridine.
L: lipase PS (*Pseudomonas fluorescens*).
PPY: 4-pyrrolidinopyridine.
SPI: Spirocyclic Tin Initiators = dibutyltin oxide + pentaerythritol ethoxylate.
$[(DAIP)_2Ca]_2$: calcium complex (where: DAIP-H = 2-[(2-dimethylamino ethylimino)methyl]phenol) catalyst.
salen: tBu[salen]AlMe.
salan: Cl[salan]AlMe.
[d)] THMB: 1,3,5-tris(hydroxymethyl)benzene.
[e)] TMP: 1,1,1-tris(hydroxymethyl)propane.
[f)] UPy: 2-ureido-4[1*H*]-pyrimidione end group.
[g)] THME: 1,1,1-tris(hydroxymethyl)ethane.
[h)] 3Bn-DPE, 2Bn-DPE, 1Bn-DPE: dipentaerythritol with three, two, and one blocked OH groups, respectively.
[i)] Pyr: pyrene (from 4-(1-pyrene)butanoic acid).
[j)] APD: 2-aminopropane-1,3-diol.
[k)] AESO: acrylated epoxidized soybean oil.
[l)] M: methacrylate end-group.
[m)] ZnP: zinc *p*-tetraaminophenylporphyrin.
[n)] APDH: 2-amino-2-(hydroksymethyl)propane-1,3-diol.
[o)] DTMP: di(trimethylolpropane).
[p)] TfP: tetrahydroxy-functionalized perylene: *N,N'*-bis-(2,6-diisopropylphenyl)-1,6,7,12-tetrakis-[4-(2-hydroxyethyl)phenoxy]perylene-3,4,9,10-tetracarboxylic acid diimide and *N,N'*-bis-(4-bromo-2,6-diisopropylphenyl)-1,6,7,12-tetrakis-[4-(2-hydroxyethyl)phenoxy] perylene-3,4,9,10-tetracarboxylic acid diimide.
[q)] THMPP: tetrakis-(p-hydroxymethylphenyl) porphyrin.
[r)] MTHMPP: meso-tetrakis-(p-hydroxymethylphenyl) porphyrin.
[s)] HHMB: hexakis-(hydroxymethyl)benzene.
[t)] HfP: hexahydroxy functionalized perylene: *N,N'*-bis-(4-[3-butyn-1-ol]-2,6-diisopropylphenyl)-1,6,7,12-tetrakis-[4-(2-hydroxyethyl)phenoxy] perylene-3,4,9,10-tetracarboxylic acid diimide.
[u)] HHMPCTP: hexakis-[p-(hydroxymethyl)phenoxy]cyclotriphosphazene.
[v)] Q8M8H: octakis-(dimethylsiloxy) silsesquioxane.
[w)] HMEX: product of cationic polymerization of 3-hydroxymethyl-3-ethyloxetane containing on average 13-OH groups.

Please cite this article in press as: Michalski A, et al. Star-shaped and branched polylactides: Synthesis, characterization, and properties. Prog Polym Sci (2018), https://doi.org/10.1016/j.progpolymsci.2018.10.004

Table 2
Star polymers with a specified number of PDLA arms.

star				
f [a)]	core	PDLA arm end groups[b)]	catalyst[c)]	Ref.
3	TMP[d)]	-OH (26 500)	Sn	[466]
3	TMP[d)]	-OH (50 800)	Sn	[299]
3	TMP[d)]	-UPy[e)] (14 600-75 500)	Sn	[163,165]
3	glycerol	-OH (4000-67 000)	Sn	[303]
3	glycerol	-OH (9000-100 000)	Sn	[305]
3	glycerol	-OH (2800-33 600)	Sn	[64]
4	pentaerythritol	-OH (34 700)	Sn	[466]
4	pentaerythritol	-OH (7600-40 200)	DMAP	[69]
4	pentaerythritol	-OH (6200-27 700)	Sn	[302]
4	pentaerythritol	-OH (2700-30 000)	Sn	[304]
4	pentaerythritol	-OH (3300-15 500)	L	[102]
4	pentaerythritol	-OH (64 600)	Sn	[299]
4	pentaerythritol	-OH (12 400)	*p*-TSC	[117]
4	BTCA[f)]	-OH (6200-27 700)	Sn	[302]
4	erythritol	-OH (2800-33 600)	Sn	[64]
6	dipentaerythritol	-OH (6200-27 700)	Sn	[302]
6	dipentaerythritol	-OH (7600-40 200)	DMAP	[69]
6	dipentaerythritol	-OH and –COOH(15 000-20 000)	Sn	[121]
6	dipentaerythritol	-OH (47 500-66 800)	Sn	[466]
6	dipentaerythritol	-OH (86 000)	Sn	[297]
6	dipentaerythritol	-OH (5900-10 200)	Sn	[304]
6	inositol	-OH (66 800)	Sn	[299]
6	inositol	-OH (35 100)	Sn	[466]
6	inositol	-OH (4600-25 400)	L	[102]
6	sorbitol	-OH (2800-33 600)	Sn	[64]
6	sorbitol	-OH (1000-10 000)	Sn/TPhT	[198]
6	xylitol	-OH (2800-33 600)	Sn	[64]
8	polyglycerine-06	-OH (8600-26 300)	L	[102]
13	HMEX[g)]	-OH (125 000)	Sn	[297]
22	polyglycerine-20	-OH (18 100-34 000)	L	[102]

[a)] *f*: number of arms.
[b)] in brackets M_n (g/mol) of star polymer.
[c)] polymers were obtained by "*core-first*" method; descriptions of used catalyst:
Sn: stannous octoate (tin(II) octoate, stannous 2-ethylhexanoate), $Sn(Oct)_2$.
DMAP: 4-dimethylaminopyridine.
p-TSC: p-toluenesulfonic acid.
L: lipase PS (*Pseudomonas fluorescens*).
TPhT: tetraphenyltin.
[d)] TMP: 1,1,1-tris(hydroxymethyl)propane.
[e)] UPy: 2-ureido-4[1*H*]-pyrimidione end group.
[f)] BTCA: 1,2,3,4-butanetetracarboxylic acid.
[g)] HMEX: product of cationic polymerization of 3-hydroxymethyl-3-ethyloxetane containing on average 13-OH groups.

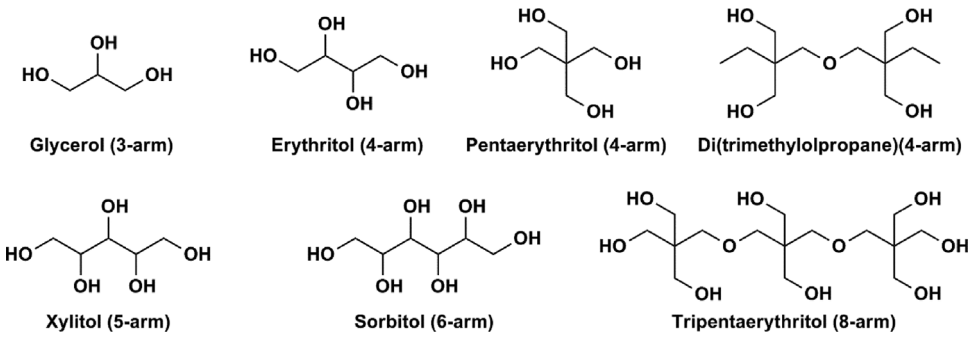

Fig. 4. Examples of simple structure initiators used in PLA polymerization.

The kinetics of the formation of star-shaped PLLAs with a low number of arms (3–10) was reported only in a few papers, mainly for L,L-lactide (L,L-LA) polymerization in the bulk initiated with the core molecules containing hydroxyl groups in the presence of $Sn(Oct)_2$ as the co-initiator (catalyst) [60,75,84–86]. First, there is only one report that described the polymerization kinetics in THF at 72 °C [60]. Second, the synthesis of a 4-arm star-shaped PLA was performed in DMF by varying the reactant concentrations and reaction temperature [61]. In these two reports, there was no evidence of intramolecular transesterification (back-biting), and the presence of cyclic oligolactides was not observed for the polymerization of L,L-lactide using $Sn(Oct)_2$ and pentaerythritol [84]. Interestingly, the polymerization of L,L-LA using $Sn(Oct)_2$ and a primary amine did not differ mechanistically from alcohol-initiated ROP [87]. MALDI-TOF mass spectrometry [84] and mid-infrared ATR-FTIR spectroscopy [60] were used for the monitoring of L,L-lactide polymerization.

The structural analysis of star PLLA polymers synthesized using the "core-first" approach revealed that in many cases, the complete conversion of initiator hydroxyl groups did not occur. Kim et al.

Please cite this article in press as: Michalski A, et al. Star-shaped and branched polylactides: Synthesis, characterization, and properties. Prog Polym Sci (2018), https://doi.org/10.1016/j.progpolymsci.2018.10.004

reported that when pentaerythritol and $Sn(Oct)_2$ were employed for L,L-lactide polymerization, the full conversion of four pentaerythritol hydroxyl groups was not achieved until the feed mole ratio of L,L-LA to pentaerythritol was ≥ 32 [75]. This effect was attributed to steric hindrance around the core. It was suggested that the secondary hydroxyl groups of the core molecule were associated with a slow initiation activity compared with the primary alcohol groups, and the polymerization rate of the PLLA arms apparently increased with the hydroxyl functionalities under a fixed molar ratio of monomer to initiator [85].

3.2. Catalysts

Star PLAs were synthesized using various structures of catalysts [32], which are reported in Tables 1–8, and selected structures are shown in Fig. 6. In a review of Gupta and Kumar, catalyst systems applied for the synthesis of linear PLAs were described in detail [31].

Table 3
Star polymers with a specified number of PDLLA arms.

star		PDLLA end groups[b)]	catalyst[c)]	Ref.
f[a)]	core			
3	glycerol	-OH (5800)	Sn	[426]
3	glycerol	-OH and M[d)] (14 300-34 200)	Sn	[314]
3	cholic acid	-OH (5900-10 600)	Sn	[417,467]
		-OH (5400)	Sn	[468]
		-OH (5900-23 100)	Sn	[469]
		-OH (11 300)	Sn	[470]
3	cholic acid	-OH (5000)	Sn	[426]
3	cholic acid	-OH (3300-7500)	SnO	[242]
3	tris(2-aminoethyl)amine	-OH (7800)	DBU	[70]
3	triethanolamine	-OH (14 200-32 540)	SLYAC	[111]
3	THMB[e)]	-OH (5020)	Sn	[342]
3	THME[f)]	-OH, maleimide (7740)	Al	[110]
3	TMP[g)]	-OH	Sn	[60]
3	PTA[h)]	-OH (2000-3400)	SnO	[119]
4	ethoxylated pentaerythritol	OH and –Um[i)] (1500-9500)	Sn	[140] [147]
4	ethoxylated pentaerythritol	adenine and thymine (6730-46 000)	Sn	[138]
4	ethoxylated pentaerythritol	-OH	STI	[95]
4	pentaerythritol	-OH (1500-39 800)	Sn	[195]
4	pentaerythritol	-OH (15 100-29 800)	Sn	[471]
4	pentaerythritol	-OH (4640)	Sn	[342]
4	pentaerythritol	-OH (1700-4000)	Sn	[85]
4	pentaerythritol	-OH (2700-14 400)	L	[102]
4	pentaerythritol	-OH (11 000-22 000)	Sn	[341]
4	pentaerythritol	-OH (1700-4000)	Sn	[154]
4	pentaerythritol	-OH and M[d)]	Sn	[145]
4	pentaerythritol	-OH and -ethynyl (5900-14 200)	DMAP	[135]
4	pentaerythritol	-SH (5000)	DMAP	[406]
4	methyl-D-glucopyranoside	-OH (550 and 2280)	DMAP	[428]
4	TPE-4OH[j)]	-OH (1800-23 720)	TPE-4-OH-[Lu]	[472]
4	TAPP[k)]	-OH (7500)	Sn	[473]
6	dipentaerythritol	-OH (8200-78 500)	Sn, salen, salan	[109,289]
6	dipentaerythritol	-OH (9900)	Sn	[342]
6	dipentaerythritol	-OH (23 200-47 900)	Sn	[471]
6	dipentaerythritol	-OH	Sn	[60]
6	dipentaerythritol	-OH, maleimide (10 250)	Al	[110]
6	inositol	-OH (4100-8200)	L	[102]
6	polyglycerine-06	-OH and M[d)]	Sn	[145]
6	polyglycerine-06	-OH (1500-39 800)	Sn	[195]
6	polyglycerine-06	-OH (3500-15 700)	Sn	[85]
6	sorbitol	-OH and M[d)] (800-14 800)	Sn	[146]
6	sorbitol	-OH (14 300-34 200)	Sn	[314]
6	sorbitol	-OH (3300-9300)	SnO, TSA, $ZnCl_2$, $SnCl_2$, $FeCl_3$	[115]
6	HHMB[l)]	-OH (13 800)	Sn	[342]
8	OC[m)]	-OH (4200-16 800)	Sn	[445]
8	POSS[n)]	-OH (5600-19 600)	Sn	[445]
8	POSS[n)]	-OH (DP ~ 110, 220, 420, 530)	Sn	[442]
8	polyglycerine-06	-OH (3200-25 600)	L	[102]
8	polyglycerine-06	-OH (3500)	Sn	[154]

Please cite this article in press as: Michalski A, et al. Star-shaped and branched polylactides: Synthesis, characterization, and properties. Prog Polym Sci (2018), https://doi.org/10.1016/j.progpolymsci.2018.10.004

Table 3 (*Continued*)

star		PDLLA end groups[b)]	catalyst[c)]	Ref.
f [a)]	core			
10	polyglycerine-06	-OH (3000)	Sn	[85]
10	polyglycerine-10	-OH and M[d)]	Sn	[145]
12	polyglycerine-10	-OH (3500)	Sn	[154]
21	*β*-cyclodextrin	-OH (1850)	DMAP	[428]
22	polyglycerine-20	-OH (9700-36 300)	L	[102]

[a)] *f*: number of arms.
[b)] in brackets M_n (g/mol) of star polymer, DP: degree of polymerization.
[c)] usually polymers were obtained by "*core-first*" method; descriptions of used catalyst:
Sn: stannous octoate (tin(II) octoate, stannous 2-ethylhexanoate), $Sn(Oct)_2$.
SnO: stannous oxide.
DBU: 1,8-diazabicyclo[5.4.0]-undec-7-ene.
SLYAC: salan-ligated yttrium alkyl complex, polymerization results in heterotactic star-shaped architecture.
Al: aluminum alkoxide.
STI: spirocyclic tin initiators.
L: lipase PS (*Pseudomonas fluorescens*).
DMAP: 4-dimethylaminopyridine.
TPE-4OH-[Lu]: TPE-Labelled Lutetium Alkoxide Complexes.
salen: tBu[salen]AlMe.
salan: Cl[salan]AlMe.
TSA: p-toluenesulfonic acid.
[d)] M: methacrylate end group.
[e)] THMB: 1,3,5-tris(hydroxymethyl)benzene.
[f)] THME: 1,1,1-tris(hydroxymethyl)ethane.
[g)] TMP: 1,1,1-tris(hydroxymethyl)propane.
[h)] PTA: pyrimidine-2,4,5,6-tetramine.
[i)] Um: urethane methacrylate end group.
[j)] TPE-4OH: tetrahydroxylfunctionalized tetraphenylethenes.
[k)] TAPP: meso-tetrakis-(p-aminophenyl)porphyrin.
[l)] HHMB: hexakis-(hydroxymethyl)benzene.
[m)] OC: organic core composed of 4-dimethylamino-pyridinium-p-toluenesulfate (DPTS) and 2,2,5-trimethyl-1,3-dioxane-5-carboxylic acid (TMDC).
[n)] POSS: polyhedral oligomeric silsesquioxanes.

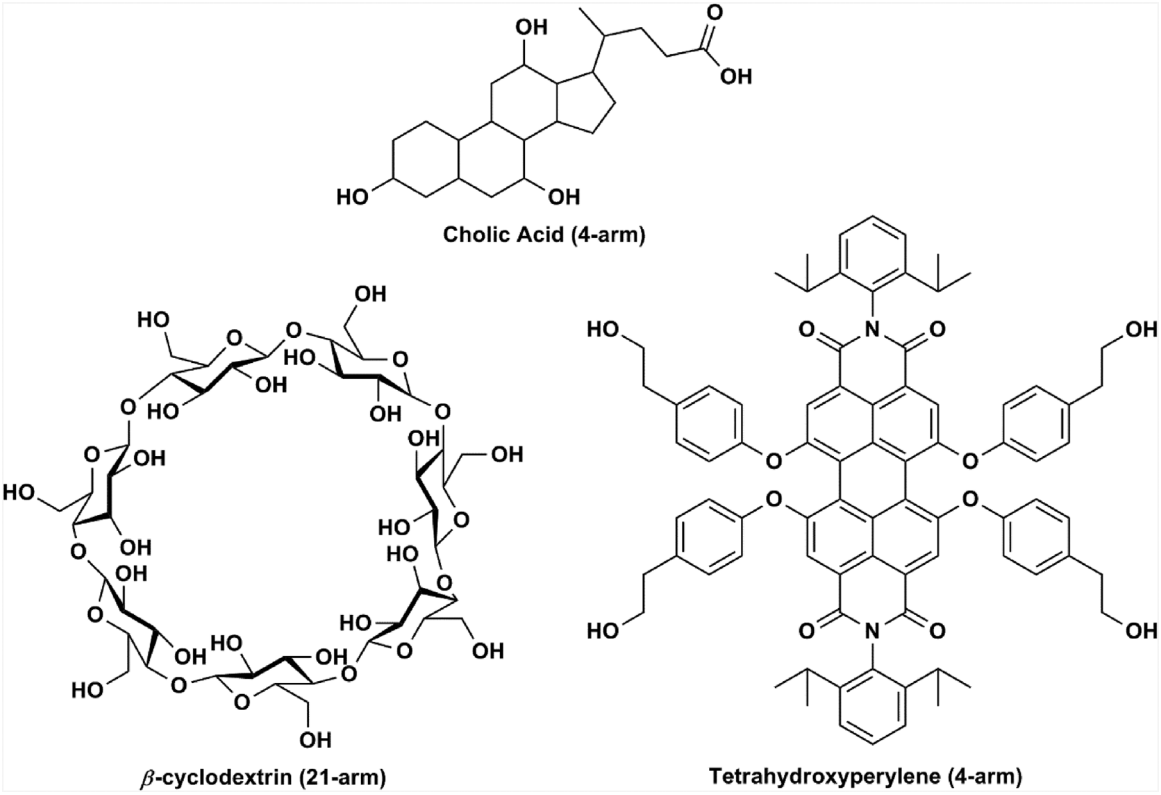

Fig. 5. Examples of initiators with more sophisticated structures used in PLA polymerization.

Please cite this article in press as: Michalski A, et al. Star-shaped and branched polylactides: Synthesis, characterization, and properties. Prog Polym Sci (2018), https://doi.org/10.1016/j.progpolymsci.2018.10.004

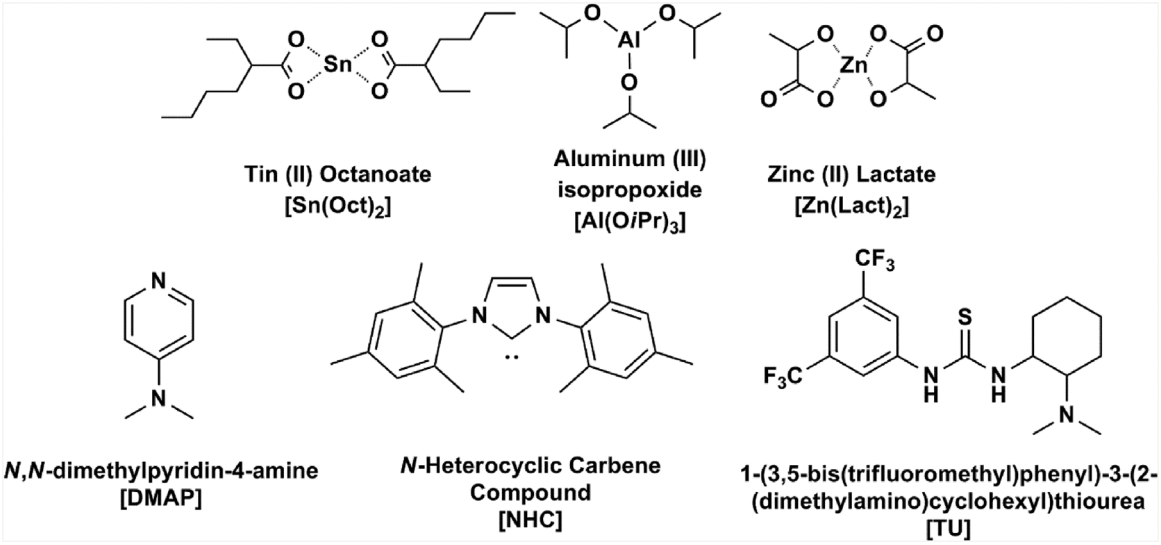

Fig. 6. Structure of organometallic catalysts and organocatalysts used in PLA polymerization.

Nearly all reports used stannous octoate ($Sn(Oct)_2$) to promote star formation. $Sn(Oct)_2$ is a very efficient initiator, and its utility results in PLAs with a low degree of racemization (even at high temperatures); additionally, it has low toxicity. $Sn(Oct)_2$ is a ubiquitous catalyst in an aliphatic polyester synthesis that produces atactic PLA chains [29]. Additionally, $Sn(Oct)_2$ is accepted by the FDA (Food and Drug Administration, USA) for biomedical applications [88].

Table 4
Star-block PLA copolymers with a specified number of arms. Structure of stars: [core] $(\mathbf{A}\text{-}\mathbf{B})_n$; block **A** is an inner part of arm (connected to the core) and block **B** is an outer part of arm.[a)]

star		arm: block copolymer A-B		arm end groups	catalyst[c)]	Ref.
f[b)]	core	**A**	**B**			
3	BTCTC[d)]	PDLLA	PMPC[e)] (56 000*)	azido	Sn/(*a-f*)	[137]
3	BTCTC[d)]	PCL (3500)	PLLA (2500-4000)	OH	$AlEt_3$	[474]
3	β-cyclodextrin	MPEG	PDLLA (14 000-17 100*)	metoxy	Sn/(*a-f*)	[414]
3	cholic acid	PLGA (D,L-lactide)	TPGS[f)] (17 800*)	D-α-tocopheryl	Sn/(*a-f*)	[159] [161]
3	glycerol	PLGA (D,L-lactide)	PEG (23 300*)	$-NH_2$	Sn/coupling reaction	[379]
3	glycerol	PLGA (D,L-lactide)	MPEG (6200*; 6900*)	$-NH_2$	Sn/coupling reaction	[380]
3	glycerol	PDLLA	PCL (2700-8100*)	-OH	Sn	[315]
3	glycerol	PDLLA	PCL (1180-11 900*)	-OH	Sn	[318]
3	glycerol	PDLLA	PCL (2900*)	-OH, norfolocaxin	Sn	[103]
3	glycerol	PCL (1250,7800*)	PDLLA	acrylate	Sn	[140] [148] [149]
3	glycerol	PCL	PDLLA (2830*)	-OH	Sn	[98]
3	glycerol	PLLA (3400-6540)	PEO (16 690-18 600*)	metoxy	Sn/(*a-f*)	[374] [375]
3	glycerol	PTMC (9900-63 000)	PLLA (29 900-87 000*)	-OH	β-diiminate zinc complex	[114]
3	glycerol	PLLA (47 600-99 700)	PDLA (85 500*)	-OH	Sn	[308]
3	hydroxyl-terminal PDMS[g)]	PDMS[g)]	PDLLA (6600-8800*)	-OH, Bu (PDMS)	Sn/(*a-f*)	[475]
3	3star-PCL**	PCL (900)	PLLA and PDLLA (2830*)	-OH	KMDS	[101]
3	PPO triols	PPO** (3300)	PLLA PDLLA (4200-6600*)	-OH	Zn powder	[476]
3	PTA[h)]	PTA[h)]	PDLLA (2000-2600*)	-OH	melt polycondensation	[119]

Table 4 (*Continued*)

star		arm: block copolymer A-B		arm end groups	catalyst[c)]	Ref.
f[b)]	core	**A**	**B**			
3	THMB[i)]	PLLA	PHB	-OH	indium complexes	[477]
3	THME[j)]	PDLLA (980-11 700*)	PGA	-OH	DBTO	[478]
3	TMP[k)]	PEG (9760)	PLLA (26 140*)	-OH	Sn	[56]
3	TMP[k)]	PCL	PLLA (14 560*)	-OH	Sn	[355]
3	TMP[k)]	PCL and PTMC	PLLA	-OH	Sn	[84]
3	TMP[k)]	PCL (6100-21 200)	PDLLA (11 500-36 200*)	-OH	Sn	[55]
3	TMP[k)]	PCL	PLLA (27 900*)	-OH	Sn	[449]
3	TMP[k)]	D,L-PLGA (6800)	PLLA (12 600-27 400*)	-OH	Sn	[82]
3	TMP[k)]	PLLA (10 000*)	PGA	UTM[l)]	Sn	[141]
3	TMP[k)]	PDLLA (6840-35 010*)	PGA	-OH	Sn	[479]
3	TMP[k)]	PDLLA (11 600-17 620)	PNIPAAm (23 040-41 950*)	-Cl	Sn/ATRP	[65]
3	ethoxylated TMP	PEG	PLLA (2000-4600*) PDLLA (2000-4400*)	-OH	KMDS	[100]
3	triethanolamine	PEG	PDLLA (3900-10 800*)	-OH	Sn	[28]
3	Tween 80[m)] (1310)	PEG	PDLLA (8600; 15 500*)	-OH	Sn	[410]
3	3 arm PEG**	PEG (3200)	PLLA (7500-12 100*)	-OH	Sn	[118]
3	cholic acid	PCL-*ran*-PLA	(12 000*)	-OH	Sn	[418]
3	cholic acid	PCL-*ran*-PLA	MPEG (15 000*)	$-OCH_3$	Sn	[418]
4	4 arm PEG**	PEG (5920)	PLLA (19 800-24 700*)	-OH	$AlEt_3$	[26]
4	4 arm PEG**	PDLLA	PEG (11 500-34 400*)	-OH	Sn	[416]
4	4 arm PEG**	PEG (10 000)	PLLA (21 800, 32 000*)	-OH	Sn	[480]
4	4 arm PEG	PEG (11 500-34 400*)	PDLLA	-OH, -COOH	Sn	[123]
4	4 arm PEG**	PEG	PLLA (6980-57 600*)	-OH	Sn	[377]
4	4 arm PEG**	PEG (4300)	PLLA (10 700-18 700*)	-OH	Sn	[118]
4	4 arm PEG-NH_2	PEG	PDLLA (9000, 10 600*)	-OH	triazole carbene	[74]
4	pentaerythritol	PLLA	heparin (10 600*)	-OH	Sn/(*a-f*)	[438]
4	pentaerythritol	PDL[n)]	PDLLA	-OH	Sn	[225]
4	pentaerythritol	PEG (10 920)	PLLA (28 460*)	-OH	Sn	[56]
4	pentaerythritol	D,L-PLGA (12 400)	PLLA (26 700-45 200*)	-OH	Sn	[82]
4	pentaerythritol	PLGA (D,L-lactide)	PEG (33 200*)	$-NH_2$	Sn/coupling reaction	[379]
4	pentaerythritol	PLLA	PEG (23 090*)	$-OCH_3$	Sn/(*a-f*)	[80]
4	pentaerythritol	PDLLA	PEG (13 600-42 500*)	$-OCH_3$	Sn/(*a-f*)	[424]
4	pentaerythritol	PLLA (72 000)	PDLA (54 000)	-OH	Sn	[68]
4	pentaerythritol	PDLA (15 200-54 500*)	PLLA (8500-30 700)	-OH	Sn	[481]
4	pentaerythritol	PLLA (13 000-30 700)	PDLA (22 000-35 200*)	-OH	Sn	[306,307]
4	pentaerythritol	PCL	PLLA (27 100*)	-OH	Sn	[449]
4	pentaerythritol	PCL	PLLA	-OH	Sn	[453]

Please cite this article in press as: Michalski A, et al. Star-shaped and branched polylactides: Synthesis, characterization, and properties. Prog Polym Sci (2018), https://doi.org/10.1016/j.progpolymsci.2018.10.004

Table 4 (*Continued*)

star		arm: block copolymer A-B		arm end groups	catalyst[c)]	Ref.
f[b)]	core	**A**	**B**			
4	pentaerythritol	PCL	PLLA (17 450*)	-OH	Sn	[355]
4	pentaerythritol	PCL (12 900)	PLLA (36 000-43 800*)	-OH	Sn	[370]
4	pentaerythritol	PCL	PDLLA (186 000*)	-OH	Sn	[196]
4	pentaerythritol	PCL	PDLA (6290-25 950*)	-OH, acrylate	Sn	[142]
4	pentaerythritol	PLLA	PCL (7470-16 700*)	-OH, acrylate	Sn	[151]
4	pentaerythritol	PDLLA	PCL (3100*)	-OH, norfolocaxin	Sn	[103]
4	pentaerythritol	PCL	PLLA (4660-165 000*)	-OH, acrylate	Sn	[482]
4	pentaerythritol	PGA	PLLA (9000-14 000*)	-OH	Sn	[412]
4	pentaerythritol	PTMC	PDLLA (157 000-166 000*)	-OH	Sn	[196]
4	pentaerythritol	PDLLA (7580-32 910*)	PGA	-OH	Sn	[479]
4	pentaerythritol	PDLLA (11 800*)	PGA	-OH	DBTO	[483]
4	pentaerythritol	PLLA (11 230-50 050*)	CCAT[o)] trimer	-COOH	Sn	[399]
4	pentaerythritol	PDLLA (7000*)	PNVP[pp)] (13 500*)	xanthate	Sn/RAFT	[405]
4	pentaerythritol	PCL	PLLA (38 000-65 000*)	-OH	Sn/DBU	[171]
4	pentaerythritol	PDLLA	PHPMA[q)] (9200-22 600*)			[406]
4	pentaerythritol	PDLLA	PNVP[pp)] (11 200-27 600*)			[406]
4	pentaerythritol ethoxylate	PEG	PLLA (2100-5500) PDLLA (2100-5600)	-OH	KMDS	[100]
4	pentaerythritol ethoxylate	PEG	PLLA PGA (2490-6570*)	-OH -acrylate	Sn	[143]
4	pentaerythriol triazide	PLA	PDMAEMA[r)]	-OH, Br	Sn/(*a-f*) (ATRP) and click chemistry	[133]
4	pentaerythriol triazide	PLA	PCL (61 300, 87 100) DXO[s)] (72 900, 75 000)	-OH	Sn/ spirocyclic tin	[94]
4	carboxylated pentaerythritol	MPEG (550)	PLGA (7700-7900*)	$-OCH_3$	Sn/(*a-f*)	[439]
4	carboxylated pentaerythritol	MPEG (550, 750)	PLGA (5700-9900*)	$-OCH_3$	Sn/(*a-f*)	[441]
4	porphyrin (TAPP[t)])	PGLA (D,L-lactide)	TPGS[f)] (10 100*)	D-α-tocopheryl	Sn/(*a-f*)	[160]
4	porphyrin-$(OH)_4$	PLLA (13 950-29 110)	PGAMA[u)] (20 510, 32 770*)	-OH, BSPA[v)]	Sn/(*a-f*)	[168]
4	porphyrin (THMPP[w)])	PLLA	PNIPAAm (35 400*)	benzyl	DMAP/RAFT	[170]
4	Tetronic 1107**	poloxamine	PLLA PLDLA (60 300, 93 300*)	-OH	Sn	[484]
4	Tetronic 1107**	poloxamine	PLLA	-OH	Sn	[435]
5	BIS-TRIS[x)]	PCL (11 060)	PLLA (17 100-36 500*)	-OH, -BSPA[v)]	Sn	[382]
6	cyclophosphazene	PCL (6500-22 500)	PLLA (45 200-102 300*)	-OH	Sn	[485]
6	dipentaerythritol	PLLA (28 800*)	PCL	-OH	Sn	[449]
6	dipentaerythritol	PLLA (107 300-184 600*)	PCL (68 600)	-OH	Sn	[452]
6	dipentaerythritol	PCL (8500-17 200)	PLLA (14 300-26 200*) PDLA (17 100, 26 500*) PDLLA (14 300-37 300*)	-OH	Sn	[486]

Please cite this article in press as: Michalski A, et al. Star-shaped and branched polylactides: Synthesis, characterization, and properties. Prog Polym Sci (2018), https://doi.org/10.1016/j.progpolymsci.2018.10.004

Table 4 (*Continued*)

star		arm: block copolymer A-B		arm end groups	catalyst[c)]	Ref.
f[b)]	core	**A**	**B**			
6	dipentaerythritol	PCL (10 600-27 100)	PLLA (33 300-62 300*)	-OH	Sn	[487]
6	dipentaerythritol	PCL (7160,11 820)	PLLA (17 300-43 180*)	-OH	Sn	[356]
6	dipentaerythritol	PLLA (3800-6000)	PEG (13 600-29 000 *)	-OH	Sn	[398]
6	dipentaerythritol	PLGA	PEG (43 300*)	-NH_2	Sn/coupling reaction	[379]
6	dipentaerythritol	PLLA	PEG (23 120*)	-OH, -COOH	Sn/(*a-f*)	[80]
6	HHMPCTP[y)]	PCL (11 000-21 100)	PLLA (17 500-37 500*)	-OH	Sn	[372]
6	HHMPCTP[y)]	PCL (6400-21 100)	PDLLA PGA (28 300-40 800*)	-OH	Sn	[488]
6	HHDTP[z)]	PLLA (25 500-64 000)	PS PNAS[aa)] (38 300-15 500*)	methine	Sn/ATRP	[381]
6	inositol	PLLA (21 600-40 800*)	CCAT[o)] trimer	-COOH	Sn	[399]
6	mannitol	PLGA (15 900*)	TPGS[f)] (23 900*)	D-α-tocopheryl	Sn	[158]
6	PNIPAAm macromonomer	PLLA (247 100*)	PNIPAAm	-OH	Sn/(*a-f*)	[383]
6	D-sorbitol	PLLA (27 630-28 600*)	PCL	-OH	Sn	[449]
6	D-sorbitol	PTMC PCL (9000-29 900)	PDLLA PGA	-OH	Sn	[199]
6	D-sorbitol	PLLA (50 300-108 600)	PDLA (85 600*)	-OH	Sn	[308]
8	8-arm PEG-OH**	PEG (21 800, 43 500)	PLLA (27 200-53 300*)	-OH	Zn	[112]
8	8-arm PEG-OH**	PEG (10 000)	PDLLA (20 700*)	-OH	Sn	[480]
8	8-arm PEG-OH** and PEG-NH_2	PEG (20 600, 23 700)	PLLA (28 300-32 200*)	-OH	Sn	[324,326, 332]
8	8 arm PEG-NH_2	PEG (20 600)	PLLA (24 300-28 700*)	-acrylate	Sn	[144]
8	8 arm PEG-NH_2**	PEG (21 800)	PLLA/PDLA (22 700*)	methacrylate	Sn	[113]
8	8-arm PEG-OH**	PEG (23 800)	PLLA (24 300-28 700*)	-pyridine	Sn	[329]
8	8-arm PEG-OH**	PEG (12 500, 21 800)	PLLA (13 900-29 800*)	-OH	Zn	[328]
8	8 arm PEG-OH**	PEG (7100)	PLLA (21 200-42 300*)	-OH	$AlEt_3$	[26]
8	8 arm PEG-OH**	PEG (10 000, 35 000)	PLLA (44 600, 71 400*)	-OH	K/naphthalene	[434]
8	8 arm PEG-OH**	PEG (20 000)	PLLA (20 000-69 000*)	-OH	K/naphthalene	[300]
8	8 arm PEG-OH**	PEG (5000)	PLLA (11 600-15 200*)	-cholic	Sn	[136]
8	PDI-80[bb)]	PDLLA	PEEP[cc)] (59 200-65 800*)	-OH	DBU	[384]
8	POSS[dd)]	PCL	PDLLA (122 000*)	-OH	Sn	[443]
8	POSS[dd)]	PAA[ee)]	MPEG-*b*-PLLA (131 670*)	-OH	Sn/SET-LRP and click reaction	[425]
8	POSS[dd)]	PCL	PLLA (5500) PDLA (20 600*)	-OH	Sn	[446]
11	PGS[ff)]-OH	PGS[ff)] (2850)	PLLA (9030-115 530*)	-OH	Sn	[167]
10-20	BMI[gg)]	PDLLA-CTA[hh)]	PS	-OH	RAFT	[169]

Table 4 (*Continued*)

star		arm: block copolymer A-B		arm end groups	catalyst[c)]	Ref.
f[b)]	core	**A**	**B**			
21	t-β-CD[ii)]	POX[ij)] (18 300*)	PLA	-OH	Sn	[413]
32	$POSS(OH)_{32}$	PDLLA (25 100-118 800)	PDMAEMA[r)] (110 100-220 600*)	-OH, -Br	Sn/ATRP	[130]

[a)]in brackets M_n (g/mol) of arm and/or star polymer is given; M_w in italic; M_n of star polymer is denoted by * (in column "**A**" for star with **A** arms only and in column "**B**" for star with **A-B** arms); commercial product is denoted by **.
[b)]*f*: number of arms.
[c)]usually polymers were obtained by "*core-first*" method; *a-f* (in parenthesis) denotes "*arm-first*" method; descriptions of used catalysts:
Sn: stannous octoate (tin(II) octoate, stannous 2-ethylhexanoate), $Sn(Oct)_2$.
$AlEt_3$: triethylaluminum.
KMDS: potassium hexamethyldisilazide, $KN[SiMe_3)]_2$.
DBTO: dibutyltin oxide.
triazole carbene: 1,3,4-triphenyl-4,5-dihydro-1H-1,2,4-triazol-5-ylidene.
DBU: 1,8-diazabicyclo[5.4.0]-undec-7-ene.
spirocyclic tin: mixture of dibutyltin oxide and pentaerythritol ethoxylate.
DMAP: 4-dimethylaminopyridine.
Zn: single-site ethylzinc complex - $(Zn(Et)[SC_6H_4(CH(Me)NC_4H_8)-2])$.
SET-LRP: single electron transfer living radical polymerization.
[d)]BTCTC: 1,3,5-benzenetricarbonyl trichloride.
[e)]PMPC: poly(2-methacryloyloxyethyl phosphorylcholine).
[f)]TPGS: D-α-tocopheryl polyethylene glycol 1000 succinate.
[g)]PDMS: polydimethylsiloxane.
[h)]PTA: pyrimidine-2,4,5,6-tetramine.
[i)]THMB: 1,3,5-tris(hydroxymethyl)benzene.
[j)]THME: 1,1,1-tris(hydroxymethyl)ethane.
[k)]TMP: 1,1,1-tris(hydroxymethyl)propane.
[l)]UTM: urethane trimethacrylate.
[m)]Tween 80: polyoxyethylene (20) sorbitan monolaurate.
[n)]PDL: poly(ε-decalactone).
[o)]CCAT: carboxyl-capped aniline trimer.
[p)]PNVP: poly(*N*-vinylpyrrolidone).
[q)]PHPMA: poly(*N*-(2-hydroxypropyl)methacrylamide).
[r)]PDMAEMA: poly(dimethylaminoethyl methacrylate).
[s)]DXO: 1,5-dioxepan-2-one.
[t)]TAPP: 5,10,15,20-tetrakis-(4-aminophenyl)porphyrin.
[u)]PGAMA: poly(gluconamidoethyl methacrylate).
[v)]BSPA: benzylsulfanylthiocarbonylsufanylpropionic acid.
[w)]THMPP: tetrakis-(p-hydroxymethylphenyl)porphyrin.
[x)]BIS-TRIS: bis(2-hydroxyethyl)amino-tris(hydroxymethyl)methane.
[y)]HHMPCTP: hexakis-[p-(hydroxymethyl)phenoxy]cyclotriphosphazene.
[z)]HHDTP: 2,3,6,7,10,11-hexakis-(10′-hydroxydecanoxyl)triphenylene.
[aa)]PNAS: poly(*N*-acryloxysuccinimide).
[bb)]PDI-8OH: perylene diimide.
[cc)]PEEP: poly(ethyl ethylene phosphate).
[dd)]POSS: polyhedral oligomeric silsesquioxane.
[ee)]PAA: poly(acrylic acid).
[ff)]PGS: poly(glycerol-sebacate).
[gg)]BMI: bis(maleimidoethane).
[hh)]CTA: (dodecylthiocarbonothioylthio)-2-methylpropionic acid, polylactide macro-chain transfer agent.
[ii)]t-β-CD: $(tosyl)_7$-β-cyclodextrin; 14−OH groups (for LA polymerization) and 7-tosyl groups (for 2-ethyl-2-oxazoline polymerization).
[ij)]POX: poly(2-ethyl-2-oxazoline).

The polymerization of L,L-LA in bulk with $Sn(Oct)_2$ as a catalyst was usually undertaken at 130 °C [21,82,89,90]. The processes carried out at a high temperature of 190 °C caused a number of side reactions, such as transesterification, which led to linear and cyclic homopolymers [91]. Spirocyclic tin initiators based on tin-substituted polyethylene ethoxylate [18,92–96] and a cyclic stannoxane [97] were also used successfully. Other catalysts, such as calcium hydride [86,98], stannous acetylacetonate [99], potassium hexamethyldisilazide [100,101], tetraphenyl tin [75], $Bi(OAc)_3$ [17], and enzymes mainly lipase [102,103], were employed, as well.

The catalytic activities of Bi(III) acetate ($Bi(OAc)_3$) and of creatinine towards the ring-opening polymerization of L,L-lactide were compared with those of a $Sn(Oct)_2$-based system and a system catalysed by enzymes. In all cases, high and moderate molar mass poly(L-lactide)s were obtained. The $Bi(OAc)_3$-based system was comparable with $Sn(Oct)_2$ at 140 °C [104]. However, the reactivity of creatinine was lower than that of $Bi(OAc)_3$ but high compared with that of the enzyme lipase *Pseudomonas fluorescens* [104].

N-Heterocyclic carbenes [105] and 4-dimethylaminopyridine (DMAP) [106] were used as organic catalysts in PLA star synthesis. By this manner, 4-arm stars from amine-substituted poly(ethylene glycol)s and 6-arm stars from a luminescent ruthenium complex were prepared, respectively. The use of (−)sparteine/*N*′-(3,5-bis(trifluoromethyl)-phenyl)-*N*-cyclohexyl-thiourea (**1,** Fig. 7) as a catalyst for ROP of L,L-LA was also reported [107,108].

The aluminum salen and salan complexes (**2a, 2b,** Fig. 7) allowed for the stereocontrolled synthesis of PLA stars [32,109–111], whereas zinc amino-, thio-phenolate [112,113] and β-diiminate complex [114] and bis(calcium)pentaerythritol [86] catalysts expanded the range of metal-based mediators of PLA star synthesis. The stereoregular α,ω-chain end functional star-shaped homopolymers (PLLA arms) and copolymers (PLLA-*b*-PS arms) were synthesized with aluminum methyl complexes by the stereospecific ring-opening polymerization of *rac*-lactide [110]. In

Please cite this article in press as: Michalski A, et al. Star-shaped and branched polylactides: Synthesis, characterization, and properties. Prog Polym Sci (2018), https://doi.org/10.1016/j.progpolymsci.2018.10.004

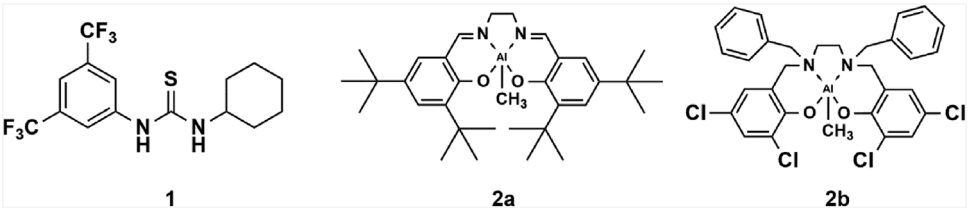

Fig. 7. Structure of catalysts for ROP of L,L-LA: (−)sparteine/*N*′-(3,5-bis(trifluoromethyl)-phenyl)-*N*-cyclohexyl-thiourea (**1**), the aluminum salen (**2a**) and salan complexes (**2b**).

addition, Lewis acidic catalysts based on tin and aluminum allowed for the control of the polymerization and afforded polymer stars of variable tacticity [109]. The cationic ROP of lactide was studied with castor oil as an initiator and in the presence of a trifluoromethanesulfonic acid as a catalyst [71].

3.3. Star-shaped PLA polymers by polycondensation

There are only a few reports on the synthesis of star-shaped poly(lactic acid)s by the polycondensation method. The obtained polymers usually had relatively low molar masses M_n < 4700 g/mol) [115]. The higher molar mass poly(lactic acid)s with $M_n \leq 67\,000$ g/mol were obtained by the direct polycondensation of lactic acid initiated by dipentaerythritol [116] and pentaerythritol [117] with antimony trioxide and *p*-toluenesulfonic acid as catalysts, respectively. In addition, star-shaped copolymers with 3 and 4 PEG-*b*-PLLA arms were prepared by melt polycondensation from 3- and 4-arm star PEGs as the core [118].

In the polycondensation of D,L-lactic acid (LA) with pyrimidine-2,4,5,6-tetramine (PTA), a star PLA was obtained (Fig. 8) that can be used as a novel potential polymeric flame retardant. In the first stage, compound **3** (Fig. 8) was formed with a purine unit as a core that in the next step acted as the initiator of LA polymerization [119]. A more detailed study of the polycondensation process disclosed that at a starting ratio of LA/PTA equal to 60/1, a multicore structure in the copolymer was formed [119].

Finally, 4- and 6-arm star poly(lactic acid)s with carboxylic acid terminal groups were synthesized by the direct polycondensation of lactic acid in the presence of 7 different poly(carboxylic acid) core molecules with triphenylphosphonium trifluoromethanesulfonate as a catalyst [120].

3.4. End-groups in star-shaped PLA

The synthesized star PLA polymers have different end groups (mainly hydroxyl). Others are mentioned in Tables 1–8. For example, carboxyl [30,80,121–128], halogen [30,129–133], amine [30], pyrene [134], maleimide [110], ethynyl [135], cholic [136], azido [137], adenine and thymine [138] were also reported as the end-groups.

Star-shaped PLA with unsaturated end-groups, e.g., with acrylate or methacrylate [113,133,139–154] and itaconic acid [155], were used for the formation of cross-linked structures. The synthesis of star-shaped PLA with thiol [144], furanyl [156], biotin [157], and D-α-tocopheryl polyethylene glycol 1000 succinate (TPGS) [70,158–161] end-groups were also reported. Every branched unit introduced an additional end-group in the branched PLA and an increased number of hydroxyl termini, which allowed the incorporation of more biologically active ligands at the degradable polyester [162].

The synthesis of star-shaped with 3–6 PLA arms functionalized with pyrene end-groups was reported. Analysis of both static and time-resolved spectra of the star-shaped polymers revealed dynamic segmental motion resulting in end-to-end cyclization, accompanied by an excimer formation. In macromolecules containing 3-arms, the pyrene moieties are located in the interior of the star-shaped PLAs, whereas in the case of the higher number of arms (4–6), they are located at the periphery of the star-shaped PLAs. Thus, increasing the number of arms leads to their stretching away from the centre of the star-shaped PLA macromolecule [53,134].

The telechelic and 3-arm star-shaped PLAs bearing 2-ureido-4[1*H*]-pyrimidione (UPy) end groups were synthesized by reaction of hydroxyl-functionalized polymers with the excess of UPy-NCO. The crystalline structure of supramolecular PLLAs was investigated in different crystallization temperatures (T_c). At lower T_c, the metastable β crystals are formed which may be transformed into more stable α crystals during heating. This is related to confinement effect by stacked UPy crystals and the restrained chain mobility due to strong interactions of UPy end-groups. With heating to ~90 °C the UPy-UPy H-bonds are disrupted and the transition from β to α is observed [163]. Typically, the end groups functionalization with UPy groups decreases the crystallization of PCL, PLA or their copolymers due to the decreased structural symmetry [164]. However, to enhanced the sc-PLA crystallization and crystallization rate, the star-shaped PLA can be functionalized with supramolecular end-groups able to form strong hydrogen bonding. The 1:1 blend of linear and star-shaped stereoblock supramolecular polylactides (sb-SMP) have a lower crystallization temperature in comparison to the PLLA/PDLA blends composed of un-functionalized PLAs. However, it also depends on the molar mass of PLA because with the increase of PLLA and PDLA block lengths, the contribution of UPy end groups decreases. The strong influence of UPy end-groups on sc-PLA crystallization is ascribed to stronger interactions between enantiomeric blocks in the formed stereocomplexes [165].

The comparison of the thermal stability of star PLAs with carboxyl and/or hydroxyl end-groups was performed. It was reported that the hydroxyl-terminated PLA had lower thermal stability than did carboxyl-terminated PLA, as was evidenced by the faster depolymerization rate of the hydroxyl terminated polymers and their higher tendency to undergo racemization [166]. Star-shaped PLAs with carboxylic acid terminal groups showed significantly higher solubility and degradability than did star-polymers with hydroxyl terminal groups [120].

The viscoelasticity of star telechelic PLA ionomer melts could be modulated by varying the number of ionic groups per molecule [122]. Pentaerithritol ethoxylate–poly(*rac*-LA) stars were functionalizing with the complementary DNA base pairs adenine and thymine [138].

4. Star-shaped PLA polymers with a specified number of arms

The structures of star-shaped PLA polymers with a specified number of arms are shown in Tables 1–6. Thus, PLA homostars (Tables 1–3), star-block PLA copolymers (Table 4), miktoarm star PLA (Table 5), and metal-centered star-shaped PLA polymers (Table 6) are presented. In each table, the star structures are given

Table 5
Miktoarm star PLA polymers.

Star structure	Arm structure[a)]			Method of synthesis[b)]	Ref.
	A	**B**	**C**		
AB_2	PEG (7300)	PLLA (16 500*) PDLA (15 900*) PDLLA (15 000*)		s1, (ROP)	[191]
	MPEG (2000, 5000)	PLLA (3790-10 700*)		s1, (ROP)	[378]
	MPEG (2000)	PLLA (15 700*) PDLLA (28 600*)		s1, (ROP)	[221]
	PF[c)] (5600-9300)	PDLLA (10 800-12 200*)		s2	[489]
	PHIC[d)] (5100-10 900)	PLLA (15 500-20 700*)		s3, (ROP)	[482]
	MPEG (2000)	PLLA-*b*-MPEG (9200-14 100*)		s4, (ROP)	[330]
	MPEG (5000)	PLLA-*b*-MPEG (18 400-23 100*)		s4, (ROP)	[330]
	PBA, PNIPAAm, PPEGA[e)]	PLA (4700-5700*)		s5, (ROP/ RAFT/ click)	[490]
	PS (8500, 4000)	PDLLA (3500, 7000)		ROP, click	[402]
	P(EA-*co*-HEA)-*b*-PS)[f)] (14 600*)	PLLA (49 600*)		s6, (ROP)	[107]
	P(EA-co HEA)-b-PS)[f)] (38 100*)	PLLA (57 800*)		s6, (ROP)	[107]
	MPEG (2000)	PLA (8100*)		s7, (ROP)	[437]
	MPEG (2000)	PLA-*b*- PPBDMMA[g)] (25 500-28 800*)		s8, (ROP)	[437]
	PTEGA[h)]	PDLLA (28 400*)		s9, (ROP)	[491]
	PTEGA[h)]	PLA (33 100*)		s9, (ROP)	[492]
	PDLA (4900*)	PLLA (10 400*)		s10	[301]
	poly(aspartic acid)	PLLA ($\leq$ 24 800*)		ROP	[493,494]
AB_3	PDLA (4900*)	PLLA (10 500*)		s10	[301]
	PCL (1300)	PLLA (11 500*)		s11, (ROP)	[495]
	PF[c)] (5100-9400)	PDLLA (10 300-14 000*)		s2	[489]
	P(EA-*co*-HEA)-*b*-PS)[f)] (11 700*)	PLLA (56 300*)		s6, (ROP)	[107]
	P(EA-*co*-HEA)-*b*-PS)[f)] (38 200*)	PLLA (69 800*)		s6, (ROP)	[107]
	PHIC[d)] (5200-9600)	PLLA (14 100-20 200*)		s3, (ROP)	[482]
	Tween-80[i)]**	PLA (8500-15 300)		ROP	[410]
	PLA	MPEG (71 900*)		s12	[157]
	PLGA	MPEG (11 400*)		s12	[157]
	poly(LA-*co*-TMC)	MPEG (14 000*)		s12	[157]

Please cite this article in press as: Michalski A, et al. Star-shaped and branched polylactides: Synthesis, characterization, and properties. Prog Polym Sci (2018), https://doi.org/10.1016/j.progpolymsci.2018.10.004

Table 5 (*Continued*)

Star structure	Arm structure[a)]			Method of synthesis[b)]	Ref.
	A	**B**	**C**		
AB_4	MPEG (2000)	PLLA (13 500*) PDLLA (9800*)		s13, (ROP)	[221]
	P(EA-*co*-HEA)-*b*-PS)[f)] (18 400*)	PLLA (58 600*)		s6, (ROP)	[107]
	P(EA-*co*-HEA)-*b*-PS)[f)] (69 700*)	PLLA (94 000*)		s6, (ROP)	[107]
A_2B_2	PS (7000, 6500)	PDLLA (9000, 15 000)		ROP, click	[402]
	PLLA (5000)	PDLA (10 400*)		s10, (ROP)	[301]
	MPEG	PLA (9100*)		s12	[157]
	PLLA (7000*)	PCHO[j)] (≤ 15 600*)		s14, (ROP)	[496]
A_2B_3	PDLA (5000)	PLLA (10 700*)		s10	[301]
A_2B_4	MPEG	PLA (8400*)		s12	[157]
A_3B_3	PLLA (5000)	PDLA (10 500*)		s10	[301]
ABC	PDMSB[k)]	PS (36 000)	PDLA	s15, (an/ROP)	[172]
	PEG (7300)	PLLA	PDLA (14 500*)	s16	[191]
	PEG (7300)	PLLA	PS (15 200*)	s16	[191]
	PEG (2000, 5000)	PS	PLLA(≤ 54 800)	s17	[497]
	PS	PLA	PEO (6000*)	s18	[498]
	PS	P*t*BM	PLLA (39 300*)	s19	[499]
	PS	PEG	PLLA (50 000*)	s20	[500]
	PS	PLLA	PEG (5900*)	s9	[492]
$A_nB_nC_n$	PS	PLLA	PEG	s21	[62]

[a)]in brackets M_n (g/mol) of arm and/or star polymer is given; M_w in italic; M_n of star polymer is denoted by *; commercial product is denoted by **.
[b)]methods of synthesis miktoarm star-block copolymers (an: anionic polymerization; Sn: Sn(Oct)2; ROP: ring opening polymerization; click: click reaction).
[c)]PF: poly[2,7-(9,9-dihexylfluorene)].
[d)]PHIC: poly(n-hexyl isocyanate).
[e)]PPEGA: poly(polyethylene glycol acrylate).
[f)]P(EA-co-HEA)-*b*-PS): poly(ethyl acrylate)-*co*-poly(hydroxyethyl acrylate)-*b*-polystyrene.
[g)]PPBDMMA: poly(2-phenylboronic esters-1,3-dioxane-5-methyl) methylacrylate.
[h)]PTEGA: poly(triethylene glycol monomethyl ether acrylate).
[i)]Tween-80: (polyoxyethylene sorbitan monooleate).
[j)]PCHO: poly(cyclohexene oxide).
[k)]PDMSB: poly(1,1-dimethyl silacyclobutane).
s1: di-functional macroinitiator was used at the end of **A** chain.
s2: copolymers were synthesized by combining the chain growth Suzuki–Miyaura coupling polymerization and ROP. Poly[2,7-(9,9-dihexylfluorene)] (PF) macroinitiators possessing two and three hydroxyl groups at the α-chain end were used.
s3: hydroxyl end-functionalized PHICs were used as macroinitiators in ROP of L,L-LA catalyzed by DBU.
s4: ROP of L,L-lactide, followed by coupling reaction.
s5: di-functional initiator with alkyne group was used and then the resulting alkyne functional PLA was reacted with azide functional polymer.
s6: di-, tri-, and four-functional macroinitiator was used at the end of **A** chain; ROP with DBU as catalyst.
s7: MPEG with two hydroxyl end-groups ($MPEG(OH)_2$) was used as macroinitiator.
s8: combination of ROP and ATRP with $MPEG(OH)_2$.
s9: initiating system was based on a dithiomaleimide containing dual ROP/RAFT initiator.
s10: combination of ROP (DBU as catalyst) and click chemistry.
s11: lipase-catalyzed ROP of ε-CL with multifunctional 1-ethyl glucopyranoside as an initiator and after deprotection ROP of L,L-lactide.
s12: MPEG esters of citric, mucic, and tartaric acids were used as initiators for LA polymerization and/or copolymerization with glycolide and trimethylene carbonate.
s13: tetra-functional macroinitiator was used at the end of **A** chain.
s14: ROP of L,L-LA followed by photoinduced free radical promoted cationic polymerization of cyclohexene oxide.
s15: hydroxy-functional PDMSB-*b*-PS macroinitiator was used for the ROP of D,L-LA.
s16: carboxylic acid functional cyclic carbonate, derived from 2,2-bis(methylol)propionic acid, was coupled to MPEG. After ring-opening of the cyclic carbonate, macroinitiator capable of initiating either controlled radical or ring-opening polymerization was formed.
s17: the combination of ROP and RAFT.
s18: arms were synthesized by combining ATRP and ROP followed by two click reactions.
s19: PS-*b*-P*t*BM copolymer was used as initiator for L,L-LA.
s20: PS-*b*-PEG copolymer was used as initiator for L,L-LA.
s21: combination of ROP, ATRP, copper-catalyzed azide–alkyne cycloaddition (CuAAC) and ROMP.

Please cite this article in press as: Michalski A, et al. Star-shaped and branched polylactides: Synthesis, characterization, and properties. Prog Polym Sci (2018), https://doi.org/10.1016/j.progpolymsci.2018.10.004

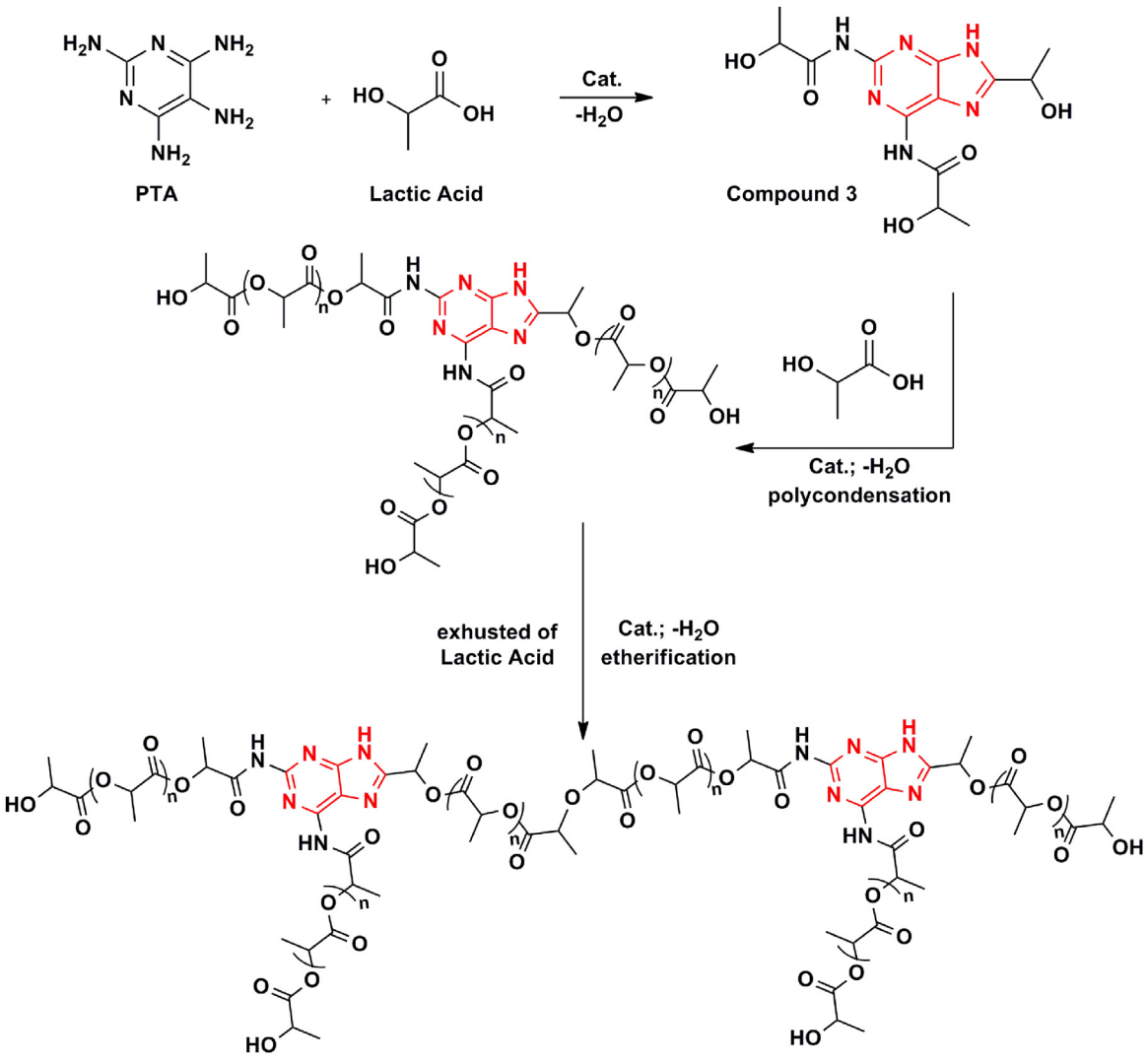

Fig. 8. Synthetic route of star PLA with a PTA [119].

in the order of the increasing number of arms. Typically, the small molecules containing multiple hydroxyl functionalities were usually used to initiate the ring opening polymerization of LA, as shown in Tables 1–6.

4.1. Homostars of PLA

In Tables 1–3, the collected data for homostars of PLLA, PDLA, and PDLLA are shown. The multi-hydroxyl compounds were used as initiators of the ROP and were subsequently transformed into the cores of stars with a specified number of arms, e.g., glycerol, 1,1,1-tris(hydroxymethyl)propane (TMP), pentaerythritol, dipentaerythritol (DPE) and its derivatives, xylitol, sorbitol, mannitol, myo-inositol, sucrose, hydroxyl-terminated cyclotriphosphazene, star-shaped poly(ethylene glycols), and natural sugars. Usually, the "core-first" method was used in the star synthesis. Considerably fewer reports were devoted to the "arm-first" method (cf. Tables 1–3).

Most of the initiators that were used as the "cores" of the star-shaped PLLAs were not favourable natural products. The utility of these non-bioresorbable residual "core" compounds may be toxic after PLLA degradation, which is especially important if these polymers are applied for the preparation of drug release delivery systems [167]. Therefore, the synthesis of a star-shaped PLLA from L,L-lactide and pure natural polyols is desirable.

For example, pentaerythritol ethoxylate was used to synthesize a 4-arm star PLA with a polymeric flexible polyol core [138,140,147]. On the other hand, tetrahydroxyperylene and hexakis-[p-(hydroxymethyl)phenoxy] cyclotriphosphazene were used to synthesize 4- and 6-arm PLA stars with rigid cores, respectively. A comparison of these star-shaped PLAs with different cores indicates that macromolecules with a rigid core exhibit a higher melting temperature [27,29].

Star-shaped PLAs using polyfunctional amines as the initiator were also obtained (Fig. 9) [70].

Star PLA was also obtained by ROP of D,L-lactide in supercritical CO_2 with D-sorbitol as a co-initiator. This process was performed at significantly reduced temperatures (as low as 80 °C) compared with bulk reactions (140 °C). As a result, a reduction in the formation of side products was observed, which led to narrower polymer dispersity and good control of the degree of branching [146].

4.2. Star-block PLA copolymers

The structures of the star-block PLA copolymers with a specified number of arms (up to 32) are shown in Table 4. Block copolymers containing PLA and PCL, PGA, PEG or PTMC were usually synthesized by the ring opening polymerization (ROP) of the respective monomers. As an alternative, RAFT [168–170] and ATRP [130,133] methods were also applied.

Please cite this article in press as: Michalski A, et al. Star-shaped and branched polylactides: Synthesis, characterization, and properties. Prog Polym Sci (2018), https://doi.org/10.1016/j.progpolymsci.2018.10.004

Table 6
Star-shaped PLA polymers and copolymers with metal ion core.

star			coordinating ion[b]	catalyst[c]	Ref.
f [a]	core	arm structure			
3	dbmOH[d] (Fe^{3+})	PDLLA	Fe^{3+}, ($M_n \leq 23\,200$)	Sn	[178]
3	dbmOH[d] (Fe^{3+})	PDLLA	Fe^{3+}, ($M_n \leq 37\,500$)	Sn	[180]
3	dbmOH[d] (Eu^{3+})	PDLLA	Eu^{3+} (arm: $M_n = 8400$)	Sn (*a-f*)	[179]
4	BHMBP[e] (Ru^{2+})	2 PDLLA + 2 PS	Ru^{2+} ($M_n = 51\,500$)	Sn (*a-f*)	[181]
5	dbmOH[d] (Eu^{3+})+ BHMBP[e]	3 dmb-PDLLA + bpy-PCL_2	Eu^{3+} (PLA arm: $M_n = 8400$)	Sn (*a-f*)	[179]
6	BHMBP[e] (Ru^{2+}, Fe^{2+})	PLLA, PDLLA, PDLLA-*b*-PCL	Ru^{2+}, Fe^{2+} ($M_n \leq 240\,000$)	Sn (*a-f*)	[183]
6	(Fe)bpy[f] (Fe^{2+})	PEG-*b*-PLLA PEG-*b*-PDLLA	Fe^{2+} ($M_n \leq 115\,600$)	Sn (*a-f*)	[182]
6	(Ru)bpy[g] (Ru^{2+})	PDLLA PDLLA-PtBA	Ru^{2+} ($M_n \leq 57\,000$) ($M_n \leq 28\,600$)	DMAP (*a-f*)	[106]

[a] *f*: number of arms.
[b] in brackets M_n (g/mol) of star polymer.
[c] usually polymers were obtained by "*core-first*" method; *a-f* (in parenthesis) denotes "*arm-first*" method; descriptions of used catalysts:
Sn: stannous octoate (tin(II) octoate, stannous 2-ethylhexanoate), Sn(Oct)2.
DMAP: 4-dimethylaminopyridine.
[d] $Fe(dbmOH)_3$: alcohol-functionalized iron(III) tris(dibenzoylmethane) complex, iron serves as both a dbm protecting group and a catalyst for lactide ring-opening polymerization.
[e] BHMBP: bis(hydroxymethyl)-2,2-bipyridine.
[f] (Fe)bpy: iron(II) tris(bipyridine) complexes.
[g] Ru(bpy): $[Ru(bpy(CH_2OH)_2)_3](PF_6)_2$, ruthenium tris(bipyridine) centers.

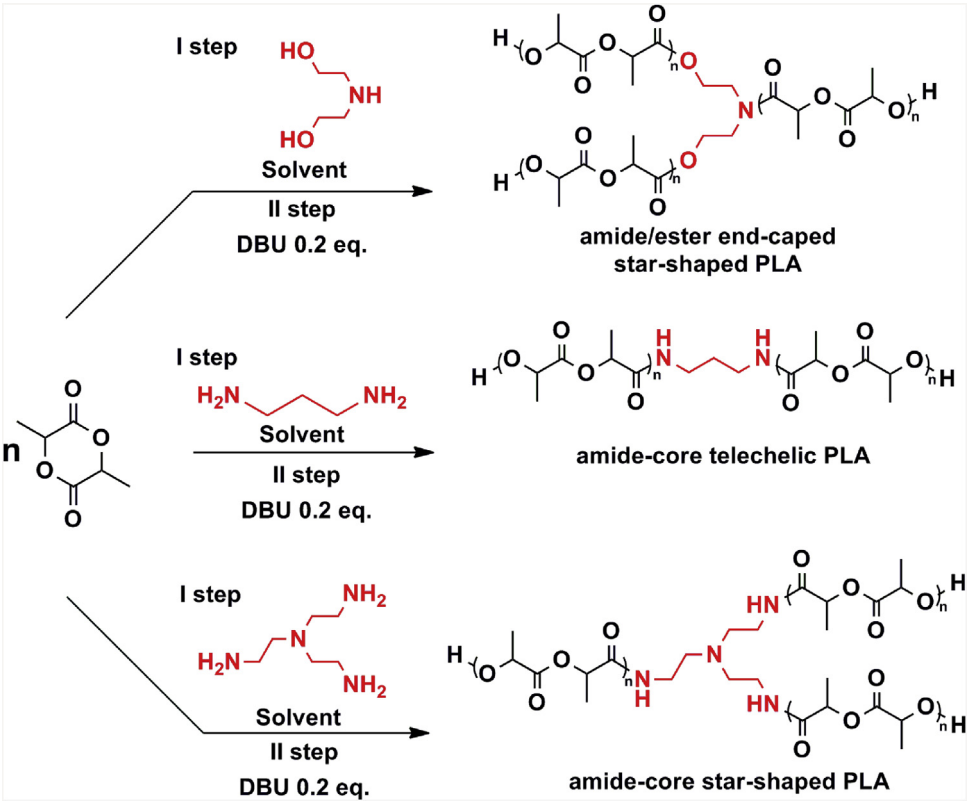

Fig. 9. Preparation of star-shaped PLA using polyfunctional amines as the initiator and DBU as the catalyst [70].

There are several reports on the synthesis of dendrigraft star-block copolymers having graft and/or comb structures. Highly branched star-comb poly(ε-caprolactone)-*block*-poly(L-lactide) (scPCL-*b*-PLLA) with M_n up to 140 000 g/mol were obtained using star-shaped hydroxylated polybutadiene (sHPB) as the macroinitiator by a simple "grafting from" strategy (Fig. 10). These star-comb double crystalline copolymers were well-defined and used to study the influence of the polymer chain topology by comparing with their counterparts in linear-shaped, star-shaped, and linear-comb shaped forms [171].

On the other hand, the amphiphilic 21-arm, star-like block copolymer β-cyclodextrin-*graft*-(poly(lactide)-*block*-poly(2-

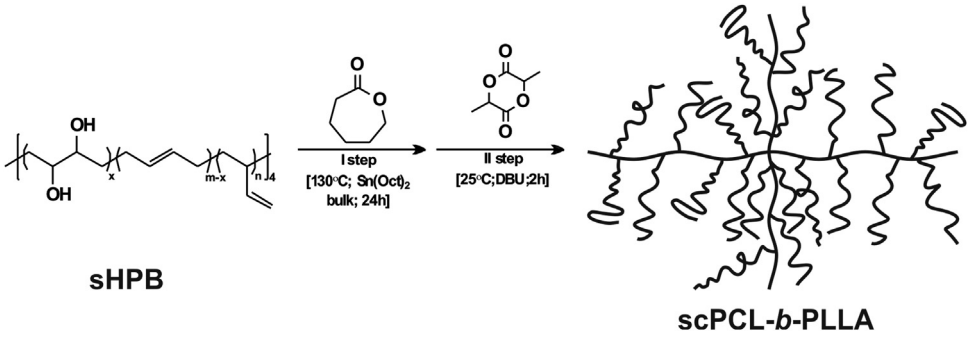

Fig. 10. Synthesis of star-comb poly(ε-caprolactone)-block-poly(L-lactide) (scPCL-*b*-PLLA) [171].

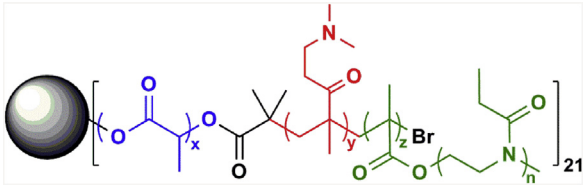

Fig. 11. Schematic structure of β-CD-*g*-(PLA-*b* -PDMAEMA-*b* -PEtOxMA)$_{21}$ [172].

(dimethylamino) ethyl multimethacrylate)-*block*-poly[oligo (2-ethyl-2-oxazoline) methacrylate]) (β-CD-*g*-(PLA-*b*-PDMAEMA-*b*-PEtOxMA)) (Fig. 11) was prepared. That copolymer formed stable micelles with β-CD and hydrophobic PLA as the inner core, reductive PDMAEMA as the middle layer, and hydrophilic PEtOxMA as the shell [172]. The simulation results showed that micellar aggregation was favored by longer hydrophobic or pH-sensitive chains, shorter hydrophilic backbones, a smaller hydrophilic side chain grafting density, and fewer polymer arms [173].

4.3. Star-shaped PLA polymers with different arm structures (miktoarm stars)

According to Hadjichristidis [174], "the term miktoarm stars was adopted for stars with chemical asymmetry." Thus, miktoarm stars are molecules having chemically different arms (**A**, **B**, **C** or **D**) linked to the branched point. Their structures, shown in Fig. 12, can be described as follows, e.g., **A$_2$B**, **ABC, A$_2$B$_2$, AB$_3$**, and **ABCD**.

Hadjichristidis developed methods for the synthesis of miktoarm polymers and published reviews describing various star structures and discussed their properties [174–177]. The summarized data of the synthesis and the structure of miktoarm star polymers, where at least one arm is built of homo- and/or copolymer of PLA, are collected in Table 5.

4.4. Metal-centered star-shaped PLA polymers

The star polymers with metal-ligand non-covalently bonded with polymeric arms are sensitive to an external stimulus, therefore their structure is often labile and can be broken by alteration of pH or heat [32]. Typically, the non-covalent cores are based on iron, ruthenium, and europium with hydroxy-substituted dibenzoylmethane (dbm) and bipyridine (bpy) ligands. For dbmOH, the ROP of LA was followed by complexation to the metal center [178–180], while bpyOH systems [106,181–183], must be first complexed with a metal ion to create a transition metal macroinitiator core. These materials are designed with a specific function, and because of their stimuli-responsiveness, luminescent materials for drug delivery and imaging or responsive chromophores can be created [29].

In Table 6, metal-centered star-shaped (co)polymers with Fe^{2+}, Fe^{3+}, Eu^{3+}, and Ru^{2+} ions are shown. Star structures were obtained by the combination of coordination chemistry with living or controlled polymerization via metalloinitiation, metallotermination, coupling, and macroligand chelation approaches (Fig. 13) [40,180].

Luminescent ruthenium tris(bipyridine)-centered star block copolymers consisting of PLA as the hydrophobic core and PAA as the hydrophilic corona should provide a multifunctional drug delivery system with the capability of optical imaging. Star copolymers were obtained by the consecutive ROP of D,L-lactide, ATRP of *tert*-butyl acrylate, and finally, the *tert*-butyl end-groups were hydrolyzed [106]. The polymeric metal complex iron tris(dibenzoylmethane-polylactide), Fe(dbmPLA)$_3$, was synthesized from D,L-lactide and Fe(dbmOH)$_3$, a hydroxyl functionalized metalloinitiator. Demetallation with dilute HCl yielded dbmPLA macroligands for chelation to other metals [180].

5. Star-shaped PLA polymers having a large core (branched and/or dendritic)

Star-shaped PLA polymers with a higher number of arms and larger cores: dendritic (up to 64 arms) and hyperbranched (up to 160 arms) are shown in Tables 7 and 8, respectively.

5.1. Star-shaped PLA polymers with a dendritic core

According to many definitions, a dendrimer is a molecule consisting of the following components: a central core; monomeric units linking branching points, symmetrically distributed in the dendrimer; and closely packed surface groups (functional groups) [184–186]. These functional groups are usually used as initiators for the formation of arms (generally by the ROP method).

All data for PLA stars with a dendritic core are collected in Table 7. Multi-arm PLA stars based on dendrimers are usually prepared by the "core-first" strategy. A typical synthesis involves the initiation of ROP from a multifunctional hydroxy- (e.g., dendritic polyols [24]) or amine-substituted initiator. In dendrimer synthesis, however, incomplete initiation was often observed due to the close packing of growing chains [29]. In Fig. 14 there is shown star-shaped PLA with Boltorn H20 as a core and 16 arms.

Dendrimer star PCL, a block-comb copolymers with 18 arms, was also prepared with poly(L-lactide) blocks grafted from poly(2-hydroxyethyl methacrylate) blocks by the ROP of L,L-lactide [188].

5.2. Star-shaped PLA polymers with a branched core

Branched polymers possess compact, highly branched, three-dimensional structure and high densities of terminal functional groups. The polymers' terminal groups can easily react with other compounds (monomers) and can be used as multifunctional initiators for star-shaped polymers [89]. In branched polymers, there is a lack of the perfect structure typically observed for dendrimers; however, branched polymers are substantially easier to synthesize.

Please cite this article in press as: Michalski A, et al. Star-shaped and branched polylactides: Synthesis, characterization, and properties. Prog Polym Sci (2018), https://doi.org/10.1016/j.progpolymsci.2018.10.004

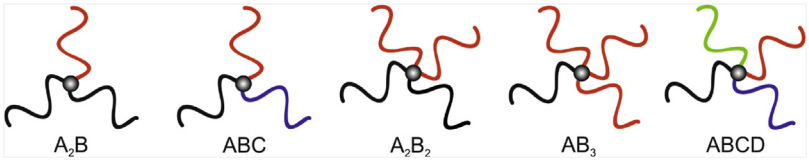

Fig. 12. Structures of miktoarm star polymers.

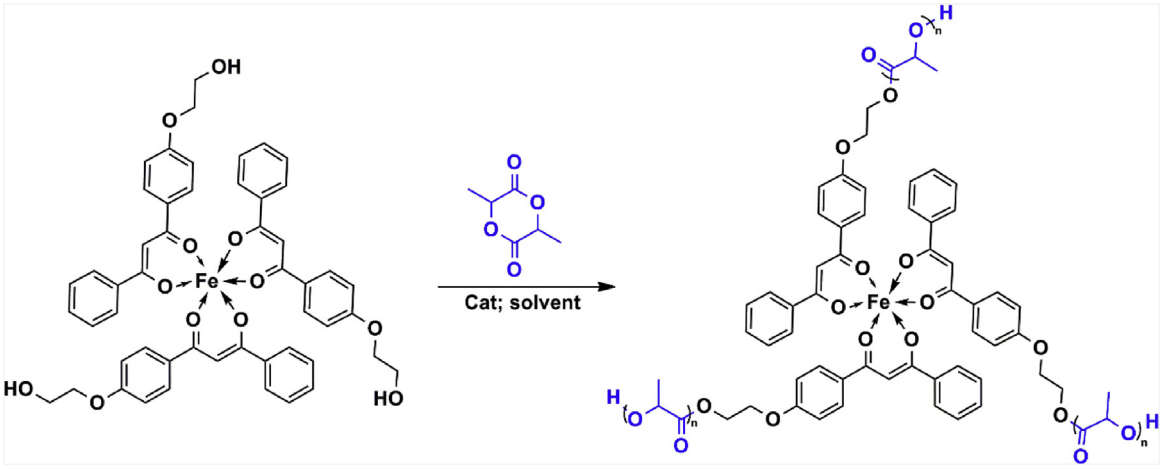

Fig. 13. Scheme of the methods of synthesis of metal-centered star-shaped PLA polymers [180].

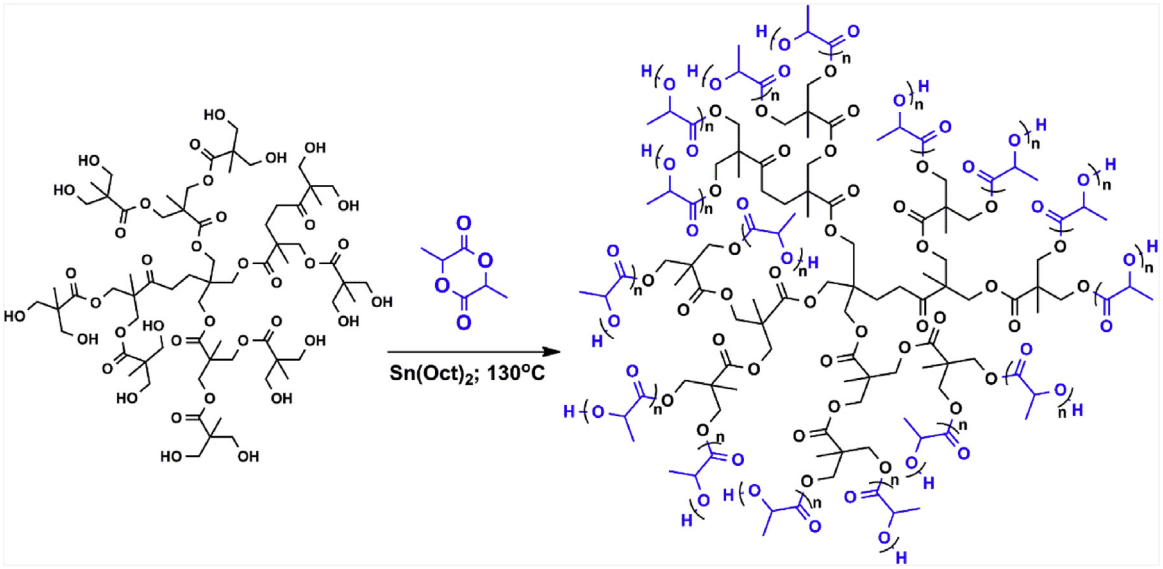

Fig. 14. Depicts the synthesis of a 16-arm star-shaped PLLA with Boltorn H20 as a core [187].

Table 7
Star-shaped PLA polymers and copolymers obtained by ROP and having dendritic core (usually $Sn(Oct)_2$ was used as catalyst).

Structure of core	Structure of arms	*f* (number of PLA arms)[a,b]	PLA end groups	Ref.
bisMPA[c] (G1-G2)	PLLA or PDLLA	6, 12 (3100-44 000*)	OH	[501]
bisMPA[c] (G1-G4)	PLLA	8, 16, 32, 64 (29 000-74 700*)	OH	[108]
bisMPA[c]-G3	PLLA	24 (24) (DP = 38)	OH	[105]
bisMPA[c]	PLLA or PDLLA	4 (4), 6 (6), 12 (12) (22 300-44 000*)	OH	[20]
bisMPA[c]	PLLA	24 (24) (~ 6400*)	OH	[105]

Table 7 (*Continued*)

Structure of core	Structure of arms	*f* (number of PLA arms)[a,b]	PLA end groups	Ref.
bisMPA[c] -G1	PDLA, PLLA	6 (6) (16 600*, 23 500*)	OH	[21]
bisMPA[c] -G2	PCL, PLLA or PDLA	12 (12) (36 300-61 500*)	OH	[21]
bisMPA[c] -G3	PCL, PLLA or PDLA	24 (24) (67 900-101 100*)	OH	[21]
bisMPA[c]-G3	PLLA-*b*-PTMC	32 (67 170-112 220*)	OH	[108]
Boltorn H20[d]	PLLA	16 (16) (17 800-157 700*)	OH	[187]
Boltorn H20[d]	PLLA-*b*-PCL	16 (16) (51 800-104 300*)	OH	[502]
Boltorn H20[d]	PLLA	16 (45 400*)	OH	[108]
Boltorn H20[d]	PLLA-*b*-PTMC	16 (45 400-56 000*)	OH	[108]
Boltorn H40[d]	PDLLA	64 (260 000*)	OH	[411]
Boltorn H40[d]	PLA	64 (26 000*)	OH	[419]
Boltorn H40[d]	PLLA-*b*-TPGS[e]	64 (55 000*)	OH	[419]
Boltorn H40[d]	PLLA-*b*-PEG	64 (108 500*)	COOH	[127]
Boltorn H40[d]	PLLA-*b*-MPEG PLLA-*b*-PEG-FA[f]	64 (20) (108 500*)	COOH	[125]
DAB-8[g]	PLLA	8 (8) (103 700*)	OH	[87]
DAB-32[g]	PLLA or PDLA	32 (32) (356 400, 376 900*)	OH	[87]
DPE[h]	PLLA-*b*-PDMAEMA[i]	18 (18) (60 500-104 300*)	OH/Br	[132]
DPE[h]	PLLA PLLA-*b*-PDMAEMA[i]-*b*-PEG	16 (89 400) 16 (≤238 000*)	OH OCH_3	[386]
PAED[j]	PLLA-*b*-PMMA or PS	6, 12, 24 (6, 12, 24) (42 700-148 000*)	OH/Br	[129,131]
PAMAM[k] (G1-G3)	6-arm PLLA	12, 24, 48	COOH	[126]
PAMAM [k]-G1	PLLA or PDLLA	8 (9200*)	OH	[334]
PAMAM [k]-G3	PLLA-*b*-PEG	32 (221 400*)	OH	[403]
PAMAM [k]-G3	PLLA	32 (16-21) (19 540-64 000*)	OH	[197]
PAMAM [k](G1-G4)	PLLA or PDLLA	8 (5-8), 16 (11-14), 32 (16-21), 64 (25-32) (9600-204 000*)	OH	[79]
PAMAM[k] (G2-G4)	PLLA	16 (26 400-67 500*), 32 (44 300*), 64 (48 900*), 128 (56 300*)	OH	[385]
POSS-$(OH)_{32}$[l]	PDLLA-*b*-PDMAEMA[i]	32 (110 100-220 600*)	OH/Br	[130]
PPI[m] (G1-G4)	PLLA	8, 16, 32, 64 (29 400-87 600*)	OH	[108]
PPI[m]-G3	PLLA-*b*-PTMC	32 (64 100-100 700*)	OH	[108]
PPI[m]-G4	PLLA PDLA	32 (377 000*) 32 (356 000*)	OH	[297]

[a] the overall number of active centers on the core is given; in brackets number of arms is given.
[b] in brackets M_n (g/mol) of arm and/or star polymer is given; M_n of star polymer is denoted by *.
[c] bisMPA: 2,2-bis(hydroxymethyl)propanoic acid based dendrimers.
[d] Boltorn H20 and Boltorn H40: the aliphatic dendritic polyester.
[e] TPGS: D-α-tocopheryl polyethylene glycol 1000 succinate.
[f] FA: folate.
[g] DAB-8 and DAB-32: amine terminated diaminobutane poly(propylene imine) dendrimer with 8 and 32 primary amino groups.
[h] DPE: dendrimer polyester (Perstorp Specialty Chemicals, Sweden).
[i] PDMAEMA: poly(2-(dimethylamino)ethyl methacrylate).
[j] PAED: poly(aryl ether) dendrimers.
[k] PAMAM: poly(amidoamine) dendrimers.
[l] POSS: multi-hydroxyl polyhedral oligomeric silsequioxane.
[m] PPI: poly(propyleneimine) dendrimers.

Please cite this article in press as: Michalski A, et al. Star-shaped and branched polylactides: Synthesis, characterization, and properties. Prog Polym Sci (2018), https://doi.org/10.1016/j.progpolymsci.2018.10.004

Table 8
Star-shaped PLA polymers obtained by ROP and having hyperbranched core.

Structure of core	Structure of arm	*f* (number of PLA arms)[a,b]	PLA end groups	Ref.
5HDON[c]	PLLA	(9300-34 100*) DB ~ 0.21	-OH, focal unit	[162]
aliphatic polyester (Boltorn H20[d])**	PLLA	16 (17 800-157 700*)	-OH	[187]
aliphatic polyester (Boltorn H20[d])**	PLLA	16 (17 800-1 577 000*)	-OH	[187]
aliphatic polyester (Boltorn H40[e])**	PDLLA	26 (26 000*)	-OH	[419]
aliphatic polyester (Boltorn H40[e])**	PLLA-*b*-MPEG	20 (108 500*)	-OH, -COOH	[125] [373]
BHB[f]	PLLA	(6800-12 100*) DB ~ 0.23-0.30	-OH	[238]
BHB[f]	PLLA PDLA	24 (259 000*) 24 (224 000*)	-OH	[297]
BHB[f]	PDLLA	(270-57 500*) DB ~ 0.018-0.469	-OH	[24,234, 239,346]
bisMPA[g]	PLLA	(49 500-147 000*)	-OH	[216]
bisMPA[g]	PLLA	(19 000-26 000*)	-OH	[22]
polyglycerol[h]	PLLA	(89 000*)	-OH	[232]
hb(PEG-*co*-PG)[i]	PLLA	67; 128 (16 000-95 000*)	-OH	[93]
*hb*M[j]	PLLA	(13 500-64 900*)	-OH	[73]
*hb*PEG[k]	PLLA	160 (122 400-246 900*)	-OH	[78]
*hb*PEI[l]	PLA	DP_n ~ 9-77	-OH	[420]
*hb*PEI [l]**	PLLA PDLLA	13 DP_n ~ 39.5-47	-OH	[261]
*hb*PG[m]	PLLA	28, 68 (2200-26 500*)	-OH	[89]
*hb*PG[m]	PLLA	(1500-10 000*)	-OH	[503, 504]
*hb*PG[m]	PLLA	13, 18, 25 (13 500-200 000*)	-OH	[91]
*hb*PG[m]	PLLA	25, 51 (35 500, 43 000*)	-OH	[366]
*hb*PG[m]	PLLA	20 (22 000-250 000*)	-OH	[231]
*m*PEI[n]	PLLA	(9860-28 800*)	-OH	[505]
*m*PG[o]	PDLA	(6700-23 000*)	-OH	[447]
*m*Si-PLLA[p]	PLLA	(89 000*)	-OH, -Me, -Si	[506]
PEHMO[q]	PLLA	13 (2300-74 000*)	-OH	[214]
PDL[r]	PDLLA	(151 000*)	-OH	[225]
PDL[s]	PLLA	(229 500-255 800)	-OH	[507]

[a] the overall number of arms is given.
[b] in brackets M_n (g/mol) of arm and/or star polymer is given; M_w in italic; M_n of star polymer is denoted by *; commercial product is denoted by **; DB: degree of branching; catalyst: $Sn(Oct)_2$.
[c] 5HDON: 5-hydroxymethyl-1,4-dioxane-2-on, the hyperbranched PLAs were obtained by ring-opening multibranching copolymerization of lactide with the cyclic inimer 5HDON.
[d] Boltorn H20: hyperbranched aliphatic polyester (Boltorn H20) containing 16 terminal hydroxyl groups.
[e] Boltorn H40: hyperbranched aliphatic polyester (Boltorn H40) containing 64 terminal hydroxyl groups.
[f] BHB: 2,2-bis(hydroxymethyl)butyric acid, condensation of AB_2 macromonomer.
[g] bisMPA: bis(hydroxymethyl)propionic acid, the hyperbranched PLAs were obtained by self-polycondensation of AB_2 macromonomer.
[h] polyglycerol: simultaneous incorporation of glycidol in PLA chain by opening the ring and the growth of PLA from OH group results in a hyperbranched architecture.
[i] *hb*(PEG-*co*-PG): hyperbranched poly(ethylene oxide)-*co*-poly(glycerol).
[j] *hb*M: hyperbranched D-mannan.
[k] *hb*PEG: hyperbranched poly(ethylene oxide).
[l] *hb*PEI: hyperbranched polyethylenimine.
[m] *hb*PG: hyperbranched polyglycerols.
[n] *m*PEI: multibranched polyethyleneimine was used as an initiator of L,L-lactide polymerization with $Sn(Oct)_2$ as a catalyst.
[o] *m*PG: multibranched polyglycerol.
[p] silyl-terminated oligomers were readily hydrolyzed into hyperbranched polymers.
[q] PEHMO: poly(3-ethyl-3-hydroxymethyloxetane).
[r] PDL: poly(ε-decalactone); branched multiblock polymers were synthesized by coupling star diblock copolymers with a substoichiometric quantity of sebacoyl chloride.
[s] PDL: poly(ε-decalactone); multiarm hydroxyl-terminated PDL-OH were used as an initiator for L,L-lactide polymerization.

These polymers were obtained usually using "core first" methods. Multi-arm star-shaped PLA (co)polymers having (hyper)branched cores are listed in Table 8.

Hetero-arm core star polymers consisting of PLA and PS arms (PLA_nPS_n) were also obtained by the reversible addition-fragmentation chain transfer copolymerization of 1,2-bis(maleimidoethane) with styrene in the presence of a polylactide macro-chain transfer agent [169]. The one-pot synthesis of star-shaped PLLAs with $M_n \leq 4200$ g/mol and the core built from bislactones was also reported [189].

Please cite this article in press as: Michalski A, et al. Star-shaped and branched polylactides: Synthesis, characterization, and properties. Prog Polym Sci (2018), https://doi.org/10.1016/j.progpolymsci.2018.10.004

6. Methods of characterization of star-shaped PLA

Polymers composed of macromolecules of a complex, nonlinear architecture require more precise and demanding analytical tools compared with those employed for the characterization of their linear counterparts. Since polymer properties are considerably affected by the architecture of the component macromolecules, detailed knowledge of their topology is an important prerequisite for further structure–property relationship studies of the resultant macromolecular materials.

The characterization of star polymers has traditionally been performed using the same instruments and techniques employed for the analysis of linear polymers, such as size exclusion chromatography (SEC) [190], proton nuclear magnetic resonance (^{1}H NMR) spectroscopy [187,190,191], and matrix-assisted laser desorption/ionization time-of-flight mass spectrometry (MALDI-ToF MS) [89,192]. In addition, differential scanning calorimetry (DSC) [18,19,30,56,58,59,66,75,81,85,99,193–198], thermogravimetry (TG) [193,197], wide-angle X-ray diffractometry (WAXD) [8,58,59,81], viscometry [8,56,59,75,199], rheological measurements [8], tensile and impact testing [75,99,195,196], and swelling measurements [56] were applied for multi-arm PLLA and L,L-lactide copolymers to investigate the effects of branching on the physical properties and highly ordered structures [200]. Due to the star-shaped structure and usually high molar mass, the typically applied method for their characterization provides only incomplete information. Therefore, the more advanced characterization techniques for the detailed analysis of star macromolecules should be applied, as e.g. multidimensional chromatography, atomic force microscopy (AFM), and transmission electron microscopy (TEM) [32].

6.1. Traditional characterization techniques (SEC and DLS)

The SEC method is usually used to determine the molar mass of polymers, including branched polymers [32,35,190,192,201]. It is worth noting that the M_n value measured by SEC is not absolute. The molar masses measurement of star/branched polymers is based on a calibration performed with the use of available commercial linear standards, and the assign M_n values are usually lower than the actual M_n. In addition, the hydrodynamic volume of star-shaped macromolecules is smaller than that of linear polymers and depends not only on molar mass but also on the number of arms, which makes their molar mass determination quite complex. SEC analysis with a multi-angle light scattering (MALS) detector allowed to determine absolute M_n value of polymers. However, this method is less reliable for the polymers with very broad dispersities [192].

Dynamic light scattering (DLS) provided information about the hydrodynamic size of star polymers in solution. The size of star polymers is usually below 100 nm and varies dramatically with their synthesis method (e.g., core-first, arm-first, and brush-first) [32].

6.2. Spectroscopic analysis of star polymers

NMR spectroscopy is usually used for determination of specific molecular environments of the different core in a molecular structure. The observed broadened polymeric resonance peaks are derived from the inequivalent environment of individual protons in the polymer chains. Therefore, for more specific characterization multidimensional NMR spectroscopy is usually applied [32]. ^{1}H NMR spectra are also used for molar mass determination. The integration of methine protons from terminal group adjacent to the —OH group or protons in branching moiety is employed and compared with methine protons from the PLA main chain.

Additionally, Danko et al. evaluated the molecular dynamics of star-shaped PLLA functionalized with pyrenyl end-groups using static and time-resolved fluorescence spectroscopy in solution at room temperature [134]. The end-to-end cyclization of polymer arms with accompanying excimer formation of the covalently linked pyrene end-groups because of dynamic segmental motions was observed, and the rate of the excimer formation increased with the number of arms. The number of arms influenced the location of the pyrenyl groups. For star-shaped polylactides with few arms, the pyrene units were located in the center, while with an increasing number of arms, a stretching away from the center was observed [134].

Fluorescence spectroscopy appears to be a useful and convenient technique for the examination of the branched macromolecular structures. A number of studies on the application of this method for the characterization of the well-defined linear, dendritic, and star-shaped polymers were reported (references cited in [134]).

6.3. Two-dimensional chromatography

To determine the actual structure and size of star-shaped macromolecules on the basis of the typically applied methods are still a challenge for scientific groups. The results of SEC, NMR or MALDI-TOF analyses carried out for branched and star-shaped macromolecules cannot be interpreted in such a straightforward way as for the linear chains. For example, SEC separates macromolecules according to their hydrodynamic volume, which is different for the same M_n but different topologies. In contrast, the NMR and MALDI-TOF analyses give cumulative mean values of the molar masses and the content of a given end-group per macromolecule. However, SEC equipped with a simple RI detector would merely show the same or even narrower “molar mass” distribution for star-shaped polymers with structural imperfections compared with linear macromolecules [202], and it is not able to provide the required information. Therefore, SEC analysis with a MALS detector should be employed for the direct determination of the number of arms in the star-shaped polymers. This method, although fast and convenient, can only be used for the analysis of polymers of uniform architecture and of high enough molar mass. In these macromolecules, the radius of gyration should be higher than 10–15 nm because of the MALS detector limits. This is because polymers with different architectures usually have different hydrodynamic volumes for a given molar mass. The triple SEC detection (RI, RALS, viscosity) can enable the determination of absolute molar mass but cannot distinguish between macromolecules with varying numbers of arms.

The absolute determination of the molar mass of a star-shaped polymer is possible when the arms of this polymer can be detached from the core. Then, measurements of the absolute molar masses of the original star-shaped polymer and arms, after their detachment, can provide unambiguous information. This method was used, for instance, to analyze star-shaped poly(tetrahydrofuran), attached with easily hydrolysable ester bonds to the aromatic core [203]. However, it, unfortunately, cannot be used for branched polyesters because both core and arms were hydrolyzed simultaneously. A degradable functionality was also incorporated into the core domain using a degradable bislactone to cross-link a non-degradable linear macroinitiator – single hydroxyl-terminated polystyrene (PS—OH) under ROP conditions. Hydrolysis of this core cross-linked polymer resulted in the degradation of the core and full recovery of the original linear PS arms [204,205].

In some other instances, the addition of a small amount of a mono-functional initiator to a system with a multifunctional initiator during the synthesis of star-shaped polymers may be useful.

Please cite this article in press as: Michalski A, et al. Star-shaped and branched polylactides: Synthesis, characterization, and properties. Prog Polym Sci (2018), https://doi.org/10.1016/j.progpolymsci.2018.10.004

This excess of mono-functional initiator can produce linear polymer chains that have the same molar mass as the arms in the star-shaped polymer (identical reactivity of an active function for both initiators has to be assumed). The molar masses of the final polymers both star-shaped and linear can be determined by simple SEC analysis [204].

Traditional SEC and NMR analysis are giving only limited information on the compositional and topological structure of star polymers [190]. More detailed results were obtained by combining these techniques with other, more sophisticated methods of separation and detection because most common synthetic polymers exhibit structural heterogeneity. Thus, the optimization of each of the applied methods allows getting more reasonable results [206]. These techniques are called two-dimensional (2D) chromatography and are particularly useful for the chromatographic analysis of polymeric materials, where random distributions and structural diversity are very often observed [32,207–209].

Star-shaped polymers having a different number of arms also have a different number of functional end-groups. Because liquid chromatography at the critical point of adsorption (LC-CC) separates macromolecules according to the structure of the end-groups, both LC-CC and two-dimensional (2D) chromatography with LC-CC as the first dimension were employed. In the second dimension, ordinary SEC provided information on molar mass. The method applying critical conditions was based on the use of a solvent (usually a mixture of solvents) at a specific temperature when enthalpic and entropic factors of macromolecules stationary-phase solvent interactions cancelled each other [210,211]. Macromolecules under these conditions are separated exclusively with regard to the end-groups and independent of the molar mass. The interaction of end-groups with the column packing is responsible for the discrimination between macromolecules bearing different end-groups.

A series of papers are devoted to the synthesis and analysis of PLLA stars with various numbers of arms [212–215], and it was shown that only mixtures of stars with similar molar masses could be separated strictly with regard to the number of arms. Thus, structural imperfections can be detected regardless of the molar masses of the species. Star-shaped polymers, with strictly defined numbers of linear arms, provide useful model structures for studies of the branched macromolecular structures. Our papers [212–215] reported on the analysis of 1-, 2-, 3-, 4-, 5-, 6-, and 13-arm star-shaped PLLAs. For this purpose, we employed LC-CC analysis, which is very sensitive to macromolecular architecture and to the presence of functional groups [134,210]. It was shown that LC-CC allows for discriminating among PLLA structures with various architectures but having the same total number of hydroxyl groups, i.e., to distinguish for example the “star-shaped” (arms grown evenly from all of the OH groups) from the “comet-shaped” (arms grown from only a fraction of OH groups in a given core molecule) PLLA macromolecules of the same molar mass. The elution behavior of these very well-defined star-shaped PLLA was also discussed quantitatively on the basis of theories for polymer chromatography for large and small pores of a column packing. It was possible to derive the parameters necessary to quantitatively fit the experimental results.

The two-dimensional (LC-CC vs. SEC) chromatogram of star-shaped PLAs with 3, 4 and 6 arms with similar molar masses confirmed the unquestionable usefulness of this relatively new analytical method, as shown in Fig. 15 [214]. This method allows for the separation of a mixture of stars with similar molar masses according to their number of arms. In addition, star-shaped PLAs with various numbers of secondary OH groups at the PLAs’ arm ends, and primary OH groups attached directly to the core of the star were analyzed under critical conditions [213].

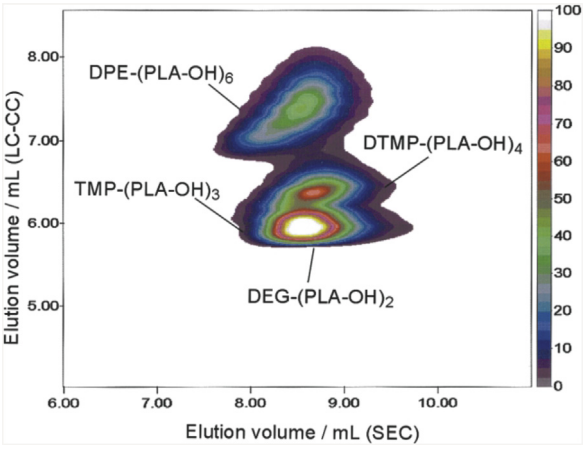

Fig. 15. Two-dimensional LC-CC versus SEC trace of the artificial mixture composed of linear PLA (DEG-(PLA-OH)$_2$) and star-shaped PLAs with 3, 4, and 6 arms: TMP-(PLA-OH)$_3$, DTMP-(PLA-OH)$_4$, DPE-(PLA-OH)$_6$ [214], Copyright 2003. Reproduced with permission from Elsevier Ltd.

7. Branched PLA

The branching of macromolecules can be achieved by applying different strategies and employing different methods of polymer synthesis [35,36,40,41]. One common method was to use the ring-opening polymerization of lactides or direct polycondensation of lactic acids with multifunctional co-monomers and catalysts in solution [17,24,216]. The synthesis and characterization of hyperbranched and highly branched polymer architectures were described by Voit and Lederer [192] and other authors [35,217]. These highly branched polymers are essentially the long-chain analogs of conventional dendrimers and hyperbranched polymers [217]. Many studies focused on the chain-branching reactions of PLA to increase the polymer melt strength [218–220].

Branching influences the crystallinity and chain entanglement of the polymers in the bulk. Traditionally, branching points are introduced by the addition of multifunctional monomers during the production of the linear polymer, which results in the formation of insoluble cross-linked materials. Soluble branched polymers can be prepared when the introduction of branching is not accompanied by an infinite network formation [216].

Only a few papers were completely devoted to branched PLAs [22,35] but in more other papers their synthesis and properties were also reported, e.g., [19,24,27,126,162,219,221].

Hyperbranched polymers with many branching points are perfect candidates for applications where strain-hardening is of crucial importance. On the other hand, there are polymers with the confined number of branching. These polymers are called long-chain branched [27].

There are two possibilities of branching in PLA: chemical (e.g., star-shaped, comb-like, and hyperbranched) and physical (co-crystallization of PLLA and PDLA). It is known that the mixing of PLLA and PDLA chains generates physical cross-linking points because of the formation of stereocomplexes [222]. Therefore, stereocomplex crystals that remain in PLA melt act as branching points, and free chain segments act as branches on the opposite chains [223].

The presence of branches in highly branched polymers prevents chain entanglements [54,127,192,224]. Typically, long-chain branching (LCB) is marked by the presence of branches that exceed the critical molar mass of entanglement and at least one interior section of entangled polymer bordered by two branching points (i.e., an entangled section with no free dangling ends) [225]. Long-chain branching (LCB) [54] means that the molecular chain between

Please cite this article in press as: Michalski A, et al. Star-shaped and branched polylactides: Synthesis, characterization, and properties. Prog Polym Sci (2018), https://doi.org/10.1016/j.progpolymsci.2018.10.004

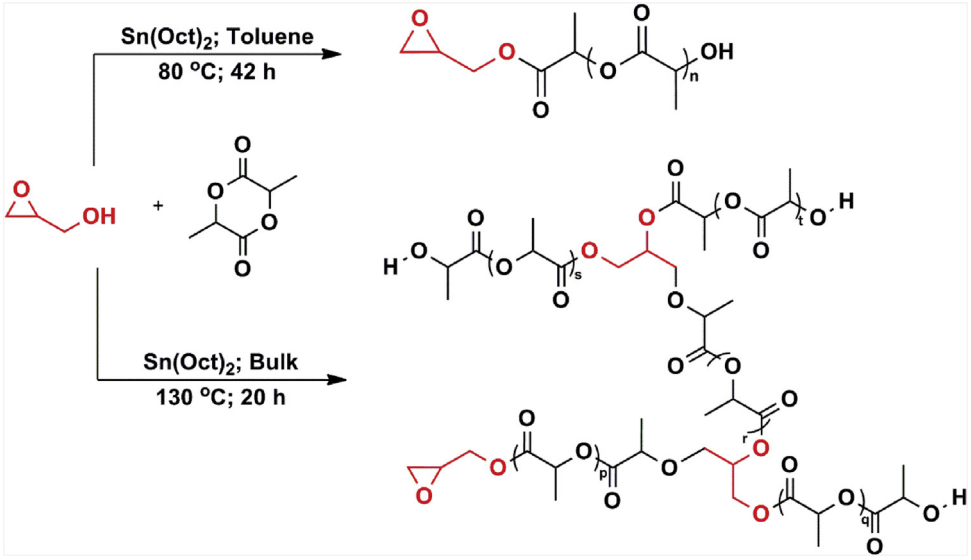

Fig. 16. ROP of lactide using glycidol as the branching monomer [219].

branch points is long enough to entangle with other chains, and thus, it results in high strength in the melt. To overcome the shortcoming of low melt strength, long-chain branches were introduced into a polyester backbone. Reactive extrusion and high-energy irradiation were usually used to get LCB for PLA [226]. Different multifunctional monomers such as epoxy [227,228] and anhydride [227] were used effectively to produce LCBs of PLA with high molar mass and high melt strength. It was difficult to get control of the molar mass and topological structure of the final products because of the randomness of branching [229]. Dorgan et al. [230] suggested that the critical length for PLA entanglement is approximately 9000 g/mol.

Branched structures with varying branching density influence the crystallinity degree and the biodegradability of PLA. The viscoelasticity of polymers is influenced by the presence of the long-chain branches and as a result decrease of their viscosity with simultaneous increase of elasticity is observed. In contrary, short-chain branches influence mainly the crystallinity of stars [231] and the lower amount of crystalline domains are formed with increasing degree of branching [35]. The introduction of branching to the PLA backbone was also proved to be one highly effective approach in tailoring the physical properties.

Several methods were used to obtain PLA with high molar mass and branching structures, namely, the ROP of lactide or polycondensation of lactic acid, with multifunctional co-monomers and catalysts in solution [17,24,193,216]. The effect of branching on PLA properties was investigated by comparing the crystallization and rheological behavior of branched PLAs to those of a linear commercial grade. DSC and optical microscopy observations revealed a remarkable improvement in PLA crystallization because of the nucleation role of branching points. Branched polymer structures improved significantly the crystallization and elongational rheology behavior [232].

7.1. Synthesis of branched PLA

7.1.1. Copolymerization

In copolymerization, the branching monomer possesses a dual role of an initiator and a monomer. Such monomer is called "inimer" and hydroxyl-substituted cyclic monomers can be used in this respect. In copolymerization, the hydroxyl group of the inimer initiated chain growth and as a result, macromolecules built from units of both monomers can be formed [35]. However, the most reactive monomer is three-membered cyclic ether – oxirane (e.g., glycidol [219,232]) and its use allow for the preparation of copolymers with the high degree of branching. In the polymerization of less reactive four-membered hydroxymethyloxetanes apart branched copolymers, linear oligomers were formed [35].

The polymerization in bulk, carried out at 130 °C, induces the simultaneous lactide and epoxide ring opening of both monomers and as a result, hyperbranched structures were formed, in which the PLA segments were separated by glycerol branching points. The molar masses of the obtained hyperbranched polymers were higher than the theoretical values (M_n from 19 800 to 100 800 g/mol), and it was related to the association of PLA linear segments. In bulk copolymerization of lactide with hydroxymethyloxetanes (3-hydroxymethyl-3-methyl-oxetane (HMMOX) and 3-ethyl-3-hydroxymethyl-oxetane (EHMOX)) catalyzed by diphenylphosphate, the lower molar masses were obtained ($M_n \leq$ 16 600 g/mol) [35].

In copolymerization where glycidol epoxide ring opening was prevented in low-temperature solution polymerizations (80 °C), an essentially linear PLA functionalized with an epoxide group was generated. In polymerizations performed in bulk at a high temperature (130 °C), a simultaneous ring opening of lactide and epoxide occurred, and as result, the branched structure was obtained (Fig. 16) [219,232].

In addition, branched PLLA was prepared through the copolymerization of L,L-LA with D,L-mevalonolactone (ML), as a bifunctional co-monomer containing both a six-membered lactone ring and pendant hydroxyl group [19]. In comparison to lactide, the lower reactivity of ML for ROP, could be a reason for the preparation of low molar mass polymers and the slow formation of branching [19,27]. Copolymerizations with a monomer ratio LA/ML = 10 were performed in the presence of two different catalysts: stannous octoate and 1-ethoxy-3-chlorotetrabutyldistannoxane (distannoxane). It was observed that in the presence of $Sn(Oct)_2$, branched polymer formation proceeded by a macromonomer formation step, accompanied by side reactions such as ester exchange and/or alcoholysis, while copolymerization catalyzed by distannoxane proceeded without side reactions [19].

(Hyper)branched PLLA copolymers were also prepared by the ring-opening multibranching copolymerization of L,L-lactide with a hydroxyl-functional lactone inimer, 5-hydroxymethyl-1,4-dioxane-2-on (5HDON). The copolymerization was performed in bulk at 130 °C or in methylene chloride using $Sn(Oct)_2$ and 1,5,7-

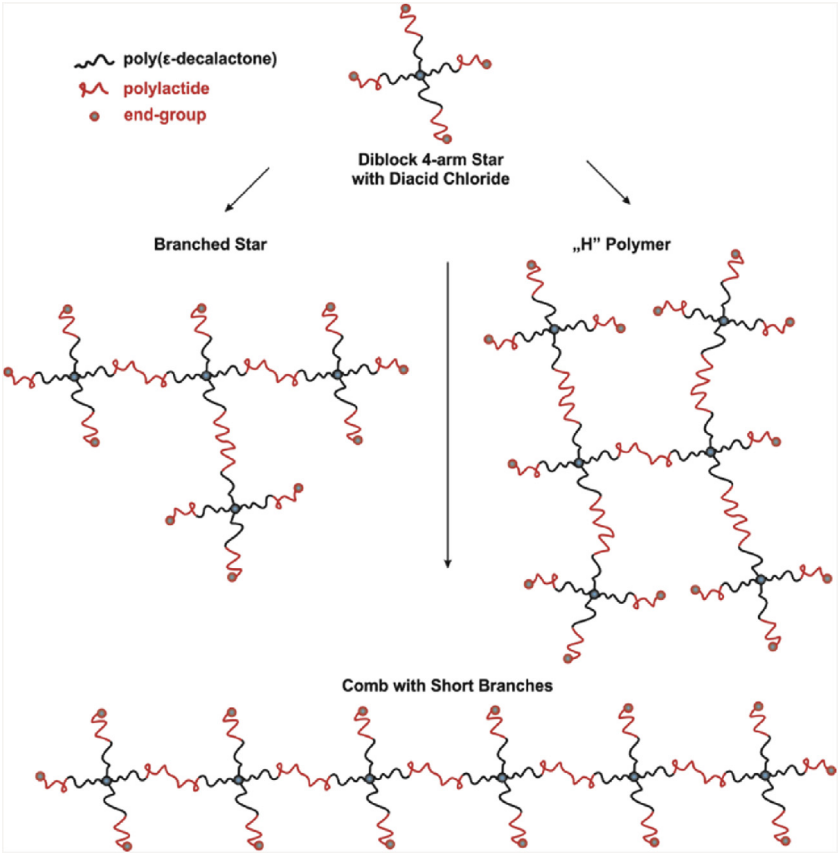

Fig. 17. Possible architectures those result from coupling the diblock star with functional end-groups: entangled branched star polymer, entangled "H" polymer, and comb polymer with short branches [225].

triazabicyclo[4.4.0]dec-5-ene (TBD) as catalysts, respectively [162]. It was observed that with a decrease of the inimer content in the reaction mixture the average chain length between two branching points increased and as a result LCB polymers were formed. The increased inimer content led to the decrease in T_g and T_m. The decrease in T_g, T_m and melting enthalpy (ΔH_m) proved that branching points were evenly distributed in the polymer [27]. A mechanism of branched polymer formation was also proposed [162].

Recently, it was reported that the cationic copolymerization of L,L-LA with glycidol and hydroxymethyl oxetanes led to branched polylactides [233]. Hyperbranched PLLA were also synthesized by enzymatic ring-opening polymerizations [234].

7.1.2. Addition of multifunctional reagents

The reaction of multifunctional reagents with star-shaped PLA usually leads to branched polymers. Thus, e.g., branched multiblock copolymers were prepared from diblock 4-arm star poly(ε-decalactone)-poly(D,L-lactide), as shown in Fig. 17 [225]. The coupling strategy utilized diacid chloride (e.g., sebacoyl chloride) and it was reacted with the hydroxyl end groups of the diblock star polymers.

The long-chain branching (LCB) of PLA was also achieved by using other reactive coupling molecules, namely, in the successive reactions of the hydroxyl end-groups of linear PLA with pyromellitic dianhydride (PMDA) and triglycidyl isocyanurate (TGIC) [227] or with PMDA and 1,4-phenylene-bis-oxazoline (PBOZ) [235]. Alternative methods were based on the melt radical reaction with pentaerythritol triacrylate (PETA) and bis(1-methyl-1-phenylethyl) peroxide (DCP) [236], or branching was attained in the reactive processing of PLA with pentaerythritol polyglycidyl ether (PGE) to enhance the molecular entanglement and melt strength of PLA [237].

7.1.3. Polycondensation

The hyperbranched PLAs were obtained in the polycondensation of different AB_2 macromonomers with lactide, mainly with 2,2-bis(hydroxymethyl)butyric acid (BHB) [24,216,238,239] or its derivatives [22] in the presence of a tertiary amine. Commercially available 2,2-bis(hydroxymethyl)propionic acid (bisMPA) was also copolymerized with LA [240]. As a condensation AB_2 monomer ("branching monomer"), 2,2-bis(hydroxymethyl)butyric acid (BHB) was more suitable than 2,2-bis(hydroxymethyl)propionic acid because of the lower polarity and better solubility of the former in molten lactide [24,238].

Branched PLA with 2,2-bis(hydroxymethyl)butyric acid (BHB) was obtained in a two-step synthesis [216,238,239]. In the first step, the AB_2 macromonomer was synthesized [240] and then self-condensed using standard coupling agents (*N*,*N*′-dicyclohexyl carbodiimide (DCC) and 4-dimethylaminopyridine (DMAP)) to form branched structures. The used mild conditions prevented etherification, as well as epimerization, which can occur under the acidic conditions applied for polycondensation. As a result, long-chain branched PLA with high molar mass and limited branching points was formed. This reaction pathway is, however, limited to AB_2 macromonomers with a molar mass below 4500 g/mol. The reactivity of the macromonomers decreases by decreasing the number of chain ends per unit volume [239]. The two-step approach of the synthesis comprises the coupling of these AB_2 macromonomers, and hence, allows precise control over the lactide chain length between the branching units in contrast to a random polycondensation (Fig. 18) [239].

Please cite this article in press as: Michalski A, et al. Star-shaped and branched polylactides: Synthesis, characterization, and properties. Prog Polym Sci (2018), https://doi.org/10.1016/j.progpolymsci.2018.10.004

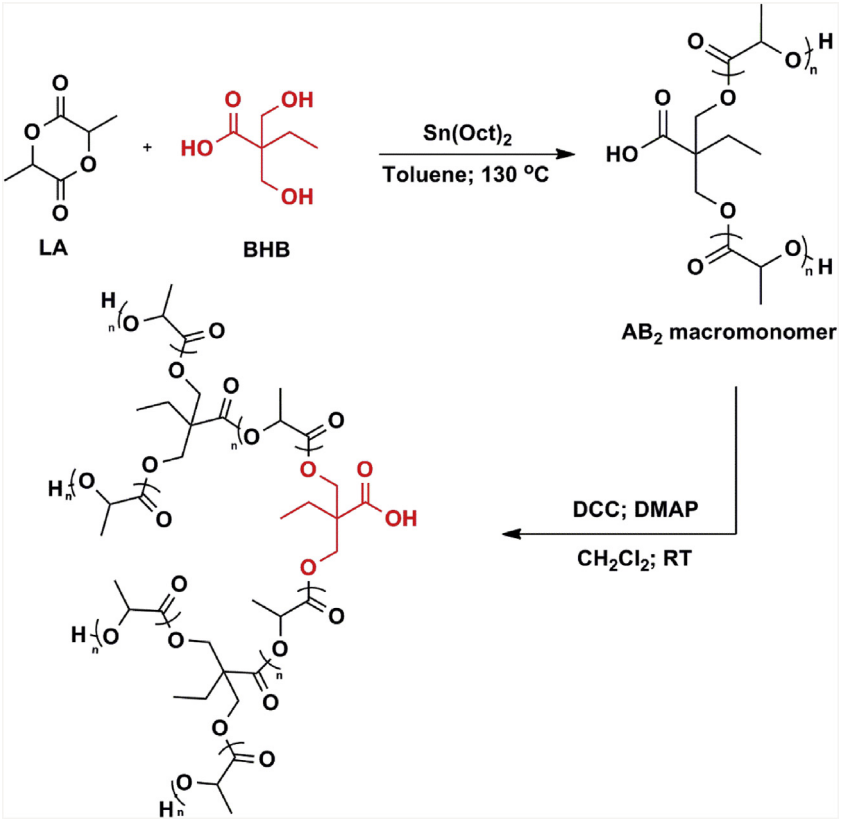

Fig. 18. Two-step synthesis of branched PLA: ROP of lactide using BHB and polyesterification of the formed AB_2 macromonomer [239].

Another approach towards branched PLA was the copolycondensation of L,L-lactide with glyceric acid, obtained from glycerol in a bioprocess using acetic acid bacteria [239].

A novel strategy for preparing biodegradable PLA materials that were based on introducing a long-chain branched block copolymer (LB-PCL-PLA) was reported recently [241], yielding materials with improved crystallinity, mechanical properties, and rheological behavior. The LB-PCL-PLA copolymer was synthesized in the reaction of single hydroxyl-terminated PLA (PLA-OH) with hydroxyl-terminated 3-arm star PCL (PCL-3OH) in the presence of hexamethylene diisocyanate (HMDI) [241].

In addition, a cholic acid (CA) can be copolymerized with lactic acid (CA/lactic acid $\leq$ 1/64), and both OH groups and COOH groups reacted, forming an asymmetrical star-shaped PDLLA with four arms. For different ratios of CA/lactic acid, various structures were obtained [242].

7.1.4. Chain extension

The addition of the chain extender to PLA caused the formation of branching that led to the reduction of thermal degradation, as well as the increase in molar mass and the onset decomposition temperature and, as a consequence, resulted in more thermally stable materials [243,244]. Usually, two multifunctional chain extenders, namely, styrene-acrylic-epoxy random oligomer (Joncryl® ADR-4368 F) [245–249] and epoxy-styrene-acrylic oligomer (CesaExtend OMAN698493), were applied [250]. It was reported that in this process a competition between polymer degradation, chain extension, and chain branching reactions occurred [227,251,252]. The reaction mechanism of the branching of PLA with polystyrene/poly(glycidyl methacrylate) random copolymer as a reactive chain extender (CE), the possible reaction between epoxy groups and carboxyl or hydroxyl end-groups of PLA chains, was discussed [253].

Branched PLA polymers were also synthesized from oligomers by the addition of highly reactive hexamethylene diisocyanate (HMDI) and 2,2′-bis(2-oxazoline) (BOX) as a chain extender. The addition of HMDI before BOX in the sequential linking produced more highly branched polymers than could be caused with the simultaneous addition. Branching and cross-linking reactions were identified as side reactions of the chain extending reactions [128].

Free radical branching in the presence of peroxides [226,254,255] or by beam irradiation [256–258] was employed to induce branching points and increase PLA molar mass. Polyisocyanates were commonly used for PLA chain extension [128,252,259] owing to the presence of terminal hydroxyl groups on the polymer chains; however, because of their toxicity, the trend is shifting towards the use of other small molecules such as tris(nonylphenyl) phosphite [230,260] and multifunctional epoxy-based chain extenders [244,249,250,261,262]. These modifications are limited as cross-linking and gelation may occur if the process is not carefully controlled.

7.1.5. Reactive extrusion

The branching was also introduced by reactive processing of the melt in the presence of some free-radical initiators or multifunctional chain extenders. This is a cheap and more convenient method because it can produce a large volume of polymers [226,227,236,263]. Typically, high-energy irradiation was applied for introducing branches, which induces free-radical reactions of a linear PLA precursor with a multifunctional monomer [257,258]. Reactive extrusion was adopted to prepare long-chain branched (LCB) structures in PLA through functional group or free-radical reactions. Different reagents, such as epoxy [248,250], anhydride [227], diisocyanate [229], and lauroyl peroxide [254] were used effectively to produce LCBs of PLA. It was also reported that the reactive extrusion of polylactide (PLA) with a free radical initiator

Please cite this article in press as: Michalski A, et al. Star-shaped and branched polylactides: Synthesis, characterization, and properties. Prog Polym Sci (2018), https://doi.org/10.1016/j.progpolymsci.2018.10.004

with a concentration ≤ 0.5% at 160–200 °C resulted in a branched polymer [226]. However, the formation of undesirable microgels was also observed during the reactive extrusion of PLA with certain peroxides or multifunctional branching agents [122].

To control this process, glycidol can be used as a chain extender for PLA in a reactive extrusion process [228], the chain extension was dominant because the chain branching process requires a higher activation energy and longer reaction time [235].

The structurally modified PDLLA was obtained through a one-step reactive extrusion–calendering process using a styrene-glycidyl acrylate copolymer as a reactive agent [251]. It was established that long-chain-branching topology was induced in the initially linear PDLLA matrix, and the melt strength, as well as melt relaxation, were increased through the creation of a higher entangled network density [262].

A reactive extrusion process based on *in situ* ultraviolet (UV) irradiation for the chain scission and branching reactions of molten polylactide (PLA) was also reported. Without the addition of trimethylolpropane triacrylate (TMPTA), random main chain scissions of PLA molecules occurred in this UV-induced reactive extrusion. With the presence of TMPTA, long-chain branched PLA was obtained, and the degree of branching in LCB PLA samples increased as the amount of TMPTA increased [264].

7.1.6. High-energy irradiation techniques

High-energy irradiation techniques can be an alternative method for inducing the radical reactions in polymers. Electron beams and γ-rays are two types of generally utilized high-energy radiation resources for polymer modification and introducing long-chain branches in PLA with a multifunctional monomer [256–258,265,266]. However, because of the limited end-group concentration and low activity of the end hydroxyl groups, hyperbranched structures are not easy to obtain for PLA through reactive processing [267].

High-melt-strength polylactides were prepared in γ-radiation-induced free-radical reactions, and this method introduced a long-chain branched structure onto a linear PLA precursor with the addition of trimethylolpropane triacrylate (TMPTA) [256,266]. The prepared long-chain branched PLA (LCB PLA) samples exhibited an increased molar mass and an elevated branching degree with increasing amounts of TMPTA incorporated during the irradiation process. The LCB PLA samples possessed unique bimodal architectures containing a linear chain fraction with low molar mass and an LCB fraction with high molar mass [265,266], and this resulted in the improved melt rheological properties and an enhancement of strain hardening under elongational flow [256,266]. It was reported that the degradation of the PLA chains occurred during irradiation by γ-rays without the addition of TMPTA [256].

A series of long-chain branched polylactic acid (PLA) samples were prepared by electron beam irradiation with or without the addition of TMPTA [258]. Samples obtained by electron beam irradiation showed only the monomodal macromolecular structure [258,266]. Electron beam radiation in the presence of glycidyl methacrylate (GMA) enhanced the melt strength of PLA. The modified PLA was prepared by varying both the amount of GMA and the irradiation dose. This modification remarkably improved their viscoelastic properties because of the formation of long-chain branching and retarding chain scission when GMA was introduced in this system. The increase in melt viscoelastic property was dependent on the irradiation dose. The gel fraction measurement revealed that chain scission and branching were more dominant than cross-linking. The biodegradability of irradiated PLA was slightly decreased by the presence of GMA [257].

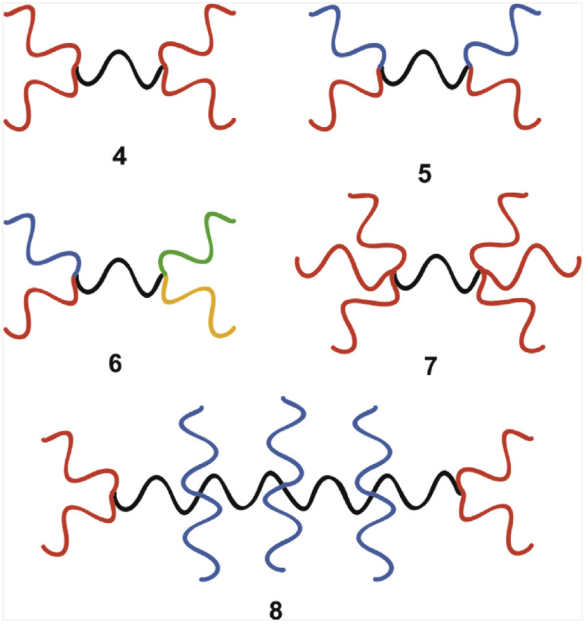

Fig. 19. Structures of H-shaped (**4**-**6**), dumbbell-shaped (**7**), and triblock molecular brush (**8**) polymers.

7.2. H-shaped and dumbbell-shaped PLA

H-shaped polymers are the block-copolymers in which two side-arms are attached to each end of a linear polymer chain (**4**-**6**). After introducing additional side-arms to a linear polymer chain, the resulted polymer has a dumbbell structure (**7**). The entanglements of the arms in H-shaped polymers are responsible for the unique structure and rheological properties [27,268]. The syntheses of H-shaped polymers were reported in many papers [74,269–274]. An example of their various structures are shown in Fig. 19: **4** (A = PS, B = PLLA) [269], (A = PEG, B = PLA) [74], (A = poly(cis-cyclooctene), B = PDLLA) [271], (A = PEG, B = PLGA) [272], **5** (A = PCL, B = PLLA, C = PDMAEMA) [270], (A = PEG, B = PLLA, C = PS) [273], **6** (A = PEG, B = PCL, C = PS, D = PLLA, E = PAA) [274].

Dumbbell-shaped block copolymers (**7**) with 8 arms (A = poly(cis-cyclooctene), B = PLLA) [271], (A = PEG, B = PDLLA) [74], (A = PEG, B = PLGA) [272], and 32 arms (A = PEG, B = PLLA) [51] were also obtained. Triblock dumbbell-shaped molecular brushes (**8**) with well-defined structures were synthesized via "grafting through" ROMP by sequential additions of poly(lactide) macromonomers bearing terminal norbornene groups [275].

8. Stereocomplexes of polylactides

Macromolecules composed of repeating units with complementary attracting sites can form intermolecular complexes [276]. Typical examples are provided by natural macromolecules, such as polysaccharides, polypeptides, or nucleic acids [277–280]. By taking a lesson from biology, polymer chemistry has developed methods of synthesis of macro- or supramolecular systems in which complementary, non-covalent interactions give rise to hierarchical assemblies, which often result in macromolecular materials with new, exceptional properties [281–288].

PLA possess an asymmetric carbon atom in each lactate repeating unit, and depending on the monomer used in polymerization: L,L-lactide, D,D-lactide, racemic [1:1 L,L/D,D-lactide] or meso L,D-lactide, semi-crystalline L-PLA and D-PLA or amorphous L,D-PLA polymers are obtained [1,13,289–291]. The intermolecular interactions of enantiomeric PLA chains of the opposite configuration

Please cite this article in press as: Michalski A, et al. Star-shaped and branched polylactides: Synthesis, characterization, and properties. Prog Polym Sci (2018), https://doi.org/10.1016/j.progpolymsci.2018.10.004

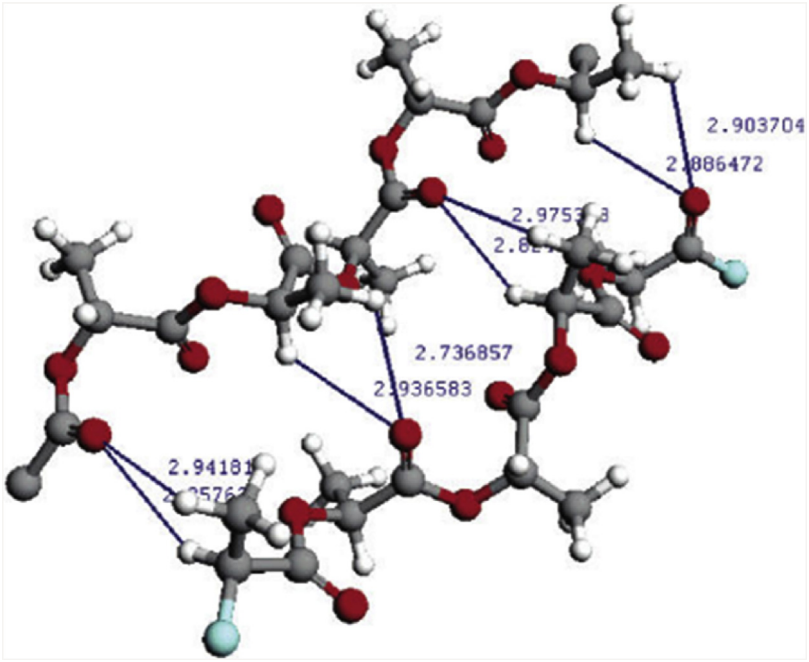

Fig. 20. Interaction of enantiomeric PLA chains leading to a stereocomplex [293], Copyright 2005. Reproduced with permission from ACS Publications.

[L-PLA and D-PLA] lead to the stereocomplex formation (sc-PLA). Initially, van der Waals bonds were proposed to be responsible for stereocomplex formation [292], but more recently a weak hydrogen bonding ($-CH_3\cdots O{=}C<$ and $\equiv CH\cdots O{=}C<$) between the L-PLA/D-PLA chains was found to keep two PLA helical chains with the opposite configuration together, as shown in Fig. 20 [293,294].

The first publication concerning stereocomplex formation between enantiomeric PLA, poly(L-lactide) [i.e., poly(L-lactic acid) (PLLA)] and poly(D-lactide) [i.e., poly(D-lactic acid) (PDLA)] was published in 1987 [222]; subsequently, numerous studies have been carried out with respect to the formation, structure, properties, degradation, and applications of the PLA stereocomplexes. It was observed that stereocomplexation enhances the mechanical properties, the thermal-resistance, and the hydrolysis-resistance of PLA-based materials. These improvements arise from a peculiarly strong interaction between L-lactyl unit sequences and D-lactyl unit sequences. In addition, stereocomplexation opens a new method for the preparation of physically cross-linked hydrogels and particles for drug delivery systems [295]. It was revealed that the crucial parameters affecting stereocomplexation were the mixing ratio and the molar masses of L-lactyl and D-lactyl unit sequences. The methods for tracing PLA stereocomplexation, the methods for inducing PLA stereocomplexation, the parameters affecting PLA stereocomplexation, and the structure, properties, degradation, and applications of a variety of stereocomplexed PLA materials were summarized in the excellent review by Tsuji [296].

We showed that equimolar mixtures of star-shaped PLA macromolecules with opposite chirality had the advantage of fast crystallization into the stereocomplex crystallites in comparison with their linear counterparts [297]. The mixture of star-shaped and linear enantiomeric PLAs also formed stereocomplexes under similar conditions. It was observed that both the low molar mass linear polymers, as well as multi-arm stars with relatively short arms, when cooled continuously from the melt or heated after rapid cooling from the melt, could more easily form the stereocomplex crystallites. In contrast, for longer linear PLAs and star-shaped PLAs with a lower number of arms (i.e., six arms), both homo- and stereocomplex crystallites were observed. These effects were explained by differences in the mobility of polymer chains in these systems as a result of cooperative interactions of the many helical arms in the PLA stars. The cooperative formation of many stereocomplex pairs in the frame of interacted enantiomeric star-shaped PLAs chains with an adequate number of arms could induce the enhancement in the thermal stability and reversibility of stereocomplex crystallites [297, 298].

Several asymmetric PLLA/PDLA blends based on linear PLLA and PDLA with different star PDLA structures (with 3, 4, and 6 arm) were prepared. The effects of PDLA on rheological behavior, crystallization behavior, nucleation efficiency and spherulite growth of PLLA were investigated [299].

It was also observed that the mixing of two enantiomeric 8-arm star-shaped copolymers with PEG-*b*-PLLA and PEG-*b*-PDLA arms led to a stereocomplex. The formed stereocomplex film exhibited a larger amount of protein adsorption than the enantiomeric films and has potential as a new class of implantable soft biomaterials. Furthermore, cell attachment efficiency and proliferation rate on the film was significantly enhanced by stereocomplexation. This stereocomplex material is expected to be applicable as a degradable temporary scaffold for tissue regeneration, and stereocomplexation was proposed as a novel method to control the protein- and cell-adhesive properties [300].

Recently, we synthesized star-shaped and linear PLAs by the controlled ring-opening polymerization (ROP) of L,L- and D,D-lactide using dipentaerythritol and 1-methyl-2-hydroxymethyl-3-butylimidazolium tetrafluoroborate as initiators. Subsequently, carboxylic end-groups were introduced into the macromolecules through the reaction of –OH end-groups with succinic anhydride. Afterwards, the un-modified and modified polylactides were used for the preparation of star-shaped and star-shaped/linear stereocomplexes in 1,4-dioxane and tetrahydrofuran (THF). In these two solvents, spontaneously precipitated stereocomplexes formed microspheres. Star-shaped stereocomplexes with hydroxyl end-groups formed in THF microspheres with diameters ranging from 1 to 4 μm, depending on the initial concentration of sc-PLA components. On the other hand, in 1,4-dioxane, the formation of uniform stereocomplex nanoparticles (~400 nm) was observed as a result of the combination of star-shaped PLA functionalized with carboxylic end-groups and linear PLA with substituted imidazolium

Please cite this article in press as: Michalski A, et al. Star-shaped and branched polylactides: Synthesis, characterization, and properties. Prog Polym Sci (2018), https://doi.org/10.1016/j.progpolymsci.2018.10.004

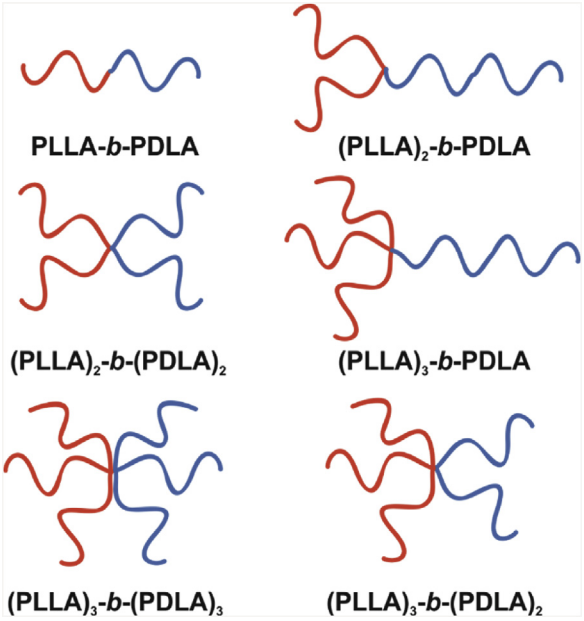

Fig. 21. Schematic illustration for the PLA stereomiktoarm star polymers [301].

end-groups. Microscopic analysis showed that nanometer-sized grains of stereocomplexes (~30 nm) aggregated to form larger stereocomplex nanoparticles. It was observed that the combination of three factors, i.e., the end-group interactions, the architecture of the enantiomeric components, and basicity of the solvent in which the stereocomplexes were prepared, influenced the properties and morphology of the final stereocomplex-based materials. It was assumed that such renewable and biocompatible PLA stereocomplex-based nanomaterials could be used as a drug delivery carrier or as a nanofiller because of the ease of the synthesis and the ability to control the size of the obtained nanoparticles by varying the concentration of the PLA components in selected solvents [121].

Frey et al. performed a systematic comparison among graft poly(L-lactide) copolymers with different topologies and studied their ability to form stereocomplexes with poly(D-lactide) (PDLA). The comb and hyperbranched copolymers based on functional poly(ethylene glycol) and poly(L-lactide) with molar masses in the range of 2000 to 90 000 g/mol and moderate molar mass distributions (M_w/M_n = 1.08–1.37) were prepared via the combination of anionic and ring-opening polymerization. Two "topological isomers," a linear poly(ethylene oxide)/polyglycerol (PEG/PG) copolymer and a branched PEG/PG copolymer, were used as backbone polymers. Furthermore, the stereocomplex formation between PDLA and the hyper-branched and comb copolymers containing poly(L-lactide) arms was studied. The stereocomplex formation was confirmed by DSC, as well as by Fourier transform IR (FTIR) and Raman spectroscopy [93].

Ouchi also prepared stereocomplexes using both branched enantiomeric polylactides (PLLA and PDLA) and compared their thermal and mechanical properties with those of linear PLLA and stereocomplexes prepared from branched and linear stereoisomers [231].

Satoh et al. reported the synthesis of stereo-miktoarm star PLAs consisting of both PLLA and PDLA arms in one molecule [301]. These polymers were prepared through ROP of D,D- or L,L-LA followed by click chemistry (Fig. 21). These 2–6 arm stereo-miktoarm star polymers ($(PLLA)_x$-*b*-$(PDLA)_y$; x and y = 1, 2, and 3) with the same molar masses (~ 10 000 g/mol) and with narrow dispersity ($Đ \approx$ 1.1) had an identical PLLA/PDLA block ratio of 1:1 [32].

The synthesis of the AB_2 and AB_3 miktoarm star polymers, composed of rigid poly(n-hexyl isocyanate) (PHIC) (A) and soft aliphatic polyester PLLA (B), was performed through the click reaction yielding di- or trihydroxy end-functionalized PHICs (PHIC-$(OH)_2$ and PHIC-$(OH)_3$) followed by the ROP of LA. The resulting PHIC-*b*-$(PLLA)_2$ and PHIC-*b*-$(PLLA)_3$ miktoarm star polymers formed micelles in DMF. The sizes of micelles prepared from those copolymers with the same compositions and molar mass decreased with increasing arm number of PLLA because of the excluded volume effect of the polyester domain [32].

Well-defined hydroxyl end-functionalized poly(*n*-hexyl isocyanate), PHIC-$(OH)_2$ and PHIC-$(OH)_3$, as rod-type macroinitiators were synthesized by the Cu-catalyzed azide–alkyne cycloaddition reactions of azido end-functionalized PHIC with ethynyl alcohol derivatives. The PHIC-$(OH)_2$ and PHIC-$(OH)_3$ were suitable macroinitiators for the ring-opening polymerization of L,L-LA which led to the synthesis of novel rod-coil type miktoarm star copolymers, PHIC-*b*-$(PLLA)_2$ and PHIC-*b*-$(PLLA)_3$, with controlled molar masses, narrow polydispersities, and controlled arm numbers. Additionally, the thermal and solution properties of the obtained miktoarm star copolymers along with the corresponding block copolymers, PHIC-*b*-PLLA, were characterized by TGA, DSC, and DLS analyses [151]. In the bulk, the formed stereocomplexes of PEG-*b*-PLLA-*b*-PDLA, miktoarm terpolymers self-assembled into micelles with enhanced stability in aqueos solutions [40].

In addition, the thermal and mechanical properties of cast films prepared from branched PLLA and stereocomplex films prepared from branched PLLA and PDLA were investigated. Moreover, the thermal and mechanical properties of 1:9 blend films prepared from the branched PLLA or PDLA with linear PLLA were investigated. The branched PLLA or PDLA acted as a good plasticizer of linear PLLA [231]. Subsequently, biodegradable branched PLLA was successfully synthesized by the bulk polymerization of LA using polyglycidol as a macroinitiator. The obtained branched PLLA film showed lower T_g, T_m, crystallinity, and higher strain at break in comparison with the linear PLLA film because of the introduced branched structure. The branched PLLA/branched PDLA stereocomplex film showed a high maximum stress and a high Young's modulus that allowed for the retention of its high strain at break. The mechanical properties of the linear PLLA/branched PLLA blend film and linear PLLA/branched PDLA stereocomplex film could easily be controlled by changing the molar mass of the branched PLA chains [231]. In addition, the stereocomplex formation between multi-armed PLLA and PDLA was also investigated [58, 297,298,302–305]. The branched structure of PLA promoted the effective physical cross-linking among crystalline domains. Thus, branched PLA can be expected to be applied as a novel biomedical material and a plasticizer of linear PLA [231]. However, branching significantly disturbed stereocomplex crystallization, which might be used for the alteration of the stereocomplexation level, and therefore, this can be a tool for the control over the release of active compounds [58].

Among the numerous reports on the synthesis of stereoblock PLLA-*b*-PDLA, little attention was paid to the properties of star shaped PLLA-*b*-PDLA copolymers and the differences between linear and multi-armed PLLA-*b*-PDLA copolymers are still unclear. Furthermore, in the blend of linear and 4-arm PLLA-*b*-PDLA/PLAs, the stereocomplexation will form between the PLLA block and PDLA block, and between the free PLA chain and enantiomeric PLA block [68,306,307].

Recently, the linear, 3-, 4-, and 6-arm star-shaped stereoblock PLA copolymers were synthesized via two-step ring-opening polymerization with 1-dodecanol, glycerol, pentaerythritol, and D-sorbitol as the initiators, respectively [306,308]. The stereoblock copolymers exhibit a faster crystallization rate than the racemic PLLA/PDLA blends. In addition, the formation of stereocomplexes

Please cite this article in press as: Michalski A, et al. Star-shaped and branched polylactides: Synthesis, characterization, and properties. Prog Polym Sci (2018), https://doi.org/10.1016/j.progpolymsci.2018.10.004

from high molar mass stereoblock copolymers was complete and reversible whereas for the racemic blends the homocrystallities were observed. Moreover, the branching effect was related to lower T_c, T_m, X_c, and long period (LP), which is ascribed to the crystalline and amorphous layer thickness, of star-shaped copolymers in comparison to linear counterparts. The mechanical properties were also affected by the branching number because the storage modulus of stereoblock copolymers decreases with increasing number of arms [308]. Tsuji and co-workers investigated the influence of linear PLAs on the crystallization of 4-arm star-shaped stereo diblock PLAs. The stereocomplex crystallinity was increased after the addition of linear counterparts; it depends on the molar mass of PLAs and was higher for low M_n PLAs [306].

9. Cross-linked PLA

9.1. Solvent-free systems

For the improvement of the poor processability of PLA, various methods were used to introduce a branched architecture into the PLA matrix, including chemical cross-linking [7,309,310], radiation-induced cross-linking, and peroxide-induced cross-linking [255]. Usually, low molar mass star-shaped PLAs with unsaturated end-groups (e.g., with acrylate and/or methacrylate end-groups [140,152–154, 311]) were used for the formation of a cross-linked structure. Biobased thermoset resins were synthesized from star PLA having glycerol [148,312,313], pentaerythritol [147,151,153], and xylitol [152] as cores. The resins were thermally cured employing a free-radical polymerization strategy [152,153]. The thermal curing was also performed with dibenzoyl peroxide as the initiator [312,313] and, *N*-dimethylaniline as the accelerator [312].

Star-shaped biodegradable polyesters and polymer networks produced from end-functionalized star polymers have been gathering increasing attention for use as biomaterials having functions, such as controlled release of drugs, stimuli-responsivity, and shape-memory, in addition to environmentally benign materials having tailor-made thermal, mechanical, and biodegradable properties [29,101,154,314–316].

The process of cross-linking was studied in several papers [154, 316]. The cross-linking density increased with the number of arms in the oligomers. The structures of the oligomers affected the cross-linking density; therefore, the properties of the cross-linked polymers. Oligomers with a higher number of arms and shorter lactide blocks exhibited greater cross-linking density and higher mechanical strength [154]. Cross-linked PLAs were obtained using different procedures, namely, from PLA macromonomers with furanyl groups and cross-linking with linkers having maleimidyl groups [156] and from star PLLA via the carbodiimide-mediated coupling [124] or after the addition of hexamethylene diisocyanate (HMDI) [61], 2,4-tolylene diisocyanate (TDI) [317], 4-(dimethylamino)pyridinium p-toluenesulfonate [124], triallyl isocyanurate (TAIC) [23], succinic anhydride [316] or using carbodiimide chemistry [316]. Star polymers with a pentaerythritol core and PLA arms having methacrylate and itaconic acid end-groups were cured by a free radical polymerization resulting in a thermoset resin [155]. The cross-linked structure was also obtained from ethynyl-functionalized 4-arm star PLA and a stoichiometric amount of the cross-linker pentaerythritol tetrakis(3-mercaptopropionate) under UV irradiation [135].

Photo-cross-linked elastomers were also obtained from 3-arm star poly(ε-caprolactone-*co*-D,L-lactide) triacrylates [148,149,318] and 4-arm star PCL-*b*-PLLA [151] or 4-arm star-poly(ε-caprolactone-*co*-L,L-lactide) triacrylates [148,149,151]. Bioabsorbable networks with a broad range of thermal, mechanical, and degradative properties were obtained by free-radically cross-linking a series of 3-arm, methacrylate-end capped poly(D,L-lactide-*co*-trimethylene carbonate) prepolymers [319].

Triallyl isocyanurate [23] and triallyl trimesate (TAM) [320] were also used as cross-linking agents for PLLA under γ irradiation. TAIC induced PLLA cross-linking at low concentration (1.0 wt.%) and low γ-ray dose (25 kGy). The gel fraction of the cross-linked PLLA increased with both TAIC concentration and γ-ray dose, whereas the degree of swelling was affected mainly by the concentration of TAIC. Cross-linking lowered the melting point and decreased the crystallinity of PLLA. Dynamic mechanical analysis showed that complete cross-linking eliminated crystallization and melting point [23].

Polyesterurethane/poly(ethylene glycol) dimethacrylate (PEGDMA) interpenetrating polymer networks (IPNs) with good shape-memory properties were synthesized using a solvent casting method. Four-arm star-shaped oligo[(rac-lactide)-*co*-glycolide] was coupled with isophorone diisocyanate to form a polyesterurethane network (PULG), and PEGDMA was photopolymerized to form another polyetheracrylate network. The IPNs were transparent with a gel content exceeding 92%. The values of strain fixity rate and strain recovery rate were above 93%. PULG and PEGDMA networks in IPNs were amorphous and did not show any characteristic diffraction peaks in X-ray diffraction pattern [321].

Other biodegradable elastomers based on the polymer network formed by the ROP of bis(ε-caprolactone-4-yl)propane and a hydroxy-terminated 3-arm star-shaped block copolymer of D,L-lactide and ε-caprolactone were reported [72,315].

Recently, the synthesis of co-networks built from 4-arm star-shaped ε-caprolactone and L,L-lactide oligomers with a degree of polymerization per arm (n = 5, 10 or 15) were reported. These stars with furan and maleimide end-groups underwent the Diels-Alder reaction and produced co-networks in which the two star-shaped oligomer units were alternatingly arranged (Fig. 22) [322].

9.2. Hydrogels

Hydrogels are highly attractive materials for use in biomedical applications, such as tissue engineering and drug delivery. Hydrogels are formed by chemical cross-linking or stereocomplex cross-linking. Recently, there appeared a review focused on the synthesis, characterization, and applications of PLA hydrogels [323]. Chemical cross-linking, in general, provides mechanically stable gels, however, it should be taken into account that there is a health risk associated with the utility of reactive macromonomers and cross-link agents. In the development of physically cross-linked hydrogels, stereocomplexation between enantiomeric PDLA and PLLA blocks in amphiphilic copolymers was reported to be a powerful tool to provide *in situ* forming gels [324].

Hydrogel medicinal implants based on PLA and its copolymers were used as drug delivery vehicles, scaffolds for tissue engineering, and tissue augmentation; for instance, copolymers of lactic and glycolic acids with PEG formed thermo-responsive hydrogels. Physical cross-linking mechanisms of PEG–PLA or PLA-polysaccharides include lactic acid segment hydrophobic interactions, stereocomplexation of D- and L-lactic acid segments, ionic interactions, and chemical bond formation by radical- or photo-cross-linking [323].

Hydrogels formed from PLA star polymers based upon 3-, 4-, and 8-arm star PEG backbones were studied for their potential biomedical applications [56,103,112,113,325–327]. Improved hydrogel properties were achieved through the aqueous mixing of equimolar solutions of star PEG–PDLA and PEG–PLLA polymers to create stereocomplex interactions between stars [112,113] and through the threading of cyclodextrins onto biodegradable polymers [29,325].

Please cite this article in press as: Michalski A, et al. Star-shaped and branched polylactides: Synthesis, characterization, and properties. Prog Polym Sci (2018), https://doi.org/10.1016/j.progpolymsci.2018.10.004

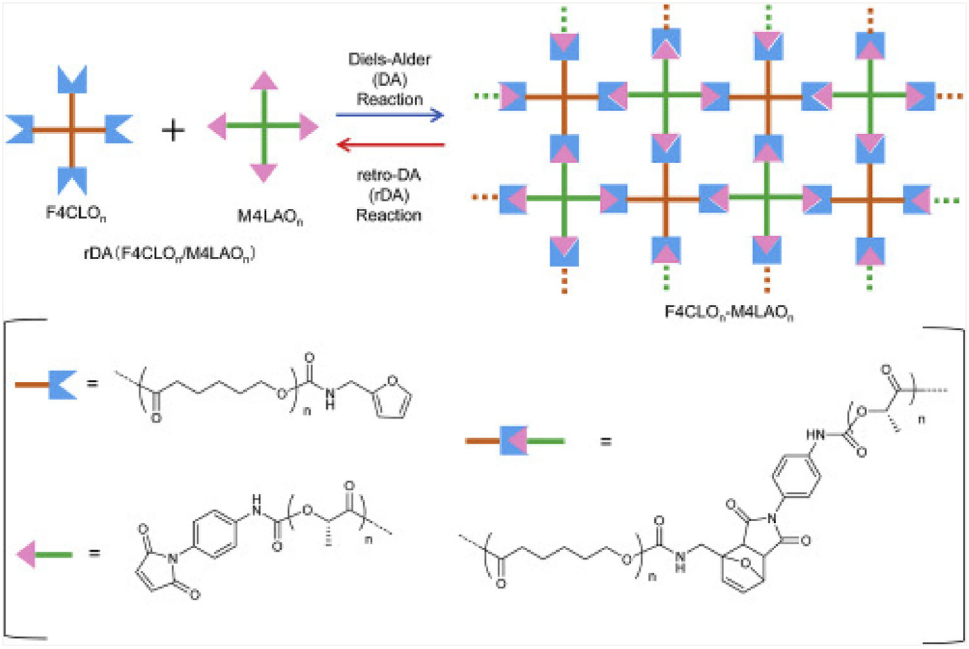

Fig. 22. Diels-Alder (DA) and retroDA (rDA) reactions of ε-caprolactone (F4CLO$_n$) and L,L-lactide (M4LAO$_n$) star oligomers [322], Copyright 2017. Reproduced with permission from Elsevier Ltd.

Stereocomplex-mediated hydrogels were obtained from the opposite chirality of 8-arm star block PEG-*b*-PLLA copolymers (PEG-*b*-(PLLA)$_8$). Rheology measurements confirmed the gel formation upon mixing of polymer solutions of opposite chirality and showed improved mechanical properties for PEG-*b*-(PLA)$_8$ hydrogels compared with the linear PLA-*b*-PEG-*b*-PLA hydrogels, which was attributed to the higher number of stereocomplexation sites of the PEG-*b*-(PLA)$_8$ star block copolymer [328]. Recently, a more detailed analysis of the physical, mechanical, and degradation properties of stereocomplexed PEG-*b*-(PLA)$_8$ hydrogels, and the mechanism of the temperature-dependent formation of stereocomplexes as studied by NMR and rheology were reported. The gelation mechanism was presented at a macromolecular level for star-shaped PEG-*b*-PLA diblock copolymers that formed a hydrogel by stereocomplexation [324]. Upon mixing PEG-*b*-(PDLA)$_8$ and PEG-*b*-(PLLA)$_8$ solutions, inter-aggregate bridging of dangling PLA chains by the formation of stereocomplexes led to spontaneous gelation. Upon heating, the rearrangement of macromolecules led to an increase in the extent of stereocomplexation. It was reported that the stereocomplexes in the mixed enantiomer PEG-*b*-(PLA)$_8$ hydrogels were rigid and highly stable up to 70 °C. That finding denotes the presence of a temperature irreversible gel system. Compared with single enantiomer hydrogels of similar concentration, stereocomplexed PEG-*b*-(PLA)$_8$ hydrogels exhibited enhanced mechanical properties and stability at 37 °C in phosphate buffered saline (PBS) [324]. Typically, 8-arm star block PEG-*b*-PLLA copolymers (PEG-*b*-(PLLA)$_8$) formed micelles in aqueous solutions and aggregates at low concentrations. The properties of two types of these star block PEG-*b*-PLLA copolymers with linking ester and amide groups (-NHCO-) between the PEG and the PLA blocks were investigated. The stable amide linking unit in the PEG-(NHCO)-(PLLA)$_8$ hydrogels slowly degraded; therefore, those hydrogels are of interest as materials for biomedical applications, such as controlled drug delivery systems and matrices for tissue engineering [326].

Eight-arm star block PEG-*b*-(PLLA)$_8$ copolymers, functionalized with pyridine, formed star block PEG-*b*-PLLA-py metallo-hydrogels in the presence of transition metal ions (Cu^{2+}, Co^{2+} or Mn^{2+}). These PEG-*b*-PLLA block copolymer hydrogels combined the excellent biocompatibility and biodegradability and could be used in a wide range of industrial and biomedical applications [329]. Chemically cross-linked PEG-*b*-PLLA hydrogels were prepared by a Michael-type addition reaction between 8-arm thiol-terminated star PEG (PEG-(SH)$_8$) and acrylated PEG-*b*-PLLA star block copolymers (PEG-*b*-(PLLA$_{12}$)$_8$-AC). These hydrogels possessed excellent mechanical properties. The degradation time of the formed hydrogels ranged from a few days to several months depending on the incorporated amount of PEG-(SH)$_8$. Lysozyme was released from the highly cross-linked PEG-*b*-(PLLA$_{12}$)$_8$-AC/PEG-(SH)$_8$ hydrogels mainly by diffusion [144]. In addition, it was reported that miktoarm star polymers PLLA/PEG formed thermo-responsive hydrogels in water at high concentrations (>22.5 wt.%) [330].

The stereocomplexation, i.e., co-crystallization, of PLLA and PDLA blocks was also exploited to introduce stable cross-links, and thereby, improve the mechanical properties of hydrogels formed by PEG-*b*-PLA star block copolymers [112,300,326,328,331]. Furthermore, it was shown that enantiomeric PEG-PLA star block copolymers with a central PEG core and outer PLA blocks gelated faster and formed stereocomplexed hydrogels with improved mechanical strength, compared with triblock PLA-*b*-PEG-*b*-PLA copolymers [112,328,332].

Star block copolymers PEG–*b*-(PLA)$_8$ and triblock copolymers of PLA-*b*-PEG-*b*-PLA were also demonstrated to form hydrogels through stereocomplexation [328]. The 8-arm star triblock copolymers of PEG–*b*-PLLA–*b*-PEG formed an irreversible hydrogel that had a very high storage modulus of 9.8 kPa at body temperature. The formation of stereocomplexes using star-shaped, hyper-branched or mixed star-shaped/linear PLA enantiomers seems to be an important way to enhance their physicochemical properties, allowing them to be used in biomedicine as drug delivery systems or materials for tissue regeneration [323,331]. Stereocomplexes of 8-arm PEG-*b*-PLA star block copolymers linked by an amide group between the PEG core and the PLA arms were recently prepared, and their aggregation behavior in water was characterized [326]. These materials were found to form gels at significantly lower polymer concentrations in comparison with the corresponding copolymers containing PLA single enantiomers, displaying higher storage moduli and stability to degradation *in vitro* [332].

Please cite this article in press as: Michalski A, et al. Star-shaped and branched polylactides: Synthesis, characterization, and properties. Prog Polym Sci (2018), https://doi.org/10.1016/j.progpolymsci.2018.10.004

10. Properties

Poly(L-lactide) is an important biodegradable thermoplastic polyester, which has potential applications in wound closure, surgical implants, scaffolds and delivery of drugs because of its biodegradability, biocompatibility and good mechanical properties. However, PLLA possesses some inherent drawbacks such as high crystallinity and low rate of degradation, which greatly limit its application in drug release systems. Therefore, modifications are necessary before successfully using this polymer [187].

A recently published review paper presented the current state and recent advances in the synthesis, characterization, properties, and applications of the star-shaped resins made from lactic acid or lactide and multi-hydroxyl core molecules. In these papers, the discussion of the role of the polymer architecture on the properties of resins was performed. Especially, rheological, physiochemical and thermomechanical properties of synthesized star-shaped resins were compared and discussed [7].

Interest in synthesis, characterization, and properties of the star-shaped PLA [8,18,30,37,82,85,197,214,215,333,334] is related, among others, to the ability of homo- and copolymers of LAs to hydrolytical and biological degradation, accompanied by useful thermomechanical properties [134]. The properties of PLA polymers and their correlation to the structure was also discussed [335].

Long-chain branching (LCB) has a significant effect on the physical properties of polymers, and even a small amount of LCB leads to great alteration on melt and solution rheological, thermal and mechanical properties [21,54,227,235,336], as well as the biodegradability of polymers [337]. The introduction of long-chain branches into PLA molecules, even in a small amount, has a significant effect on the rheological, thermal, and mechanical properties [54,223]. Branched polymers can be processed at lower temperatures than their linear counterparts, which could be advantageous, especially in the processing of thermo-labile polymers, such as PLAs [99]. Nouri et al. reported that the presence of branched PLLA increased the shear thinning, shear and extensional viscosity, and elastic modulus of linear PLLA [223]. Therefore, polylactide with different branched structures is an important modifier to improve PLLA performance [226,249,259,299,338]. Ouchi et al. demonstrated that the incorporation of polyol carbohydrates, such as glucose and dextran, could influence the surface active properties of the resulting star-shaped PLLA [146,339]. Star-shaped PLLAs would be interesting polymers as the physical properties and degradation rates should be different from those of linear PLLAs [340].

In star/branched PLAs the presence of many arms/branches with various end-groups influences the physical properties of polymers. The typical functional groups in star/branched PLAs are hydroxyl end-groups. The presence of a large number of hydroxyl chain ends enhances the polymer solubility and simultaneously improve the processing properties of the PLAs. These features are of crucial importance for their potential application in biomedical devices [35,341]. The investigation of the relation between the chain structure and critical properties, particularly crystallization and extensional rheology of high molar mass branched PLAs prepared by multifunctional initiators or initiator–comonomer molecules was reported [232].

The star-shaped PLLA, which differs from its linear counterparts of identical molar mass, exhibited significantly better properties for use as biomedical materials [29,341], such as smaller hydrodynamic radius, lower viscosity, and peculiar morphologies and thermal properties. The star-shaped PLLA degraded in a short time compared with the corresponding homopolymers. The influence of the core structure, the number of arms, arm length, and their rigidity on polymer properties was studied [29,342].

Star-shaped copolymers based on PLAs showed very interesting properties. These materials of high molar mass and relatively short PLA chains had higher hydrophilicity and faster degradation rates in comparison with linear PLA of similar molar mass [66,94,132,315]. Branching improved the toughness and processability of PLA, and the presence of PEG block introduced amphiphilicity into star copolymers. The branched polylactide copolyesters were prepared, and it was reported that solubility and solution viscosity depended strongly on the degree of branching [24,89,231]. It was observed that in dilute solutions, the linear PLLA exhibited higher intrinsic viscosity than the star-shaped one; however, in the concentrated solutions, the star-shaped PLLA gave higher values of dynamic viscosity, storage, and loss moduli than the linear one [8].

Branched and star-shaped macromolecules have also a different entanglement level and possess a higher density of chain-ends than linear chains of comparable molar mass. This affected mechanical properties, degradation behavior and physical ageing [99,230,256]. For polymers made from a 98:2 ratio of the L- to D- enantiomeric monomers, it was found that the entanglement molar mass was approximately 9000 g/mol ($Me \approx 8700$ g/mol), while the molar mass for branch entanglement was inferred to be nearly 35 000 g/mol ($Mb \approx 34\,600$ g/mol). Therefore, the ratio of the molar mass for branch entanglement to the entanglement molar mass was roughly four ($Mb \approx 4\,Me$). These results suggest that PLA may be a semi-stiff polymer that is characterized by relatively open chain conformations in the melt state [220]. It was also reported that the critical molar mass for entanglement (Mc) was close to 9000 g/mol (that corresponding to 383 backbone bonds), and the molar mass between entanglements (Me) was near 4000 g/mol (that corresponding to 165 backbone bonds) [230].

10.1. Thermal properties

Linear PLLA has a melting point of 170–183 °C, a glass-transition temperature of 55–65 °C [3,31,343–345] and a degree of crystallization approximately 70% [346]. PLLA has a narrow window of processing (12 °C) [14], whereas a 90/10 L- to D-copolymer has a much wider range of processing (40 °C) because of its lower melting temperature [3]. Polylactides were found to be highly sensitive to heat, especially at temperatures higher than 190 °C [347].

Multi-arm PLLA has a lower glass transition temperature (T_g), melting temperature (T_m), crystallization temperature (T_c), and decomposition temperature (T_d), as well as low crystallinity (X_c), compared with those of linear PLLA [8,29,35,81,197,198,200]. It was determined that the crystallization of PLLA was effectively suppressed by the formation of a star topology [187]. In addition, in the dilute solutions, the star-shaped PLLA exhibited lower intrinsic viscosity than a linear one. However, in the concentrated solutions, the star-shaped PLLA have the higher dynamic viscosity, storage, and loss moduli than the linear one and shows the greater dependence of rheological properties on temperature [8]. The relationship between viscosity and temperature was caused by the presence of arms entanglements that suppress chains longitudinal movement [27]. T_g, T_m, transition crystallization temperatures of crystalline forms, and crystal growth mechanism were not affected by the presence of branching, however, they were dependent on the M_n or M_n per arm [59,193,198,263]. The glass transition temperature and the melting temperature of the star-shaped polymers increased with increasing arm length [92] and as well with the total molar mass [140].

The most of the investigations focus on the overlapping effects derived from branched structures and some other effects (e.g., end-groups) on PLA properties. The effects of branching architecture on crystallization and thermal properties were studied using linear 2-arm and 4-arm star poly(L-lactide). Suitable polylactides were obtained using bifunctional (1,3-propanediol) and tetrafunctional

Please cite this article in press as: Michalski A, et al. Star-shaped and branched polylactides: Synthesis, characterization, and properties. Prog Polym Sci (2018), https://doi.org/10.1016/j.progpolymsci.2018.10.004

(pentaerythritol) initiator, respectively with a wide range of molar mass (M_n = 5000-60 000 g/mol). It was observed that the 4-arm star architecture delayed or disturbed non-isothermal crystallization and isothermal crystallization, compared to the 2-arm linear architecture. However, the glass transition temperature, segmental mobility, melting temperature, and other crystal features were not affected by the presence of branching. It is worth noting that these properties depended on M_n or M_n per one arm [59].

For star polymers with a cross-linked large core and a high number of arms, the core influenced the thermal properties more considerably by inducing a nonuniform distribution of segmental mobility and conformation of the arms from the core to the arm chain ends, e.g., higher chain density and more stretched chains near the core [29].

It was reported that for linear and star PLLA polymers containing 16 – 21 arms with similar molar masses (M_n = 71 000 – 72 000 g/mol) but with different degrees of crystalline perfection, the two melting peaks for the star polymer was observed, in comparison to the linear polymer in which one melting was detected [197]. The degree of crystallinity (X_c) of the star polymer (0.25) was lower than that of the linear polymer (0.41) because of the more compact structure of star polymer that disturb in the alignments of the polymer chains in the crystallization process. The decomposition temperature (T_d) for the star (287 °C) was also lower than that for the linear polymer (307 °C) [32]. The thermal properties of the multi-arm star copolymers were characterized by DSC [35,219].

It was also observed that stereocomplex film formed from two enantiomeric 8-arm star-shaped copolymers with PEG-*b*-PLLA and PEG-*b*-PDLA arms exhibited higher T_g and higher PLA crystallinity than the original enantiomeric films [266].

Double melting and crystallization peaks were observed for the miktoarm stars containing PLLA and PEG arms and an oligomeric silsesquioxane (POSS) core [348]. These separate transition curves correspond to PLLA and PEG arms that differ from their linear polymers. T_m, T_c, and X_c of the PLLA and PEG arms of the miktoarm stars are lower than those reported for the corresponding homoarm stars because of imperfections in the crystallization domains formed as a result of the presence of two different arms in the same miktoarm star [32].

A decrease of crystallinity and increase of degradation rate for star-shaped PLLA with a xylitol core was observed with the increase of the xylitol molar fraction. These polymers were amorphous when the molar fraction of xylitol was higher than 6%, or semicrystalline when the molar ratio of xylitol fell below 6% [349]. The thermal stability of star-shaped polyesters significantly decreased with the degradation of the polyester polyol obtained in an acid solution [71]. Star-shaped PLLAs exhibited a faster hydrolysis rate compared with linear polylactide because of lower crystallinity and increased number of arms [79].

It was observed that the melting temperatures (T_m) of the branched PLLA/branched PDLA stereocomplexes were in the range of 210–220 °C. For the polymers with higher molar masses (M_n ≥ 140 000 g/mol) two melting temperatures were observed. It was related to the presence of homo- and stereo-crystallities in the mixture of branched PLLA/PDLA. In addition, there was a marked difference in the melting temperatures of stereocomplexed branched and linear polylactides with similar molar masses. The lower melting temperature of stereocomplexes composed of branched polylactides was related to the size of stereocomplex crystallites and lower values with the decreasing PLA branch length was observed [35,58,231]. In addition, the T_g and T_m values of the branched PLLA increased with its increasing molar mass.

It was reported that films of linear stereoblock PLA and stereomiktoarm stars formed stereocomplex crystals with T_m greater than the films prepared from the linear and star homopolymer PLAs. The decrease in the T_m and crystallinity of the stereocomplex crystal with the increase in the arm number of the star was observed. It was caused by the higher crystalline imperfections due to the increase in the number of chains ends and branching points in the polymers [38].

Subsequently, stereocomplex formation between PLLA and PDLA in the melt state was investigated and altered via the addition of multi-branched PDLA additives. Two different 3- and 4-arm star-shaped PDLA additives were synthesized as potential heat resistance modifiers and incorporated into PLLA at 5, 10, and 20 (w/w) through melt blending. The mechanical and thermomechanical properties of these blends were compared with those of linear PLLA, as well as with blends formed by the addition of two linear PDLA analogs that had similar molar masses to their star counterparts. Blends with linear PDLA additives exhibited two distinct melting peaks at 170–180 °C and 200–250 °C that implied that two distinct crystalline domains were present, one of the homopolymer and the other of the stereocomplex, the more stable crystalline structure, formed by the co-crystallization of both poly(L-lactide) and poly(D-lactide) enantiomers. In contrast, for blends of PLLA with multi-branched PDLA a single broad melting peak was observed by X-ray diffraction (XRD) data indicating that stereocomplex crystallites were exclusively formed [350].

10.2. Crystallization

A long-chain branching (LCB) structure was found to affect the crystallization of PLA products [236,320]. The multi-branched short chain PLLA is an effective nucleating agent that is not only responsible for the acceleration of PLA crystallization in multi-directions but also for good miscibility with PLA [255,351]. The crystallization kinetics for linear PLA and LCB PLA samples were extensively investigated using polarized optical microscopy and DSC. The introduction of long-chain branched structures into PLA improved the melt viscosity of PLA and reduced the diffusion rate of PLA chain segments during the transformation of the PLA melt into crystals. Therefore, the spherulitic growth rate decreased on increasing the long-chain branching degree for LCB PLA samples. Thus, the overall crystallization rates of the LCB PLA samples are faster than that of linear PLA [338,352]. Recently, a broad review was published on PLA crystallization [353].

The initial degree of crystallinity (X_c), that is, the crystallinity of samples before reheating, was calculated by using Eq. (1):

$$X_C = \frac{\Delta H_m - \Delta H_{cc}}{93.6} \times 100\% \quad (1)$$

where ΔH_m is the melting enthalpy, ΔH_{cc} the cold crystallization enthalpy, and 93.6 the melting enthalpy in J/g of 100% crystalline PLA [338,354].

In star PLLAs, the presence of arms reduces the crystallinity of polymers [85,102,193,194,198]. The star-shaped structures possessed different arms, implying their distinct nucleation mechanisms, and the more arms of a star-shaped PLLA led to a lower spherulite growth rate and decreased crystallizability [59,64,69,90,200]. It was reported that the T_g depended on M_n, whereas the T_m or crystalline thickness, and T_c of the star depended on the M_n of the arm not on the overall M_n and were similar to those of linear polymers [59]. The star-shaped PLLA contained more crystalline imperfections because of the increased number of end-groups and branching points. These facts led to lower crystallinity, which, in turn, lowered the melting temperature of the star PLLA. On the cooling scan, the star-shaped PLLA exhibited the crystallization peak at a lower temperature on account of the aforementioned reasons [8]. At rest, the polymer chains would have a coiled structure to maximize entropy. The steric hindrance resulting from a coiled conformation has a dominant effect on the static state. As a result, the star-shaped PLLA exhibited a lower rate of crystal-

Please cite this article in press as: Michalski A, et al. Star-shaped and branched polylactides: Synthesis, characterization, and properties. Prog Polym Sci (2018), https://doi.org/10.1016/j.progpolymsci.2018.10.004

lization than the linear one in the case of quiescent crystallization, as previously discussed. Shearing leads to uncoiling and stretching of molecules, and therefore, the branching points causing steric hindrance would have a less serious effect on crystallization. In consequence, chain mobility would have a dominant effect over the steric effect in dynamic crystallization. Thus, the star-shaped PLLA gave a higher rate of crystallization than the linear one under shear [8]. The physical properties of the star and linear PLLA having wide ranges of molar masses were studied by the use of DSC, TG, and polarimetry [200]. The star-shaped PLLA polymers with more arms are expected to have faster degradation and drug release rates [90].

The crystallization of linear (2-arm) PLLA and 4-arm star PLLA was analyzed and the following phenomena were observed. Both non-isothermal and isothermal crystallization of star is disturbed, compared to the linear architecture. This leads to the higher T_{cc}, lower X_c, and radius growth rate of the spherulites (G) values for 4-arm star than to those for linear 2-arm PLLA. The presence of branching architecture in macromolecules was not influenced on the T_g and segmental mobility, T_m and crystalline thickness, and T_c. The T_m or crystalline thickness, and $T_c(\alpha)$ of star depended on M_n(arm), not on M_n, and the values were similar to those of linear, when plotted as a function of M_n(arm). Regime analysis exhibited that crystal growth mechanism depends on T_c, crystalline form, the molar mass and presence or absence of branching [58,81,303].

With the increase of the number of arms in PLLA-*b*-PDLA stars not only the melting temperature and the degree of crystallinity decrease but also the change of parameters related to the crystalline structure, such as spherulitic growth rate, crystallites size, long period, and crystalline layer thickness of PLLA-*b*-PDLA chains was observed [308]. In addition, the lower T_m of stereocomplexes of branched PLAs than those measured for the stereocomplexes prepared from linear PLAs with similar molar mass was ascribed to the decrease in the average size of the stereocomplex crystallites with the decreasing PLA branch length [231].

In contrast, the thermal properties and crystallinity (T_c, T_m, and X_c) of star-shaped PCL-*co*-PLA block copolymers were independent of the number of arms of the polymer [355]. Crystallization kinetics and the spherulitic morphology of these star block copolymers were also studied [55,340,356]. It was also stated that in 4- and 6-arm star PLLA-*b*-PEG block copolymers, the T_m, T_c, and X_c of the PLLA block within these PLLA-*b*-PEG copolymers decreased with an increasing branch arm number, whereas X_c of the PEG block within the copolymer inversely increased. Additionally, both the PLLA and PEG blocks within the block copolymer mutually influenced each other, and the crystallization of both the PLLA and PEG blocks within the PLLA-*b*-PEG copolymer could be adjusted through both the branch arm number and the arm length of each block [80].

The influence of branching in PLLA polymers on crystallization properties was studied in several papers [64,81,200,220,357,358]. Long-chain branched (LCB) PLA showed a higher crystallization rate than linear PLA during isothermal crystallization. Less perfect crystals were formed for the LCB PLA samples, that was responsible for their lower melting temperatures and crystallinities [263]. The crystallinity of branched PLA was lower than its linear counterpart, and the crystallinity of branched PLA could be controlled by tailoring the branched chain lengths [231]. It was reported that the addition of a chain extender improved the crystallization kinetics of PLA samples [250,352].

The melt elasticity of PLA was also improved by converting it into an ionomer. Ionomers are polymers containing small amounts (up to 15 mol%) of ionic groups, which associate to form nanometer-sized clusters because of the micro-phase separation from the dielectric medium of the polymer. The degree of crystallinity of the star telechelic PLLA ionomers was found to be lower than that of the precursor star polymers. The star ionomers showed two glass transition temperatures: one close to the precursor polymer and the other higher than that of the precursor polymer. These thermal attributes corroborate the hindered chain mobility of the star ionomers chains [122].

10.3. Rheology

Rheological investigations of star polymers were carried out both in solution and in melt [32]. It was reported that long-chain branching (LCB) had a significant effect on the rheological properties of polymers, and even a small amount of LCB could lead to a great increase in extensional viscosity, shear viscosity, and elasticity [227,235]. The complex viscosity, elastic and viscous modulus for chain branched PLA were improved resulting from the enhancement of molecular entanglement, and consequently, a higher draw ratio could be achieved during the subsequent hot stretching [232,237].

Multifunctional monomers, such as epoxy [218,250], anhydride [227], diisocyanate [263], and acrylate [236], were used to prepare LCB PLA with high molar masses and improved melt strengths compared with their linear precursors. The LCB structure contributed to the enhancement of the zero-shear viscosity, complex viscosity, storage modulus, melt strength, and strain hardening under elongational flow. In star PLA polymers the zero shear viscosities were dependent on the number of arms, and a higher melt viscosity was observed for stars with higher numbers of arms [220]. Branched PLLAs had high viscosity and elastic modulus at low frequencies compared with linear PLLA and an increased shear thinning behavior. Among the branched PLLAs, star-shaped PLLAs had the highest viscosity and elastic modulus, which was associated with longer branches [223]. In the dilute solutions, the linear PLLA exhibited higher intrinsic viscosity than the star-shaped one. In the concentrated solutions, the star-shaped PLLA gave higher values of dynamic viscosity, storage, and loss moduli than those of the linear one. Star PLLA exhibited also a more noticeable shear thinning behavior and greater dependence of rheological properties on temperature than the corresponding linear polymer [8]. The rheological properties of linear PLA were also improved by γ-irradiation [23] and electron beams [309,359] cross-linking.

Rheological measurements showed a dramatic increase in the elasticity of star telechelic poly(L-lactide) ionomer melts relative to that of star PLA precursor melts. The star ionomer melts were predominantly elastic (storage modulus (G') > loss modulus (G''), large relaxation time) while the star PLA precursor melts were predominantly viscous (G'' > G', short relaxation time). The viscoelastic properties of the star telechelic PLA ionomers could be modulated in a facile manner by varying the number of ionic groups per star. The influence of ionic associations of star PLA ionomers on the thermal properties and the linear viscoelastic rheological properties of the star PLA ionomers was also reported [122].

10.4. Mechanical properties

The mechanical properties of PLA can be varied to a large extent ranging from soft, elastic plastic to stiff and high strength plastic [195]. PLLA with higher molar masses exhibited better mechanical properties. With the increase of M_n of PLLA from 23 000 to 67 000 g/mol, the flexural strength increased from 64 to 106 MPa, but the tensile strength remained the same at 59 MPa [360]. PLLA possesses good mechanical properties, with elastic modulus and tensile strength in the range of 3.2–3.7 GPa and 55–60 MPa, respectively [346].

The thermo-mechanical properties of 3-arm star PTMC-*b*-PLLA copolymers with controlled molecular features, i.e., controlled functional end-groups and molar masses, rather narrow dispersity values, were also studied. The results revealed that a minimal block

Please cite this article in press as: Michalski A, et al. Star-shaped and branched polylactides: Synthesis, characterization, and properties. Prog Polym Sci (2018), https://doi.org/10.1016/j.progpolymsci.2018.10.004

size of the PTMC and of the PLLA segments within the copolymers of $M_{n,PTMC} \approx 10\,000$ g/mol and $M_{n,PLLA} \approx 23\,000$ g/mol enabled significant improvement in the elongation at break (ε_b) of PLLA up to 328%, while maintaining the Young's modulus (E = 2781 MPa) close to that of PLLA (E = 3427 MPa, ε_b = 8%) [114].

T_g of the elastomers prepared from the cross-linking of an acrylated 3-arm star poly(ε-caprolactone-*co*-D,L-lactide) prepolymer was independent of the prepolymer molar mass and was in the range from −6 to −8 °C. The Young's modulus and stress at break of the elastomers were proportional to the inverse of the prepolymer molar mass, while the strain at break increased in a linear fashion with the prepolymer molar mass. Over a degradation period of twelve weeks in phosphate buffered saline (PBS), the elastomers exhibited little mass loss, appreciable mechanical strength loss, and little dimensional or strain at break change [315, 318].

10.5. Degradation

The degradation of PLA is dependent on many factors, such as molar mass, crystallinity, purity, temperature, pH, the presence of terminal carboxyl or hydroxyl groups, water permeability, and additives acting catalytically that may include enzymes, bacteria or inorganic fillers [4,5]. The degradation time of PLA varied from 10 mo. to 4 y [361]. A major advantage of lactide-based polyesters over other biocompatible polymers is the *in vivo* degradability into non-toxic components, which can be further adjusted for the desired medical application to control drug release rates and mechanical stability. Because polymer degradation preferentially occurs in the amorphous regions of PLLA, an increase in the number of branching units (and chain ends) in branched PLAs enhances both enzymatic degradability and hydrolysis [102,362]. Star PLA with relatively short PLA chains had a higher hydrophilicity and improved degradation profiles [109,334,363,364]. The enzymatic hydrolysis rate of star PLLA monolayers was found to be dependent on the average molar mass of the PLLA arm in macromolecules, not on the overall molar mass of polymer [362].

The hydrolytic degradation and crystalline morphology change for the branching architecture and crystallinity of linear (2-arm) and 4-arm star poly(L-lactide)s was investigated. It was observed that the degradation mechanism of 2-arm PLLA changed from bulk degradation to surface degradation with kind of the polymer phase (amorphous and crystalline) and decrease with M_n. Initially crystallized star PLLA with high molar mass degraded according to bulk degradation mechanism. In contrast, a branching architecture and/or the high number of hydroxyl groups disturbed crystallization of 4-arm star PLLAs during hydrolytic degradation at 37 °C and pH = 7.4. Influence of star architecture and density of −OH groups were also observed for amorphous poly(L,D-lactide)s (2-arm and 4-arm), although the degradation was carried out in slightly different conditions [343,365].

The thermal properties and thermal degradation of linear PLLA, as well as 25- and 51-arm branched PLLA and poly(D,L-lactide-*co*-glycolide) (PLGA), polymers were reported. It was observed that the degradation kinetics of linear and branched PLLA and PLGA were not dependent on polymer architecture. This is in agreement with the suggestion that Sn-catalyzed depolymerization is the main thermal degradation pathway for linear and branched polylactones synthesized using Sn catalysts [366].

Furthermore, hydroxyl end-groups in polylactides were transformed into —Cl, —NH_2, and —COOH groups. The cold crystallization temperatures of PLA with these groups were higher than those of OH-terminated polylactides. The thermal stability of OH-terminated polylactides was poor, whereas —NH_2 and -Cl terminated polylactides were more resistant to thermal degradation. Polylactides with —Cl and -NH_2 end-groups were less resistant to hydrolytic degradation than that containing —COOH end-groups. These end-group effects increased with an increasing number of chain arms [30].

The degradation rates of star-shaped PLAs films were accelerated with an increase in the number (as well as a decrease in the molar mass) of arms [102]. Star PLAs with a higher number of arms (and chain ends) and lower molar masses of arm showed higher degradability [362]. It was reported that star-shaped PDLLA had a higher hydrolytic-degradation rate than the linear poly(D,L-lactide) with similar molar mass [52], and the hydrolytic degradation proceeded mainly via surface erosion mechanisms [341]. The degradability by enzymatic and alkaline hydrolyses of star PLA with glycerol or sorbitol core was also studied by Arvanitoyannis et al. [193,367].

Star polylactides with glycerol [193], sorbitol [198], poly(vinyl alcohol) [26], or dextran [368] core had relatively short PLA chains, which caused their high hydrophilicity and fast degradation rates in comparison with those of linear PLA with similar molar mass [334].

The 4-arm star PEG-*b*-PLA polymers are thermally stable at biological conditions. In addition, the star polymers have short degradation times compared with that of linear PLA, and therefore, PEG-*b*–PLA copolymers may be an excellent candidate for drug delivery applications [369]. Oligomeric ethylene oxide blocks in PLA star polymers enhanced water solubility for the PLA materials without adversely affecting the non-toxic, non-immunogenic and biodegradable properties of PLA [29]. A biodegradable 4-arm star copolymer comprised of poly(ε-caprolactone-*co*-lactide) (PCLLA) and PLLA blocks having elastomeric properties was obtained and investigated. A degradation study of the copolymer showed that degradation first occurred in the PCLLA core, followed by degradation in the PLA ends. Chain scission in the middle core resulted in the immediate formation of ε-CL crystals within the core and increased crystallinity over time, in both PCLLA core and PLA ends [370].

Star-shaped PLLA showed lower T_g and T_m than did linear PLLA. As a result of *in vitro* degradation, the star-shaped PLLAs showed faster degradation rates than those of linear PLLAs at 80 °C [371]. The degradation of the elastomers is dependent on the cross-link density [149].

Moreover, hydrolytic degradation of the polymer network prepared by the esterification reaction of hydroxyl-terminated 4-arm star-shaped PLA and succinic anhydride [316] and *in vitro* degradation of star-shaped poly(ε-caprolactone)-*b*-poly(L-lactide)-*b*-poly(D,L-lactide-*co*-glycolide) with a cyclotriphosphazene core were also reported [372].

The cross-linking of degradable aliphatic polyesters strongly affected the rate and mechanism of degradation (surface or bulk). The degradation behavior *in vivo* and *in vitro* of photo-cross-linked star poly(ε-caprolactone-*co*-D,L-lactide) elastomers of different cross-link densities was studied, and it was observed that the degradation behavior of the network with the lower cross-link density proved a bulk erosion degradation mechanism [148]. The degradation of the network with the greater cross-link density displayed a linear decrease in mass and mechanical strength, which is characteristic of a surface erosion mechanism. The cross-link density of biodegradable networks also affects their mechanical properties, including strength and elastic modulus [124].

The influence of the number of branches (chain ends) and the stereochemistry of PLAs on the enzymatic degradation and alkaline hydrolysis were studied. An increase in the number of branches enhanced the enzymatic degradability and the alkaline hydrolysability. The branched PLLA, PDLA, and PDLLA differed in mass loss and change in M_n of the PLA segment during the enzymatic degradation [102].

In addition, micelles formed from the star copolymer H40-PLA-*b*-MPEG showed a sustained release of the entrapped hydrophobic

Please cite this article in press as: Michalski A, et al. Star-shaped and branched polylactides: Synthesis, characterization, and properties. Prog Polym Sci (2018), https://doi.org/10.1016/j.progpolymsci.2018.10.004

model drug over a period of 4 to 58 h, and the copolymer itself degraded hydrolytically within six hours under physiological conditions [373].

10.6. Micellization

There are many papers reporting on the micellization of star-shaped copolymers containing PLA arms. To improve the gel mechanical strength and degradation properties, PEG-*b*-PLA star diblock copolymers with three [80,374,375], four [66,369,376,377] or eight arms [66,112,326,328,331] were synthesized, with a hydrophilic central core and hydrophobic arms and vice versa. These copolymers associated into micelles, although differences in the micellization properties with respect to linear diblock copolymers were observed as a result of the topological constraints of the star copolymers [328,369,377]. Depending on the block length, the chain architecture, and the number of arms, unimolecular micelles or multimolecular micellar aggregates were formed [327]. Thus, star-block PEG-*b*-PLA copolymers formed micelles in the dilute aqueous solutions. With increasing temperature, micelle size decreased dramatically. In a high-concentration solution, the star-block copolymer showed a temperature-sensitive sol-gel transition behavior [374]. The self-assembly into micellar systems of 8-arm star copolymers (PEG_{65}-*b*-$PLA_n)_8$ (where: n = 11, 13, 15) was observed in water at various concentrations and temperatures [327].

The formation of supramolecular aggregates of PEG-*b*-PLA star shaped copolymers with PEG in the central core was reported only in a few papers [327,331,369,376,377]. The star block PEG-*b*-PLA copolymer structure with an iron center formed micelle-like nanoparticles that could entrap hydrophobic drugs [182]. AB_2 type 3-miktoarm star copolymers with PEG as the A arm and PLLA as the two B arms had the ability to self-assemble into polymer vesicles (polymersomes) in aqueous solutions [378]. The host–guest properties of star PLA with a hyperbranched polyglycidol core exhibiting a core–shell structure, such as reversed micelles, were studied, and it was shown that water-soluble dyes were successfully encapsulated in a hydrophilic polyglycidol core [89].

Star-shaped block copolymers with 3, 4 and 6 (PLGA-*b*-PEG) arms were synthesized to investigate the relationship between the arm numbers of PLGA-*b*-PEG copolymers and their micelle properties [36,379]. The critical micelle concentration (CMC) decreased with increasing arm numbers in copolymers [379]. PLGA-*b*-PEG stars with 3 and 4 arms showed additionally the temperature- and concentration-dependent formation and aggregation of micelles [380]. The 6-arm star PLA polymers and copolymers with styrene and *N*-acryloxysuccinimide (NAS) with a hexahydroxy triphenylene core were obtained [381]. These polymers formed micelles, and its cross-linking afforded nanospheres that could be transformed into hollow nanospheres by hydrolysis of the PLA core [29].

The 5-arm star-block terpolymers with PCL inner blocks, PLLA middle blocks, and PDMAEMA as outer blocks were prepared using the ROP and RAFT methods. Spherical micelles with a degradable core, as well as temperature- and pH-sensitive corona, were obtained in aqueous solutions [382].

The 7-arm star block copolymer comprised of one hydrophobic PLLA arm and of 6 hydrophilic poly(*N*-isopropylacrylamide) (PNIPAAm) arms was synthesized. This amphiphilic copolymer was capable of self-assembling in water into nanosized micelles approximately 100 nm in diameter. The micelles showed reversible dispersion/aggregation in response to temperature changes through an outer polymer shell of PNIPAAm at approximately 31 °C. The reversible and sensitive thermoresponse of this micelle might provide opportunities to construct a novel drug delivery system in conjunction with localized hyperthermia [383].

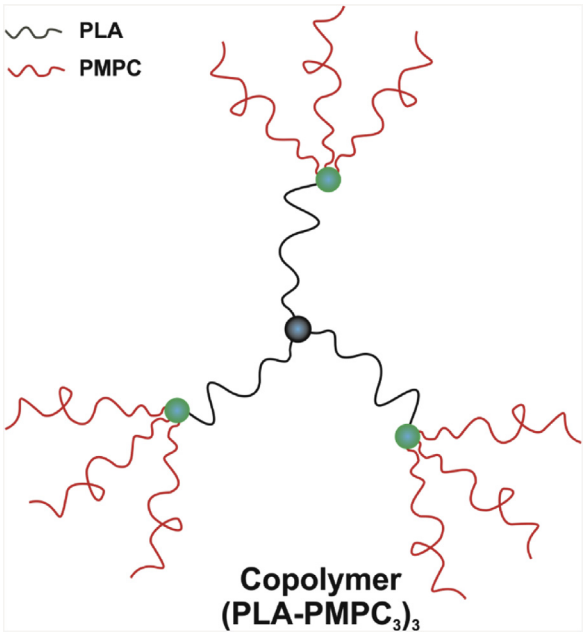

Fig. 23. Structure of star-branched polylactide and poly(2-methacryloyloxyethyl phosphorylcholine) copolymer (PLA-*b*-$(PMPC)_3)_3$ [137].

A biodegradable 8-arm star block copolymer with perylene diimide (PDI) core and poly(D,L-lactide)-*b*-poly(ethyl ethylene phosphate) (PLA-*b*-PEEP) arms formed a unimolecular micelle and can self-assemble into supramolecular micelles. These fluorescent supramolecular micelles with controllable sizes in aqueous solution can be used as a smart fluorescent drug delivery system [384]. It was reported that star PLLA with dendrimer cores also formed micelles. The synthesis of nanofibrous hollow microspheres self-assembled from star-shaped PLLA with a PAMAM core as an injectable cell carrier was reported. These nanofibrous hollow microspheres were an excellent injectable cell carrier for cartilage regeneration [385].

The synthesis of amphiphilic star-branched polylactide and poly(2-methacryloyloxyethyl phosphorylcholine) copolymers (PLA-*b*-$(PMPC)_3)_3$ with $(AB_3)_3$-style architecture via a combination of ARTP, ROP and click chemistry via an "arm-first" approach was also reported (Fig. 23). The copolymers self-assembled into micelles and had ultra-low cytotoxicity [137].

The 20-arm biodegradable and biocompatible amphiphilic hyperbranched H40-PLA-*b*-MPEG copolymer was synthesized as a hydrophobic drug delivery carrier. In aqueous solutions, the copolymer forms unimolecular micelles with the hydrophobic H40-PLA as the micelle core and the hydrophilic MPEG as the shell. The diameter of the unimolecular micelles was in the range of 11–17 nm [373].

The formation of pH- and temperature-sensitive spherical micelles from 32-arm PDMAEMA-*b*-PLA star-block copolymers, prepared using multihydroxyl polyhedral silsequioxane [POSS-$(OH)_{32}$] as the multifunctional initiator and a combination of ROP and ATRP techniques, was reported [130]. Additionally, dendritic star-block DPLLA-*b*-PDEAEMA-*b*-PEG terpolymer micelles exhibited a pH responsive property at different pH values [386].

Amphiphilic 21-arm, star-like block copolymer *β*-cyclodextrin-*graft*-(polylactide-*block*-poly(2-(dimethylamino) ethyl methacrylate)-*block*-poly[oligo (2-ethyl-2-oxazoline) methacrylate]) [*β*-CD-*g*-(PLA-*b*-PDMAEMA-*b*-PEtOxMA)] (Fig. 11) formed stable micelles. The micelle radius increased due to the stretching of the thick hydrophilic layer in the aqueous solution. This system existed as unimolecular micelles within a certain

Please cite this article in press as: Michalski A, et al. Star-shaped and branched polylactides: Synthesis, characterization, and properties. Prog Polym Sci (2018), https://doi.org/10.1016/j.progpolymsci.2018.10.004

concentration range and was able to maintain a constant particle size and a stable structure *in vivo*. This may be of great value as a drug delivery system for the efficient transport of drugs [172]. The formation of unimolecular micelles from β-CD-*g*-(PLA-*b*-PDMAEMA-*b*-PEtOxMA) star-like block copolymers was reported. That polymeric micelle could be used for encapsulating gold nanoparticles, whose mesoscopic structure was also explored. The gold nanoparticles tended to distribute in the middle layer formed by PDMAEMA, and the unimolecular micelles were capable of impeding gold nanoparticle aggregation [173].

A novel biodegradable unimolecular reversed micelle consisting of a poly(L-lactide) shell and a hyperbranched D-mannan (HBM) core, that is, a chestnut-shaped polymer (PLLA-HBM), was synthesized by the polymerization of L,L-lactide on HBM with 4-(dimethylamino)pyridine (DMAP) as the catalyst. The molar masses of the PLA chain in PLLA-HBM tended to increase with polymerization time. The number of PLLA chains on PLLA-HBM could be controlled by the ratio of DMAP to the sugar unit in HBM. The obtained copolymer, PLLA-HBM, acted as a unimolecular reversed micelle with an encapsulation ability towards the hydrophilic molecule. In addition, the entrapped hydrophilic molecules were slowly released from the core of PLLA-HBM, and the release rate was accelerated by the breaking of the PLLA shell when proteinase K was used as the hydrolase of PLLA. Hence, the unimolecular reversed micelle, PLLA-HBM, is a good candidate for biodegradable controlled-release systems [73].

11. Applications of star/branched PLA

PLA is a high strength and high modulus thermoplastic, which can be easily processed by conventional processing techniques used for thermoplastics, such as injection molding, blow molding, thermoforming and extrusion. For large-scale production, the polymer must possess adequate thermal stability to prevent degradation and maintain molar mass and properties. Its degradation is dependent on time, temperature, low-molar mass impurities, and catalyst concentration [347].

Among synthetic materials, PLLA and PLGA are common biocompatible polymers approved by the US Food and Drug Administration (FDA) and are extensively used as potential scaffold materials for tissue engineering [387]. Different biomedical applications for PLA were reported [388], e.g., as surgical applications in human tissues [361], as controlled delivery carriers [389], for orthopedic regenerative engineering [390]. Recently, there appeared a few very good reviews on the applications of PLA [391–395] and on PLA blends in biomedical applications [396].

Star PLA with pentaerythritol and dipentaerythritol cores can be used in controlled drug release [397], nanoparticle synthesis [340], and micelle formation [109,398]. Electroactive and biodegradable 4- and 6-arm star-shaped PLA coupled with carboxyl-capped aniline trimer have a great potential for applications in cardiovascular or neuronal tissue engineering [399]. The observed reduction in plasma protein absorption, as well as cell and platelet adhesion, onto the 8-arm PEG-*b*-PLLA film surface implies that the film of this polymer can be utilized as a novel bioabsorbable adhesion-prevention membrane [400].

The dendrimer-like copolymers with arms built from blocks of polystyrene, poly(L-lactide), polystyrene, and poly(*N*-acryloyloxysuccimide) were synthesized by a combination of ATRP and ROP. In the next stage, the outermost part in the dendrimer-like copolymers (polystyrene-*b*-poly(*N*-acryloyloxysuccimide)) was cross-linked with ethylene diamine, and the PLLA segments were decomposed, forming hollow particles. These hollow particles may have potential applications in catalysis and bioengineering [401].

Europium-based homostar and star block copolymers are of special interest for optical excitation and emission studies, because they exhibit high luminescent quantum efficiencies [179]. Miktoarm star polymers PS-*b*-$(PLA)_2$ and $(PS)_2$-*b*-$(PLA)_2$ have potential applications in lithography [402].

11.1. Drug encapsulation

There are many reports on the encapsulation drugs and/or its models in micelles [40,65,172,182,373,383,384,403–407], microspheres [32,34,59,366,408,409], and nanoparticles [377,410,411] formed by star/branched PLA molecules.

Micelles were formed by star copolymers: H40-PLLA [411], H40-PLA-*b*-MPEG [373], star PLGA [412] or PEG-*b*-PLA [123], star PLGA-*b*–PEG [379], and star with β-cyclodextrin (β-CD) cores [123,413]. The 32-arm star polymers with a poly(amidoamine) (PAMAM) dendrimer core and PLA arms as the inner lipophilic block and PEG as an outer hydrophilic block [403], and as well star-poly(D,L-lactide)-*b*-poly(*N*-(2-hydroxypropyl)methacrylamide) and star-poly(D,L-lactide)-*b*-poly(*N*-vinylpyrrolidone) [406] also formed micelles.

As drugs or models of drugs bovine serum albumin (BSA) [412], doxorubicin [379], doxorubicin hydrochloride (DOX·HCl) [40,414], anticancer drug etoposide [403], docetaxel [411], the dye Congo Red [413], camptothecin [65], methotrexate (MTA) [383,404,405], nimodipine [32], indomethacin [406,407], rifampicin (RIF) [409], 5-fluorouracil [377], and paclitaxel [377,406,410] were used.

In comparison with linear polymers at the same molar mass, nanocarriers based on a star-shaped polymer molecular structure showed a smaller hydrodynamic radius, lower solution viscosity, higher drug content, and higher drug entrapment efficiency [161]. For example, the self-assembly behavior of amphiphilic PEG-*b*-$(PLLA)_2$ miktoarm star copolymers was examined in aqueous solutions [378]. Taking advantage of this behavior, the efficient encapsulation of the anticancer drug doxorubicin hydrochloride was achieved [40,378].

Star PLLA possesses more terminal groups that are capable of connecting with target molecules, which could largely transport the encapsulated drugs to the targeted organs and tissues [54,334,415]. Star PLLA showed a significantly shorter degradation time than that of the linear one, which is quite beneficial for the subsequent preparation of drug-loaded microspheres [59,366,408]. For example, Ouyang and coworkers [412] prepared BSA-loaded star-shaped PLGA microspheres through a double emulsion/solvent evaporation method. The release experimental results showed that BSA-loaded microspheres release the BSA in a controlled manner and exhibited full release [409]. A 4-arm star PLLA with an erythritol core formed microspheres that were loaded with rifampicin as a model drug. These microspheres were comparatively investigated in terms of size, morphology, drug encapsulation efficiency, drug releasing profile, and drug release kinetics [409]. The guest encapsulations (methyl orange) of star polymers bearing a PEI core and well-controlled PLLA or PDLLA arms were also investigated. The guests encapsulated by the star nanocarriers can be released in a sustained way, and the guest release rate was modulated through varying the arm length or the type of the PLA arms [261]. Furthermore, polymersomes of amphiphilic block copolymers could encapsulate water-soluble cargos, such as pharmaceutical molecules and biomolecules, within the water-filled inner compartment [416].

Docetaxel-loaded dendritic copolymer H40-PDLLA nanoparticles were prepared and used as a model to evaluate whether the dendrimer-based NPs were sequestered by autophagy and degraded through the autophagic pathway. In addition to being degraded through the endolysosomal pathway, the nanoparticles of dendritic polymers were also sequestered by autophagosomes and fused with lysosomes [411].

Biodegradable recombinant human erythropoietin and fluorescein isothiocyanate-labelled dextran-loaded microspheres [397]

Please cite this article in press as: Michalski A, et al. Star-shaped and branched polylactides: Synthesis, characterization, and properties. Prog Polym Sci (2018), https://doi.org/10.1016/j.progpolymsci.2018.10.004

were prepared from 4- and 8-arm star block PEG-*b*-PLLA or PEG-*b*-PLLG copolymers [66].

11.2. Drug delivery

The polymer architectures play a crucial role in the drug delivery control and in the fabrication of drug delivery systems. Typically, star PLLA has a more compact structure with smaller hydrodynamic radius than linear PLLA of similar molar mass, lower solution viscosity, and peculiar morphologies, which means that it is not easily stranded in the blood and ensures the bioavailability of the drug encapsulated [81,326]. The micelles showed a more complete release of the drug than did the diblock copolymers, and the lower hydrodynamic radius of star-shaped polymers may result in better clearance of the carrier polymer from the body [377]. This could help to overcome the side effects of chemotherapy by reducing the adverse effects to the normal cells.

PLA star polymers were studied for their potential effectiveness as drug delivery vectors and self-assembled micelles. The morphology [182,340,374,381], solution properties [8,30,56,97,326], and loading potential [103,406,413,417] were investigated [29]. Different star PLA polymers with a core built from porphyrin [160], cholic acid [159,161,418], Boltorn H40 [419], mannitol [158] and arms containing D-α-tocopheryl polyethylene glycol 1000 succinate (TPGS) blocks were used in the drug delivery systems. Docetaxel [158–160,418,419], paclitaxel [161,406], chlorambucil [132], indomethacin [406] were used in the drug delivery tests in breast cancer therapy [158,419], liver cancer [418], cervical cancer [159,160], and in breast cancer treatment [158,161]. It should also be mentioned that the dendritic PLAs were applied in the embedding and controlled release of bovine serum albumin (BSA) [197,334], chlorambucil [132], and Rose Bengal [420], as models of controlled release drug delivery systems [29].

Star polymers are proposed as "smart" drug delivery carriers that can sustainably deliver the drug to the target tissue [32,421,422] (Fig. 24) or as a depot for the thermosensitive drugs [318]. It was found that the star polymers showed short degradation times compared with linear PLA and PLA–*b*-PEG copolymers, suggesting use as a short-term drug release agent [369]. Star-block copolymers showed the high possibility to be used as an injectable drug delivery system for long-term delivery of drugs, such as protein drugs and insulin [374].

There are many reports on employing star PLA polymers in various drug delivery systems. It was disclosed that the steady drug (indomethacin) release rate from 4-arm star MPEG-*b*-PLA micelles was higher than that of 6-arm star micelles [423]. The amphiphilic 4-arm star-shaped PDLLA-*b*–PEG copolymers with PEG (M_n = 850 and 2000 g/mol), with hydrophobic inner PDLLA segments and hydrophilic PEG external segments have good potential for the formulation of delivery carriers for bioactive compounds [424]. Amphiphilic miktoarm copolymers with one PLA and three PEG arms for the avidin-biotin system were synthesized. These stars provided at one end a hydrophilic surface that masked the hydrophobic core and prevented reticuloendothelial uptake; whereas on the other end, they provided a hydrophobic core that can interact with drugs [157]. Micelles based on POSS-(PAA-(PLLA-*b*-PEG)$_4$)$_8$ copolymer have promising applications in controlled drug delivery because: (1) they possess better stability *in vivo* than the conventional multimolecular micelles; (2) the PLA membrane of the micelles can encapsulate some hydrophobic drugs; and (3) their inner PAA hydrophilic cavities can load some hydrophilic drugs via electrostatic interactions, such as DOX·HCl [425]. The drug-release properties of star-shaped PLA attached to a poly(amidoamine) [334] or PEI [420] dendrimer core were also reported. The transport capacity of nanocarriers depended on the length of the PLA arms, and longer arms gave rise to higher transport capacities [420].

Star-shaped PDLLA was successfully used for the preparation of novel drug delivery systems of norfloxacin [103]. The presence of the PLA arms with different reactive terminal groups and the core of cholic acid (CA) provided greater cell affinity that resulted in advantages for applications in drug-release microspheres and tissue engineering [242,417,426]. Other 4- and 6-arm star PLLA-*b*-PEG copolymers were synthesized for drug delivery systems [80,398]. The 4-arm star-poly(D,L-lactide)-*block*-poly(*N*-(2-hydroxypropyl)methacrylamide) and star-poly(D,L-lactide)-*block*-poly(*N*-vinylpyrrolidone), copolymers formed micelles loaded with indomethacin and paclitaxel. Thermosensitive 3-arm PLA-*b*-PNIPAAm star block copolymers formed nanoscale micelles with a spherical core-shell architecture that can be used for camptothecin drug release [65]. Such micelles could prove useful for drug delivery applications [406].

The drug-loaded star-shaped nanoparticles (NPs) had a lower solution viscosity, smaller hydrodynamic radius, higher drug loading content and higher drug encapsulation efficiency than did the drug-loaded linear NPs with the same molar mass and composition [160,427]. The presence of a cyclodextrin core in star PLA was interesting in the frame of drug delivery applications [428]. Amphiphilic 21-arm star block copolymers with a cyclodextrin core were used for the formation of gold nanoparticles (GNPs) for targeted tumor therapy and diagnosis in biomedical fields since the sizes and morphologies of GNPs can be easily tuned to achieve prolonged blood circulation time [172].

In addition, it was reported that a 20-arm hyperbranched H40-PLA-*b*-MPEG copolymer showed no cytotoxicity against a human endothelial cell line. Therefore, it was suggested that the micelles formed from this copolymer could be a suitable candidate for drug delivery applications because of their stability, biocompatibility, higher drug loading, and controlled release ability [373]. Wang et al. [334] and Xi et al. [79] reported the synthesis, thermal properties, and controlled drug release profiles of a star-shaped poly(amidoamine) (PAMAM)-PLLA hybrid with a dendritic hydroxyl-terminated PAMAM macroinitiator [90].

Amphiphilic dendrimer-like star polymers (DLSPs) with a hydrophobic star-shaped PLLA core and a hydrophilic poly(amidoamine) (PAMAM) dendron shell were functionalized with carboxylic acid, primary amine, and triethylene glycol functional groups. These functional DLSPs exhibited a unique unimolecular micelle (14–28 nm) behavior in aqueous solution with a small amount of aggregation (205–344 nm), and large differences in thermal behaviors depending on the nature of various surface groups were observed. These polymers with an excellent water solubility (ca. 10–25 mg mL^{-1}) enhanced greatly the solubility of hydrophobic drugs, and therefore, they are the excellent candidates for controlled hydrophobic drug delivery [126].

The vesicle structures (polymersomes) with controlled size and morphologies were formed from 4-arm star PEG-*b*-PDLLA block copolymers with different hydrophobic lengths. These polymersomes were able to encapsulate up to 35 wt.% of hemoglobin under mild conditions in water. The encapsulated hemoglobin kept its own bioactivity and was capable of binding oxygen. Therefore, this hemoglobin-encapsulated 4-arm PEG-*b*-PLA polymersomes could have the potential to be applied as an artificial oxygen carrier for transfusion [416].

The metal complex star (i.e., Fe(dbm-PLA)$_3$; cf. Table 6) was investigated as a sensitive luminescent material for drug delivery. Their unique properties are related to both fluorescence and room temperature phosphorescence in the solid state caused by the acidic environment which induces the demetalation and liberation of dbm end-functionalized linear PLA. These dual-emissive

Please cite this article in press as: Michalski A, et al. Star-shaped and branched polylactides: Synthesis, characterization, and properties. Prog Polym Sci (2018), https://doi.org/10.1016/j.progpolymsci.2018.10.004

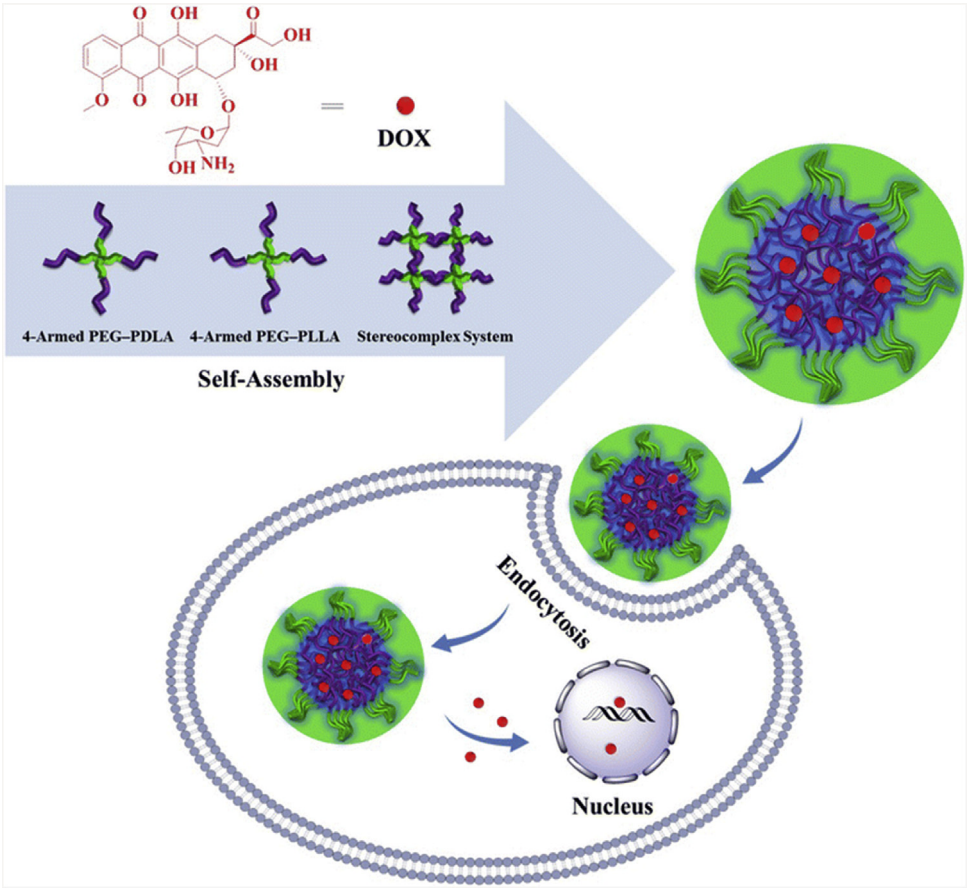

Fig. 24. Star-shaped PLA acting as a drug delivery system [421]. Copyright 2018. Reproduced with permission from Springer Open.

properties endow the medical imaging applications of the proposed system. [32].

11.3. Star/branched PLA as medical materials

PLA was approved by the Federal Drug Administration (FDA, USA) for use as a suture material because of features that offer crucial advantages [429,430]. Biomedical applications of PLA, its copolymers, and networks were reviewed in many papers [29,387,429,431,432].

Tissue engineering was used to create artificial substitutes for defective tissues and organs and tissue regeneration. The matrix can be served as a substrate for the attachment, growth, and migration of cells or can be utilized as a drug carrier to activate cellular function in the region [7]. Bioabsorbable polymers are preferred candidates for developing therapeutic devices such as temporary prostheses, three-dimensional porous structures as scaffolds for tissue engineering and as controlled/sustained release drug delivery vehicles [429]. Because of the increased cross-linking the structure and mechanical properties of PLA-based polymers were improved greatly [150]. For tissue engineering of hard tissues such as bone, strong and rigid biodegradable materials are desired. Polylactide is such a material, and it has a long track record of successful application in the clinic and in the preparation of tissue engineering scaffolds [314].

Star-shaped PLA polymers with hyperbranched polyglycerol [89], cholic acid [417], polyhedral oligomeric silsesquioxanes [18], and POSS [433] core are attractive materials for biomedical applications.

Star PLLA-*b*-PEG block copolymers have different gelation behavior from the hydrogels made from linear block copolymers [374,375]. It was reported that 8-arm PEG-*b*–PLA–cholesterol copolymer formed a gel at 34 °C in water, but the 8-arm star PEG-*b*–PLA itself did not form a gel at the same temperature. This cholesterol-substituted hydrogel promoted cell proliferation and might be used as a tissue engineering scaffold [136,323]. A biodegradable 8-arm star-shaped PEG-*b*-PLLA block copolymer was synthesized to create a novel implantable soft material [434]. Highly oriented chain branched PLA with enhanced mechanical properties and good blood compatibility was fabricated through solid hot drawing technology. The tensile strength and modulus of samples increased significantly by stretching. The results of *in vitro* blood compatibility showed that, compared with neat PLA, oriented samples after chain branching exhibited less platelet adhesion, BSA and BFG protein adsorption, longer activated partial thromboplastin (APTT) and thrombin (TT) clotting times, and a lower hemolysis ratio, indicating that the samples with high molecular orientation exhibited an appreciably better blood compatibility than did neat PLA [237]. Good survival was obtained for embedded HepG2, and two UVSMC cell types incorporated into 4-arm star PLA based on poloxamine [435]. Collagen-containing cross-linked derivatives of star-shaped PLAs based on poloxamine T1107 as the core were also produced [435].

The irreversible gel formation temperature-responsive process (thermogelling) was reported for enantiomeric 8-arm star-shaped triblock copolymers PEG-*b*–PLLA-*b*–PEG (Stri-L) and PEG-*b*–PDLA-*b*–PEG (Stri-D) that formed stable stereocomplexes at higher temperatures (e.g., 37 °C). Thermogelling polymer systems are expected to be useful for tissue engineering and because of easy entrapment of water-soluble pharmaceutical or bioactive agents. For example, proteins could be used as a depot for sustained release after a simple injection with a syringe at the target site of a human

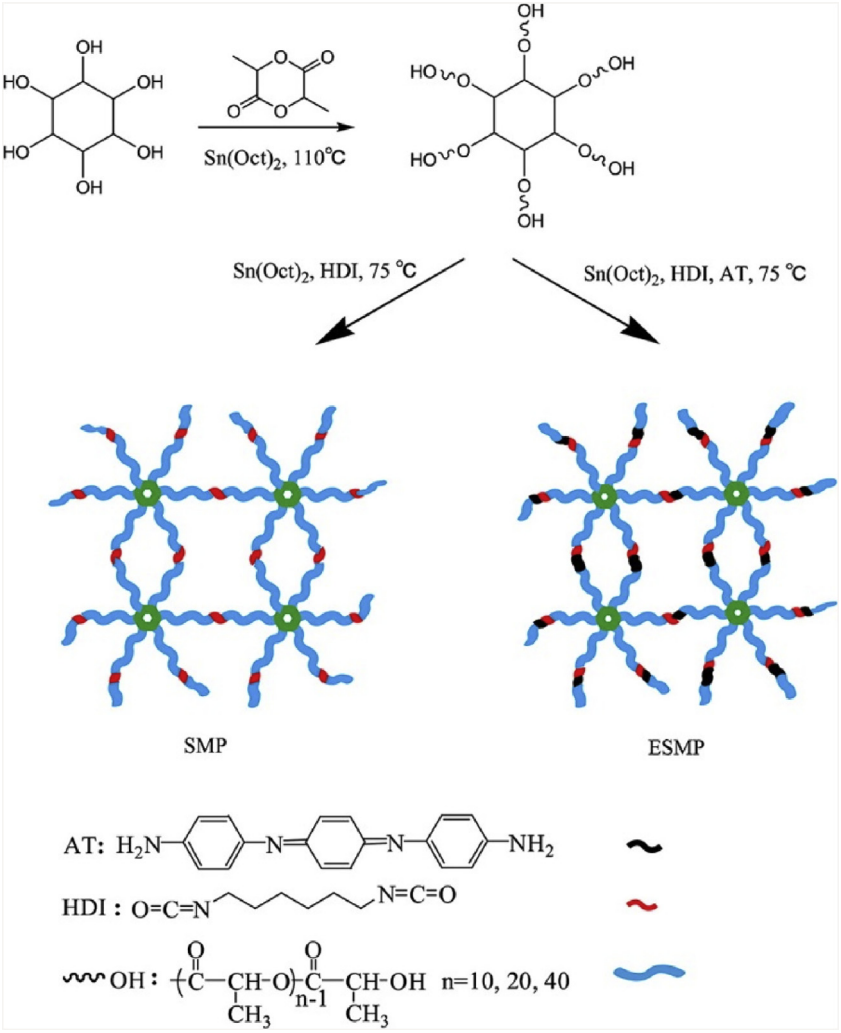

Fig. 25. The synthesis of strong electroactive shape memory polymer networks based on star-shaped PLA and an aniline trimer [436] Copyright 2018. Reproduced with permission from ACS Publications.

body [331]. When the star PLLA was used to prepare the drug-loaded microspheres that were intended to cure human beings, the raw materials ideally should be nontoxic and bioresorbable. The employment of the nonbioresorbable residual polyols may be harmful to the human body after the degradation of star PLLA [167]. Pure natural polyhydroxyl initiators (e.g., erythritol) which are nontoxic and endogenous to the human metabolic system are significantly better when confronted with the requirements for controlled drug delivery systems [409].

Implants from inositol-based star-shaped PLLA-*b*-PEG (star-shaped INO-PLLA-PEG) were reported. They showed controlled elastomeric mechanical properties (~18 MPa in tensile strength, ~200 MPa in modulus, and ~200% in elongation), biodegradability and osteoblast biocompatibility. These results make INO-PLLA-PEG implants highly promising for bone tissue regeneration and drug delivery applications [150]. Melchels et al. reported photo-cross-linked methacrylate-terminated 3- and 6-arm star-shaped poly(D,L-lactide) oligomers usable as tissue engineering scaffolds [314]. The synthesis of strong electroactive shape memory polymer (ESMP) networks based on star-shaped PLA and an aniline trimer was reported. The 6-arm PLAs with various chain lengths were chemically cross-linked to synthesize the shape memory polymer (SMP) (Fig. 25). The SMP and ESMP exhibited strong mechanical properties (modulus higher than 1 GPa) and excellent shape memory performance: short recovery time (several seconds), high recovery ratio (over 94%), and high fixity ratio (nearly 100%). These intelligent SMPs and electroactive SMP with strong mechanical properties, tunable degradability, good electroactivity, biocompatibility, and enhanced osteogenic differentiation of C2C12 cells show great potential for bone regeneration [436].

The synthesis of hollow magnetic silica microspheres (HMS) with PLA-*b*-PEG arms loaded with ioversol by physical coating was also reported. These microspheres encapsulating superparamagnetic iron oxide (Fe_3O_4) were used as a magnetic target for increasing the local concentration of the contrast media in magnetic resonance imaging and computed tomography technology [367].

In contrast, Y-shaped glucose-responsive poly(ethylene glycol)-*b*-[poly(lactic acid)-*b*-poly(2-phenylborate ester-1,3-dioxane-5-methyl) methylacrylate)]$_2$ seems to be a promising candidate that holds great potential in the treatment of diabetes [437].

11.4. In vitro *and* in vivo *investigations*

The toxicity of star and branched PLA was studied *in vitro* and *in vivo* as controlled drug-loaded biomaterials [158,159,438,439]. Investigations *in vitro* and *in vivo* were performed with micelles [125,137], microspheres [440], hydrogels [136], elastomers [149], star-shaped PLA porphyrin-cored-cross-linked aggregates [168], and PLA with a branched architecture [267]. For example, the colorimetric test MTT for assessing cell metabolic activity showed that

the cytotoxicity of star-shaped porphyrin-cored poly(L-lactide)-*b*-poly(gluconamidoethyl methacrylate) (SPPLA-*b*-PGAMA) block copolymers against COS-7 cells was very low, and when given a longer irradiation time, more BEL-7402 cancer cells died. These star-shaped porphyrin-cored SPPLA-*b*-PGAMA block copolymers can be used in photodynamic therapy [168].

Star poly(D,L-lactide) showed clearly improved cell adhesion in comparison with the linear counterparts [426]. It was reported that 4-arm star-shaped PLA with heparin end-groups (sPLA-HEP) demonstrated *in vitro* a low protein adsorption and platelet adhesion on sPLA-HEP when compared with star-shaped PLA (without heparin end-groups). Immobilized heparin also enhanced cell activity on biodegradable polymer surfaces. In addition, the heparin content of sPLA-HEP was higher than in linear PLA-HEP, and therefore, its bioactivity was also enhanced [438]. An improved property for cell adhesion and the cell proliferation of 3T3 mouse fibroblasts and ECV304 human endothelial cells on the cholic-acid-functionalized star PDLLA was observed compared with the linear PDLLA [426]. Chapanian et. al. reported that the rate of *in vivo* was faster than the rate of *in vitro* degradation for elastomers obtained from 3-arm star PDLLA triacrylate and 3-arm star-poly(ε-caprolactone-*co*-D,L-lactide) triacrylate. Both elastomers *in vivo* undergo bulk hydrolysis along with surface erosion occurring due to the physiological environment [149]. It was also reported that highly oriented long-chain branched PLA with enhanced mechanical properties exhibited significantly better blood compatibility than neat PLA [267].

The aqueous solution (polymer concentration, above 3 wt.%) of amphiphilic, partially cholesterol-substituted 8-arm PEG-*b*-PLLA (8-arm PEG-*b*-PLLA-cholesterol) exhibited instantaneous temperature-induced gelation at 34 °C, unlike 8-arm PEG-*b*-PLLA. An extracellular matrix micrometer-scale network structure was created by self-assembly between cholesterol groups, with a favorable porosity for the three-dimensional proliferation of cells inside the hydrogel. L929 cells encapsulated in the hydrogel were viable and proliferated three-dimensionally inside the hydrogels. Thus, 8-arm PEG-*b*-PLLA-cholesterol is a promising candidate as a novel injectable cellular scaffold [136].

Nanoparticles from star-shaped block copolymers with mannitol [158], porphyrin [160], and cholic acid [159] as cores and having D-α-tocopheryl polyethylene glycol 1000 succinate (TPGS) as end-groups were loaded with docetaxel, and their anticancer performance *in vitro* [160] and *in vivo* [158,159] was studied in breast cancer [158] and cervical cancer [159,160] therapies. It was reported that a 4-arm star PLGA-*b*-MPEG copolymer solution loaded with various drugs such as anti-HIV drugs, anti-inflammatory drugs, or contraceptive drugs could form gels at body temperature when sprayed into various body parts [439,441]. Gel biodegradation at body temperature studied *in vitro* and *in vivo* proceeded by hydrolysis of ester bonds [439]. Additionally, the *in vitro* study indicated that thermosensitive, star-shaped porphyrin-cored poly(L-lactide)-*block*-poly(*N*-isopropylacrylamide) showed apparent phototoxicity towards BEL-7402 cancer cells [170].

The *in vitro* degradation of the amphiphilic hyperbranched block copolymer with a dendritic Boltorn-H40 core, a hydrophobic PLLA inner shell, and a hydrophilic MPEG and folate-conjugated poly(ethylene glycol) (PEG–FA) outer shell (H40–PLA-*b*-MPEG/PEG–FA) degraded into polymer fragments within six weeks. The doxorubicin (DOX)-loaded micelles from H40–PLA-*b*-MPEG/PEG–FA block copolymer were used for the study of the sustained release of the entrapped DOX over a period of approximately 40 h. The results indicated that these block copolymers have great potential as tumor-targeted drug delivery nanocarriers [125]. Thermoresponsive micelles were formed from 7-arm star block copolymer PLLA-*b*-PNIPAAm composed of one hydrophobic PLLA arm and 6 hydrophilic PNIPAAm arms [383,404]. The *in vitro* release of the anticancer drug methotrexate (MTX) loaded in the micelles was investigated and showed a drastic thermoresponsive fast/slow switching behavior according to the temperature-responsive structural changes of a micellar shell structure [383]. An enhanced blood circulation time of 3,3′-dioctadecylindocarbocyanine (DiI) and the plasma half-life of DiI in micelles formed from an amphiphilic star-branched PLA and poly(2-methacryloyloxyethyl phosphorylcholine) copolymers (PLA-*b*-$(PMPC)_3)_3$ (cf. Fig. 23) in comparison to linear PLA-*b*-PEG was observed. The micelles themselves had an ultra-low cytotoxicity and exhibited superior suppression of serum protein adhesion compared with that of PLA-*b*-PEG [137].

The PLA star polymers also acted as a support for DNA co-precipitate complexes, as well as *in vitro* drug delivery vectors. They were also linked through condensation of multiple cholic acid oligo-PLA macromolecules to form PLA-co-cholate chains [242].

12. Organic–inorganic hybrid materials

Organic–inorganic hybrid materials received significant attention for their greatly improved physical and mechanical properties of PLA. Polyhedral oligomeric silsesquioxane (POSS), applied as a hybrid material, consists of silicon and oxygen atoms arranged in an inner eight-cornered cage with the Si atoms positioned at the corners [442]. The functionalized silsesquioxane cages of the regular octahedral structure were used as initiators for the ring opening polymerization of L,L-LA, catalyzed by $Sn(Oct)_2$, giving, as a result, biodegradable hybrid star-shaped POSS-PLLA and linear systems with an octasilsesquioxane cage as a core and PLLA arms. POSS presents a unique class of inorganic structures that can be exploited in the generation of hybrid polymer systems with advantageous properties [433]. The synthesis of a novel amphiphilic multi-arm star-like block copolymer POSS-(PAA-(PLLA-*b*-$PEG)_4)_8$ was reported (Fig. 26) [425].

A highly branched hybrid copolymer based on POSS was designed to reduce the brittleness of PDLLA. Good compatibility and distribution between POSS-*g*-PCL-*b*-PLA and PDLLA matrix were realized simply by adding the PLA segment; however, aggregation inevitably occurred. The yield stress decreased and elongation at break increased as the content of POSS-*g*-PCL-*b*-PLA increased. That finding is observed because of the core–shell structure of POSS-*g*-PCL-*b*-PLA, which significantly improved the toughness of the polymer matrix [443].

Syntheses of POSS hybrid star systems bearing 8 chains of polylactide were initiated from POSS bearing octa(glicydyl ether) [63] or octa(3-hydroxypropyl) [444] moieties. In the next step, the POSS-PLLA was further transformed into the POSS-containing star-shaped organic/inorganic hybrid amphiphilic block copolymers, poly(L-lactide)–*block*–poly(*N*-isopropylacrylamide) (POSS-PLLA–*b*–PNIPAAm) by the RAFT polymerization of *N*-isopropylacrylamide (NIPAAm) [444]. Star-shaped POSS-PLLA–*b*–PNIPAAm amphiphilic block copolymers self-assembled into vesicles in aqueous solution. The vesicular wall and coronas were composed of the hydrophobic POSS core and PLLA, and hydrophilic PNIPAAm blocks, respectively. With temperature decreasing from 34 to 30 °C, the hydrodynamic radius (R_h) sharply increased to 93 nm (from ~53 nm). At temperatures below 30 °C, the R_h nearly did not change during the heating and cooling processes, indicating that the transition process was reversible. These block copolymers could be applied in biological and medical fields [444].

Star-shaped POSS-PLA-based polyurethanes (POSS-PLAUs) were synthesized by cross-linking star-shaped polyhedral oligomeric silsesquioxane multi-arm polylactides (POSS-PLA) with polytetramethylene glycol (PTMEG) and hexamethylene diisocyanate (HMDI). All the POSS-PLAUs had excellent shape

Please cite this article in press as: Michalski A, et al. Star-shaped and branched polylactides: Synthesis, characterization, and properties. Prog Polym Sci (2018), https://doi.org/10.1016/j.progpolymsci.2018.10.004

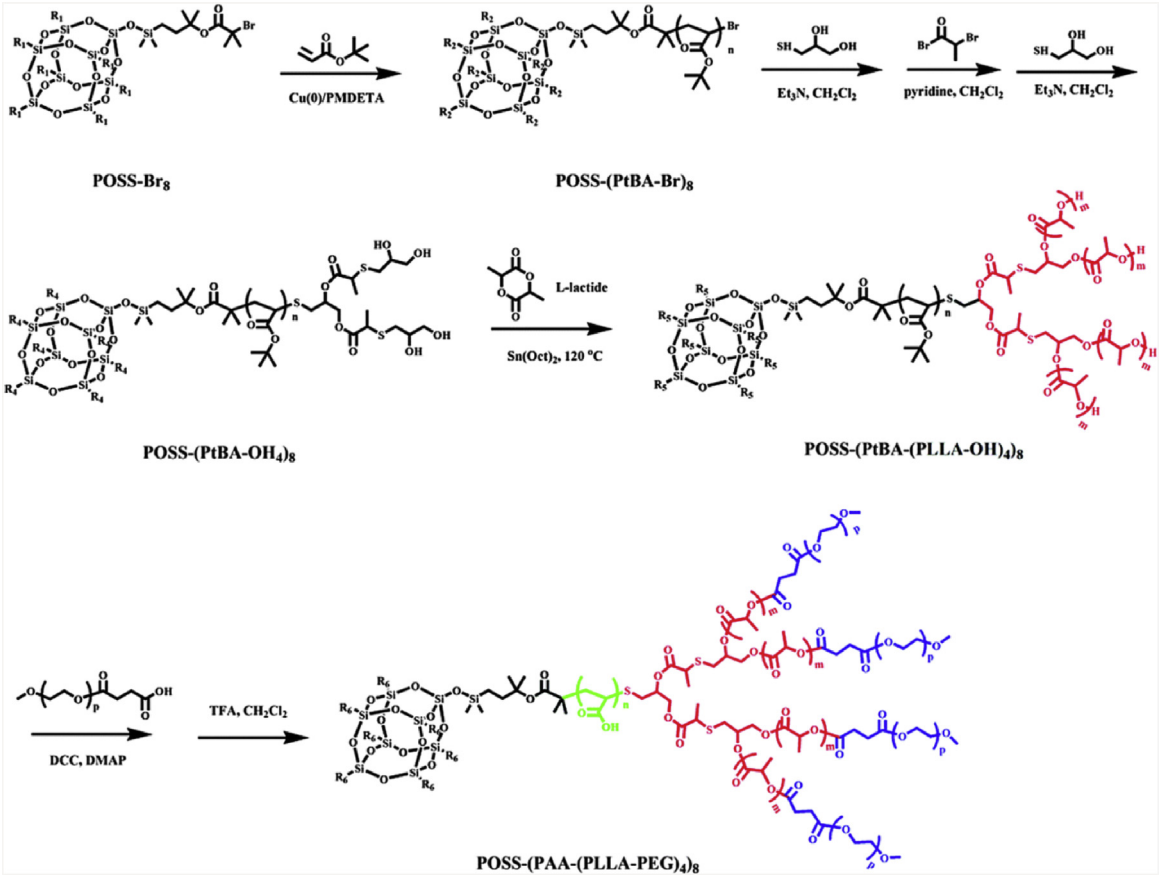

Fig. 26. Synthetic route to a novel amphiphilic multi-arm star-like block copolymer POSS-(PAA-(PLLA-*b*-PEG)$_4$)$_8$ [425]. Copyright 2018. Reproduced with permission from RSC Publications.

memory properties with high shape fixity ratios above 99%, shape recovery ratios of approximately 84% for the first cycle and above 89% for the second cycle. POSS-PLAUs with a shorter arm length showed faster recovery speed because of the higher content of POSS cores [442]. A thermal-responsive shape memory polymer (SMP), polymer network with urethane cross-linking, was imparted with a "permanent" shape above a critical transition temperature (T_{trans}) when it was cast in a mold. Such a permanent shape, formed at the elastic state of the material without external stress, was retained (memorized) as the SMP cools to a temperature below its T_{trans}. The reported POSS-SMPs have great potential as self-fitting tissue scaffolds and implants, for instance, in the reconstruction of skeletal and craniofacial defects that are characterized with complex and irregular geometries, particularly at weight-bearing locations [445].

Homo- and hetero-arm star-shaped inorganic–organic hybrid polymers with a polyhedral oligomeric silsesquioxane (POSS) core were also prepared via click chemistry of azide POSS [POSS-(N_3)$_8$], alkynyl poly(L-lactide), and alkynyl poly(ethylene oxide). The melting and crystallization behaviors of these polymers can be adjusted by altering the PLLA to PEG reagents ratio. The hybrid polymers showed different thermostabilities because of the different compositions of the polymers. The hydrophilicity of the star-shaped hybrid polymers could be improved and adjusted by the alteration of the composition of PLLA and PEG segments. The hybrid polymers can self-assemble into micelles in water, and the micelles were characterized by DLS and TEM. The size of the micelles changed with the change of the ratio of PLLA and PEG in polymers [348].

Polyhedral oligomeric silsesquioxane (POSS) initiated the ring-opening copolymerization of a mixture of ε-caprolactone and L,L-lactide forming poly(ε-caprolactone-*co*-L,L-lactide) as the rubbery core; next the polymerization of D,D-lactide resulted in poly(D-lactide) (PDLA) as the outer shell. The outer PDLA layer could facilitate strong interactions between core – shell rubber particles and the PLLA matrix via formation of a stereocomplex [446].

13. Blends of linear PLA with star/branched PLA

One of the methods for the improving properties of PLA can be blending of the star and/or branched PLA with a linear one. Blends of linear PLLA and star-shaped PLA were reported in many papers [9, 27, 140, 219,232,334,369,413,447–449].

Multiple 4-arm star-shaped PLLAs, with various molar masses, were blended with commercial linear PLLA. The initial degradation temperature of linear PLLA was increased by blending with star PLLA. The use of star-shaped PLLA in the blend modified the runability, heat sealability, and barrier properties because of the increase in melt viscosity; at the same time, the thermal stability improved by branching of the polymer and shifting the start of degradation temperatures to higher temperatures [9]. Blends of the star-shaped PLLA with linear PLLA containing up to 30% branched structure revealed an increase in viscosity. A viscosity increase was evident even at 10% branched content [223]. It was reported that the elongation of the blend of star PLA random copolymers with PLLA increased with the number of arms of the copolymer [449].

After mixing of linear PLA with 3-arm star-shaped PLA, the remarkable flexibility and heat resistance of resulting material was observed, because the mixing of PLAs with different architectures increase the plasticization and crystallization of the blend [27]. Polymer blends consisting of linear PLLA and different proportions of dendritic PLLA-based copolyesters, characterized by different degrees of branching, showed more pronounced hydrophilic char-

acter and higher susceptibility to biodegradation with an increase in the degree of branching [346].

Solution blending investigations of linear PLLA with star/branched PDLA were reported [58, 59,297,447]. Star PDLA additives, along with their linear analogs, were melt blended with linear PLLA to promote the formation of the PDLA/PLLA stereocomplex [350]. The stereocomplex formation was observed during the addition of star PDLA into linear PLLA. Short chain-branched additives were applied commercially to commodity polymers to add ductility to highly crystalline morphologies. The addition of star PDLA generally resulted in the enhancement of the thermal, mechanical, and heat resistance of linear PLLA [350]. The incorporation of star PDLA chains into the linear PLLA matrix additionally caused the entanglements of chains apart from the formation of stereocomplexed segments. By contrast, only dendritic spherulites were formed in the highly disentangled blends [450].

The rheology of blends of linear and branched PLA architectures was comprehensively investigated [260]. It was reported that the presence of star-shaped PLLA increased the shear thinning, shear and extensional viscosity, and elastic modulus of linear PLLA. In addition to the presence of a branched architecture, physical cross-links because of the stereocomplex formation existed between PLLA and PDLA chains. Based on the rheological characterizations in shear and extensional mode, a great improvement in PLA melt rheological properties was observed for blends containing the stereocomplex structure compared with the linear/branched enantiopure blends [223].

The multi-arm PLLA accelerated the crystallization rate of PLLA by acting as a nucleating agent at environmental temperatures lower than its melting temperature, and the melting enthalpy of the PLLA/multi-arm PLLA blends increased greatly compared with that of linear PLLA. The increase in the viscosity of PLLA at low frequencies after adding multi-arm PLLA indicated strong interactions between PLLA and multi-arm PLLA. The tensile strength was increased up to 73.7 MPa with the increase of multi-arm PLLA up to 10% and achieved a maximum at 10% of star content. The homogeneous surface indicated better interfacial adhesion between PLLA and multi-arm PLLA phases, and the structural difference between PLLA and multi-arm PLLA had little influence on the compatibility of PLLA blends. Additionally, all PLLA/multi-arm PLLA blends showed low thermal stability compared with neat PLLA, and their thermal stabilities were observed to depend on the arm number and arm length of the multi-arm PLLA. These results showed that the multi-arm PLLA can not only function as a substituent for nucleating agents but can also be used as a melt enhancer [451].

Blends of a low-molar mass star copolymer of ε-caprolactone and D,L-lactide with a linear oligo(ε-caprolactone) were prepared and characterized as a possible biodegradable injectable drug-delivery vehicle. The melting characteristics, melt viscosity, and degree of crystallinity of the blends were measured, and an *in vitro* degradation study was performed over a period of twelve weeks. The star copolymer degraded fastest, with a more than 60% mass decrease over this period. The melt viscosity of the blends increased as the star copolymer content increased [98].

The preparation of other blends with star PLLA (or its copolymers) and linear polymers was also described [72,452,453]. For example, amorphous 6-arm star-shaped poly(D,L-lactide-*co*-glycolide)s that were toughened with poly(TMC-*co*-ε-CL) rubber had excellent mechanical properties in the blend [99].

14. Nanocomposites

Long-chain branched PLA (LCB-PLA) nanocomposites with different clay loadings were prepared via melt extrusion. Joncryl® ADR-4368 F, an epoxy-based chain extender (CE), was used to produce LCB-PLA nanocomposites by compounding the neat PLA with 0.8 wt.% of CE in the extruder [454]. Recently, the polymeric composites with 4-arm star PLA with a zinc porphyrin core immobilized on the surface of carbon nanotubes (CNTs) were constructed by a simple ultrasonic process using the non-covalent method. Because of the strong π–π interactions between CNTs and the zinc porphyrin of the star PLA, the CNT/PLA composites were easily obtained, while the intrinsic graphitic structure of CNTs was retained [455].

Enantiomeric PLAs that contain approximately 1 wt.% of multiwalled carbon nanotubes (MWCNTs) were prepared by the ring-opening polymerization of L,L-LA or D,D-LA in the presence of MWCNTs modified with organic spacers terminated with —OH groups. PLA stereocomplexes were prepared from equimolar mixtures of PLLA and PDLA additionally containing a small amount of MWCNT-*g*-PLA, either during precipitation from solution or during thin-film formation by the slow evaporation of the solvent. Moreover, their crystallization in the form of stereocomplexes after melting was completely reversible without the formation of any homo-chiral crystallites. On the other hand, the addition of MWCNTs (not modified with PLA) to the mixture of PLLA and PDLA did not improve the thermal properties of the obtained stereocomplexes. The reported results showed that the thermal stability of the high-molar-mass PLA stereocomplexes was strongly influenced by the presence of the PLA-functionalized MWCNTs, even though their concentration in the final material was as low as 0.5 wt.%. Shish-kebab morphologies for the thin-film stereocomplexes containing 1 wt.% of MWCNT-*g*-PLA were observed by atomic force microscopy [456].

The bio-stereocomplex-nanocomposite materials were also generated by the stereocomplexation of polylactide-graft-acetylated cellulosic nanowhiskers in the solution. Perfect stereocomplexes were easily obtained in a relatively short mixing time (5 min) from various solution concentrations up to 20% (w/v). The bio-stereocomplex-nanocomposites have excellent stereocomplex memory to re-form the stereocomplex after melting, which is the main limitation of stereocomplex materials in industrial processes [457].

15. Outlook

The increasing number of publications concerning the synthesis of branched and star-shaped polylactides demonstrate the great interest in this field. The alteration of the architecture from linear polylactide (PLA) to a star-shaped induces the modification of the polymer's physiochemical, mechanical, and diffusional properties. Therefore, the utility of star-shaped polymers increases for many applications; however, because of the biocompatibility of PLA, it is especially useful in biomedical applications or biocomposites. In biomedical applications, the star-shaped architecture of PLA macromolecules provides the unique opportunity to design specific properties by adjustment of the polymer degradation rate or the hydrophilicity with the desired application, such as control drug release rate.

In addition, the cross-linkable star PLA systems provide several advantages for biocomposite manufacturing, such as lower viscosities, good processability, and thermomechanical properties. Moreover, their extended network is more compatible with natural fibers, and all of these described features allows for the reduction of the biocomposite final costs. However, star polymers have a high number of end-groups that influence their properties and usually causes faster degradation, e.g., in the case of hydroxyl groups. Therefore, to increase their thermal stability a suitable stabilizer should be added. On the other hand, the possibility of the introduction of different groups at the arm ends in star polymers allows the

Please cite this article in press as: Michalski A, et al. Star-shaped and branched polylactides: Synthesis, characterization, and properties. Prog Polym Sci (2018), https://doi.org/10.1016/j.progpolymsci.2018.10.004

formation of the various chemically cross-linked structures, which could be thermolabile and/or chemically stable.

PLAs, especially PLAs with non-linear architecture, are notably expensive polymers, and they therefore will not be used as the mass materials and cannot replace common petrochemical polymers (e.g., polystyrene) in the near future. Therefore, biodegradable and biocompatible PLAs with sophisticated structures can be applied primarily in medicine, where the properties of the material are the most important and the price does not play a significant role. However, there is growing interest in the specific application of PLA as a filament in 3D printing.

Acknowledgements

The work was supported by the National Science Centre Poland grant No DEC-2013/09/B/ST5/03616 (Biela and Brzezinski) and grant No UMO-2013/09/B/ST5/03619 (Lapienis and Michalski).

References

[1] Pretula J, Slomkowski S, Penczek S. Polylactides-methods of synthesis and characterization. Adv Drug Deliv Rev 2016;107:3–16.
[2] Kale G, Auras R, Singh SP, Narayan R. Biodegradability of polylactide bottles in real and simulated composting conditions. Polym Test 2007;26:1049–61.
[3] Garlotta D. A literature review of poly(lactic acid). J Polym Environ 2002;9:63–84.
[4] Fambri L, Migiliaresi C. Crystallization and thermal properties. In: Auras R, Lim LT, Selke SEM, Tsuji H, editors. Poly(lactic acid): synthesis, structures, properties, processing, and applications. New York: John Wiley & Sons Inc; 2010. p. 113–24.
[5] Nampoothiri MK, Nair NR, John RP. An overview of the recent developments in polylactide (PLA) research. Bioresour Technol 2010;101:8493–501.
[6] Jamshidian M, Tehrany EA, Imran M, Jacquot M, Desobry S. Poly-lactic acid: production, applications, nanocomposites, and release studies. Compr Rev Food Sci Food Saf 2010;9:552–71.
[7] Jahandideh A, Muthukumarappan K. Star-shaped lactic acid based systems and their thermosetting resins; synthesis, characterization, potential opportunities and drawbacks. Eur Polym J 2017;87:360–79.
[8] Kim ES, Kim BC, Kim SH. Structural effect of linear and star-shaped poly(L-lactic acid) on physical properties. J Polym Sci Part B: Polym Phys 2004;42:939–46.
[9] Khajeheian MB, Rosling A. Preparation and characterization of linear and star-shaped poly L-lactide blends. J Appl Polym Sci 2016;133, 42231/1-8.
[10] Sawyer DJ. Bioprocessing - no longer a field of dreams. Macromol Symp 2003;201:271–81.
[11] Bogaert JC, Coszach P. Poly(lactic acids): a potential solution to plastic waste dilemma. Macromol Symp 2000;153:287–303.
[12] Raquez JM, Mincheva R, Coulembier O, Dubois P. Ring-opening polymerization of cyclic esters: industrial synthesis, properties, applications, and perspectives. In: Matyjaszewski K, Moller M, editors. Polymer science: a comprehensive reference. Amsterdam: Elsevier Ltd; 2012. p. 761–78.
[13] Duda A. ROP of cyclic esters. Mechanisms of ionic and coordination processes. In: Matyjaszewski K, Moller M, editors. Polymer science: a comprehensive reference. Amsterdam: Elsevier Ltd; 2012. p. 213–46.
[14] Lim LT, Auras R, Rubino M. Processing technologies for poly(lactic acid). Prog Polym Sci 2008;33:820–52.
[15] Drumright RE, Gruber PR, Henton DE. Polylactic acid technology. Adv Mater 2000;12:1841–6.
[16] Auras R, Harte B, Selke S. An overview of polylactides as packaging materials. Macromol Biosci 2004;4:835–64.
[17] Kricheldorf HR, Hachmann-Thiessen H, Schwarz G. Telechelic and star-shaped poly(L-lactide)s by means of bismuth(III) acetate as initiator. Biomacromolecules 2004;5:492–6.
[18] Finne A, Albertsson AC. Controlled synthesis of star-shaped L-Lactide polymers using new spirocyclic tin initiators. Biomacromolecules 2002;3:684–90.
[19] Tasaka F, Ohya Y, Ouchi T. One-pot synthesis of novel branched polylactide through the copolymerization of lactide with mevalonolactone. Macromol Rapid Commun 2001;22:820–4.
[20] Atthoff B, Trollsas M, Claesson H, Hedrick JL. Poly(lactides) with controlled molecular architecture initiated from hydroxyl functional dendrimers and the effect on the hydrodynamic volume. Macromol Chem Phys 1999;200:1333–9.
[21] Trollsas M, Atthoff B, Claesson H, Hedrick JL. Dendritic homopolymers and block copolymers: tuning the morphology and properties. J Polym Sci Part A: Polym Chem 2004;42:1174–88.
[22] Trollss M, Kelly MA, Claesson H, Siemens R, Hedrick JL. Highly branched block copolymers: design, synthesis, and morphology. Macromolecules 1999;32:4917–24.
[23] Jin F, Hyon SH, Iwata H, Tsutsumi S. Crosslinking of poly(L-lactide) by γ-irradiation. Macromol Rapid Commun 2002;23:909–12.
[24] Gottschalk C, Frey H. Hyperbranched polylactide copolymers. Macromolecules 2006;39:1719–23.
[25] Albertsson AC, Varma IK, Lochab B, Finne-Wistrand A, Kumar K. Design and synthesis of different types of poly(lactic acid). New York: John Wiley & Sons Inc; 2010. p. 43–58.
[26] Breitenbach A, Kissel T. Biodegradable comb polyesters: part 1. Synthesis, characterization and structural analysis of poly(lactide) and poly(lactide-co-glycolide) grafted onto water-soluble poly(vinyl alcohol) as backbone. Polymer 1998;39:3261–71.
[27] Corneillie S, Smet M. PLA architectures: the role of branching. Polym Chem 2015;6:850–67.
[28] Zhu KJ, Song B, Yang S. Super microcapsules(SMC). I. Preparation and characterization of star polyethylene oxide (PEO)-polylactide (PLA) copolymers. J Polym Sci Part A: Polym Chem 1989;27:2151–9.
[29] Cameron DJA, Shaver MP. Aliphatic polyester polymer stars: synthesis, properties and applications in biomedicine and nanotechnology. Chem Soc Rev 2011;40:1761–76.
[30] Lee SH, Kim SH, Han YK, Kim YH. Synthesis and degradation of end-group-functionalized polylactide. J Polym Sci Part A: Polym Chem 2001;39:973–85.
[31] Gupta AP, Kumar V. New emerging trends in synthetic biodegradable polymers - polylactide: a critique. Eur Polym J 2007;43:4053–74.
[32] Ren JM, McKenzie TG, Fu Q, Wong EHH, Xu J, An Z, et al. Star polymers. Chem Rev 2016;116:6743–836.
[33] Rasal RM, Janorkar AV, Hirt DE. Poly(lactic acid) modifications. Prog Polym Sci 2010;35:338–56.
[34] Zhang X, Wang C, Fang S, Sun J, Li C, Hu Y. Synthesis and characterization of well-defined star PLLA with a POSS core and their microspheres for controlled release. Colloid Polym Sci 2013;291:789–803.
[35] Bednarek M. Branched aliphatic polyesters by ring-opening (co)polymerization. Prog Polym Sci 2016;58:27–58.
[36] d'Arcy R, Burke J, Tirelli N. Branched polyesters: preparative strategies and applications. Adv Drug Deliv Rev 2016;107:60–81.
[37] Spinu M, Jackson C, Keating MY, Gardner KH. Material design in poly(lactic acid) systems: block copolymers, star homo- and copolymers, and stereocomplexes. J Macromol Sci Part A Pure Appl Chem 1996;33:1497–530.
[38] Yildirim I, Weber C, Schubert US. Old meets new: combination of PLA and RDRP to obtain sophisticated macromolecular architectures. Prog Polym Sci 2017;76:111–50.
[39] Hu S, Zhao J, Zhang G, Schlaad H. Macromolecular architectures through organocatalysis. Prog Polym Sci 2017;74:34–77.
[40] Hadjichristidis N, Pitsikalis M, Iatrou H, Driva P, Sakellariou G, Chatzichristidi M. Polymers with star-related structures: synthesis, properties, and applications. In: Matyjaszewski K, Moller M, editors. Polymer science: a comprehensive reference. Amsterdam: Elsevier Ltd; 2012. p. 29–111.
[41] Wurm F, Frey H. Hyperbranched polymers: synthetic methodology, properties, and complex polymer architectures. In: Matyjaszewski K, Moller M, editors. Polymer science: a comprehensive reference. Amsterdam: Elsevier Ltd; 2012. p. 177–98.
[42] Datta R, Henry M. Lactic acid: recent advances in products, processes and technologies - a review. J Chem Technol Biotechnol 2006;81:1119–29.
[43] Bhardwaj R, Mohanty AK. Advances in the properties of polylactides based materials: a review. J Biobased Mater Bioenergy 2007;1:191–209.
[44] Lasprilla AJR, Martinez GAR, Lunelli BH, Jardini AL, Maciel Filho R. Poly-lactic acid synthesis for application in biomedical devices - a review. Biotechnol Adv 2012;30:321–8.
[45] Bigg DM. Polylactide copolymers: effect of copolymer ratio and end capping on their properties. Adv Polym Technol 2005;24:69–82.
[46] Tsuji H, Sugiura Y, Sakamoto Y, Bouapao L, Itsuno S. Crystallization behavior of linear 1-arm and 2-arm poly(L-lactide)s: effects of coinitiators. Polymer 2008;49:1385–97.
[47] Maharana T, Pattanaik S, Routaray A, Nath N, Sutar AK. Synthesis and characterization of poly(lactic acid) based graft copolymers. React Funct Polym 2015;93:47–67.
[48] Jenkins AD, Kratochvil P, Stepto RFT, Suter UW. Glossary of basic terms in polymer science. Pure Appl Chem 1996;68:2287–311.
[49] Baron M, Hellwich KH, Hess M, Horie K, Jenkins AD, Jones RG, et al. Glossary of class names of polymers based on chemical structure and molecular architecture: (IUPAC recommendations 2009). Pure Appl Chem 2009;81:1131–86.
[50] Wilks ES. Compendium of polymer terminology and nomenclature: IUPAC recommednations 2008. Cambridge: Royal Society of Chemistry; 2009. p. 261–72.
[51] Gong F, Cheng X, Wang S, Wang Y, Gao Y, Cheng S. Biodegradable comb-dendritic tri-block copolymers consisting of poly(ethylene glycol) and poly(-lactide): synthesis, characterizations, and regulation of surface morphology and cell responses. Polymer 2009;50:2775–85.
[52] Yuan W, Zhu L, Huang X, Zheng S, Tang X. Synthesis, characterization and degradation of hexa-armed star-shaped poly(L-lactide)s and poly(D,L-lactide)s initiated with hydroxyl-terminated cyclotriphosphazene. Polym Degrad Stab 2005;87:503–9.
[53] Danko M, Libiszowski J, Wolszczak M, Racko D, Duda A. Fluorescence study of the dynamics of star-shaped poly(ε-caprolactone)s in THF: a comparison with a star-shaped poly(lactide)s. Polymer 2009;50:2209–19.
[54] McKee MG, Unal S, Wilkes GL, Long TE. Branched polyesters: recent advances in synthesis and performance. Prog Polym Sci 2005;30:507–39.

Please cite this article in press as: Michalski A, et al. Star-shaped and branched polylactides: Synthesis, characterization, and properties. Prog Polym Sci (2018), https://doi.org/10.1016/j.progpolymsci.2018.10.004

[55] Dong CM, Qiu KY, Gu ZW, Feng XD. Synthesis of star-shaped poly(ε-caprolactone)-b-poly(DL-lactic acid-alt-glycolic acid) with multifunctional initiator and stannous octoate catalyst. Macromolecules 2001;34:4691–6.
[56] Choi YK, Bae YH, Kim SW. Star-shaped poly(ether-ester) block copolymers: synthesis, characterization, and their physical properties. Macromolecules 1998;31:8766–74.
[57] Castillo RV, Mueller AJ. Crystallization and morphology of biodegradable or biostable single and double crystalline block copolymers. Prog Polym Sci 2009;34:516–60.
[58] Sakamoto Y, Tsuji H. Stereocomplex crystallization behavior and physical properties of linear 1-Arm, 2-Arm, and branched 4-Arm poly(L-lactide)/Poly(D-lactide) blends: effects of chain directional change and branching. Macromol Chem Phys 2013;214:776–86.
[59] Sakamoto Y, Tsuji H. Crystallization behavior and physical properties of linear 2-arm and branched 4-arm poly(l-lactide)s: effects of branching. Polymer 2013;54:2422–34.
[60] Moravek SJ, Messman JM, Storey RF. Polymerization kinetics of rac-lactide initiated with alcohol/stannous octoate using in situ attenuated total reflectance-fourier transform infrared spectroscopy: an initiator study. J Polym Sci Part A: Polym Chem 2009;47:797–803.
[61] Eldessouki M, Buschle-Diller G, Gowayed Y. Solution-based synthesis of a four-arm star-shaped poly(L-lactide). Des Monomers Polym 2016;19:180–92.
[62] Burts AO, Gao AX, Johnson JA. Brush-first synthesis of core-photodegradable miktoarm star polymers via ROMP: towards photoresponsive self-assemblies. Macromol Rapid Commun 2014;35:168–73.
[63] Zou J, Chen X, Jiang XB, Zhang J, Guo YB, Huang FR. Poly(L-lactide) nanocomposites containing octaglycidylether polyhedral oligomeric silsesquioxane: preparation, structure and properties. Express Polym Lett 2011;5:662–73.
[64] Hao Q, Li F, Li Q, Li Y, Jia L, Yang J, et al. Preparation and crystallization kinetics of new structurally well-defined star-shaped biodegradable poly(L-lactide)s initiated with diverse natural sugar alcohols. Biomacromolecules 2005;6:2236–47.
[65] Xu F, Zheng SZ, Luo YL. Thermosensitive t-PLA-b-PNIPAAm tri-armed star block copolymer nanoscale micelles for camptothecin drug release. J Polym Sci Part A: Polym Chem 2013;51:4429–39.
[66] Li Y, Kissel T. Synthesis, characteristics and in vitro degradation of star-block copolymers consisting of L-lactide, glycolide and branched multi-arm poly(ethylene oxide). Polymer 1998;39:4421–7.
[67] Li CY, Hsu SJ, Cl Lin, Tsai CY, Wang JH, Ko BT, et al. Air-stable copper derivatives as efficient catalysts for controlled lactide polymerization: facile synthesis and characterization of well-defined benzotriazole phenoxide copper complexes. J Polym Sci Part A: Polym Chem 2013;51:3840–9.
[68] Shao J, Tang ZH, Sun JR, Li G, Chen XS. Linear and four-armed poly(L-lactide)-block-poly(D-lactide) copolymers and their stereocomplexation with poly(lactide)s. J Polym Sci Part B: Polym Phys 2014;52:1560–7.
[69] Yuan MW, He ZG, Li HL, Jiang L, Yuan ML. Synthesis and characterization of star polylactide by ring-opening polymerization of L-lactic acid O-carboxyanhydride. Polym Bull (Berl) 2014;71:1331–47.
[70] Alba A, du Boullay OT, Martin-Vaca B, Bourissou D. Direct ring-opening of lactide with amines: application to the organo-catalyzed preparation of amide end-capped PLA and to the removal of residual lactide from PLA samples. Polym Chem 2015;6:989–97.
[71] Ristic IS, Marinovic-Cincovic M, Cakic SM, Tanasic LM, Budinski-Simendic JK. Synthesis and properties of novel star-shaped polyesters based on L-lactide and castor oil. Polym Bull (Berl) 2013;70:1723–38.
[72] Takase H, Shibita A, Shibata M. Semi-interpenetrating polymer networks composed of diisocyanate-bridged 4-Arm star-shaped L-Lactide oligomers and poly(epsilon-caprolactone). J Polym Sci Part B: Polym Phys 2014;52:1420–8.
[73] Satoh T, Tamaki M, Kitajyo Y, Maeda T, Ishihara H, Imai T, et al. Synthesis of unimolecular reversed micelle consisting of a poly(L-lactide) shell and hyperbranched D-mannan core. J Polym Sci Part A: Polym Chem 2005;44:406–13.
[74] Coulembier O, Kiesewetter MK, Mason A, Dubois P, Hedrick JL, Waymouth RM. A distinctive organocatalytic approach to complex macromolecular architectures. Angew Chem Int Ed 2007;46:4719–21.
[75] Kim SH, Han YK, Kim YH, Hong SI. Multifunctional initiation of lactide polymerization by stannous octoate/pentaerythritol. Makromol Chem 1992;193:1623–31.
[76] Lang M, Wong RP, Chu CC. Synthesis and structural analysis of functionalized poly(ε-caprolactone)-based three-arm star polymers. J Polym Sci Part A: Polym Chem 2002;40:1127–41.
[77] Lang M, Chu CC. Functionalized multiarm poly(ε-caprolactone)s: synthesis, structure analysis, and network formation. J Appl Polym Sci 2002;86:2296–306.
[78] Schoemer M, Frey H. Organobase-catalyzed synthesis of multiarm star polylactide with hyperbranched poly(ethylene glycol) as the core. Macromol Chem Phys 2011;212:2478–86.
[79] Zhao Y, Shuai X, Chen C, Xi F. Synthesis and characterization of star-shaped poly(L-lactide)s initiated with hydroxyl-terminated poly(Amidoamine) (PAMAM-OH) dendrimers. Chem Mater 2003;15:2836–43.
[80] Cai C, Wang L, Dong CM. Synthesis, characterization, effect of architecture on crystallization, and spherulitic growth of poly(L-lactide)-b-poly(ethylene oxide) copolymers with different branch arms. J Polym Sci Part A: Polym Chem 2006;44:2034–44.
[81] Tsuji H, Miyase T, Tezuka Y, Saha SK. Physical properties, crystallization, and spherulite growth of linear and 3-Arm poly(L-lactide)s. Biomacromolecules 2005;6:244–54.
[82] Dong CM, Qiu KY, Gu ZW, Feng XD. Synthesis of star-shaped poly(D,L-lactic acid-alt-glycolic acid)-b-poly(L-lactic acid) with the poly(D,L-lactic acid-alt-glycolic acid) macroinitiator and stannous octoate catalyst. J Polym Sci Part A: Polym Chem 2001;40:409–15.
[83] Penczek S, Cypryk M, Duda A, Kubisa P, Slomkowski S. Living ring-opening polymerization of heterocyclic monomers. In: Müller AHE, Matyjaszewski K, editors. Controlled and living polymerizations. Weinheim: Wiley-VCH Verlag GMBH & CO KGaA; 2009. p. 241–96.
[84] Kricheldorf HR, Ahrensdorf K, Polylactones Rost S. 68: star-shaped homo- and copolyesters derived from ε-caprolactone, L,L-lactide and trimethylene carbonate. Macromol Chem Phys 2004;205:1602–10.
[85] Korhonen H, Helminen A, Seppala JV. Synthesis of polylactides in the presence of co-initiators with different numbers of hydroxyl groups. Polymer 2001;42:7541–9.
[86] George KA, Schue F, Chirila TV, Wentrup-Byrne E. Synthesis of four-arm star poly(L-lactide) oligomers using an in situ-generated calcium-based initiator. J Polym Sci Part A: Polym Chem 2009;47:4736–48.
[87] Kowalski A, Libiszowski J, Biela T, Cypryk M, Duda A, Penczek S. Kinetics and mechanism of cyclic esters polymerization initiated with tin(II) octoate. Polymerization of ε-Caprolactone and L,L-Lactide Co-initiated with primary amines. Macromolecules 2005;38:8170–6.
[88] Karidi K, Pladis P, Kiparissides C. A theoretical and experimental kinetic investigation of the ROP of L,L-Lactide in the presence of polyalcohols. Macromol Symp 2013;333:206–15.
[89] Gottschalk C, Wolf F, Frey H. Multi-arm star poly(L-lactide) with hyperbranched polyglycerol core. Macromol Chem Phys 2007;208:1657–65.
[90] Wang L, Dong CM. Synthesis, crystallization kinetics, and spherulitic growth of linear and star-shaped poly(L-lactide)s with different numbers of arms. J Polym Sci Part A: Polym Chem 2006;44:2226–36.
[91] Kundys A, Plichta A, Florjanczyk Z, Zychewicz A, Lisowska P, Parzuchowski P, et al. Multi-arm star polymers of lactide obtained in melt in the presence of hyperbranched oligoglycerols. Polym Int 2016;65:927–37.
[92] Odelius K, Finne A, Albertsson AC. Versatile and controlled synthesis of resorbable star-shaped polymers using a spirocyclic tin initiator-reaction optimization and kinetics. J Polym Sci Part A: Polym Chem 2005;44:596–605.
[93] Geschwind J, Rathi S, Tonhauser C, Schoemer M, Hsu SL, Coughlin EB, et al. Stereocomplex formation in polylactide multiarm stars and comb copolymers with linear and hyperbranched multifunctional PEG. Macromol Chem Phys 2013;214:1434–44.
[94] Odelius K, Albertsson AC. Precision synthesis of microstructures in star-shaped copolymers of ε-caprolactone, L-lactide, and 1,5-dioxepan-2-one. J Polym Sci Part A: Polym Chem 2008;46:1249–64.
[95] Kricheldorf HR, Polylactones Fechner B. 59. Biodegradable networks via ring-expansion polymerization of lactones and Lactides with a spirocyclic tin initiator. Biomacromolecules 2002;3:691–5.
[96] Kricheldorf HR, Fechner B. Polylactones. LVIII. Star-shaped polylactones with functional end groups via ring-expansion polymerization with a spiroinitiator. J Polym Sci Part A: Polym Chem 2002;40:1047–57.
[97] Finne A, Albertsson AC. Polyester hydrogels with swelling properties controlled by the polymer architecture, molecular weight, and crosslinking agent. J Polym Sci Part A: Polym Chem 2003;41:1296–305.
[98] Tomkins A, Kontopoulou M, Amsden B. Preparation and characterization of blends of star-poly(ε-caprolactone-co-D,L-lactide) and oligo(ε-caprolactone). J Biomater Sci Polym Ed 2005;16:1009–21.
[99] Joziasse CAP, Veenstra H, Topp MDC, Grijpma DW, Pennings AJ. Rubber toughened linear and star-shaped poly(d,l-lactide-co-glycolide): synthesis, properties and in vitro degradation. Polymer 1997;39:467–73.
[100] Lemmouchi Y, Perry MC, Amass AJ, Chakraborty K, Schacht E. Novel synthesis of biodegradable star poly(ethylene glycol)-block-poly(lactide) copolymers. J Polym Sci Part A: Polym Chem 2007;45:3966–74.
[101] Lemmouchi Y, Perry MC, Amass AJ, Chakraborty K, Schacht E. Novel synthesis of biodegradable linear and star block copolymers based on ε-caprolactone and lactides using potassium-based catalyst. J Polym Sci Part A: Polym Chem 2008;46:5363–70.
[102] Numata K, Srivastava RK, Finne-Wistrand A, Albertsson AC, Doi Y, Abe H. Branched poly(lactide) synthesized by enzymatic polymerization: effects of molecular branches and stereochemistry on enzymatic degradation and alkaline hydrolysis. Biomacromolecules 2007;8:3115–25.
[103] Sobczak M, Witkowska E, Oledzka E, Kolodziejski W. Synthesis and structural analysis of polyester prodrugs of norfloxacin. Molecules 2008;13:96–106.
[104] Malberg S, Basalp D, Finne-Wistrand A, Albertsson AC. Bio-safe synthesis of linear and branched PLLA. J Polym Sci Part A: Polym Chem 2010;48:1214–9.
[105] Coulembier O, Dove AP, Pratt RC, Sentman AC, Culkin DA, Mespouille L, et al. Latent, thermally activated organic catalysts for the on-demand living polymerization of lactide. Angew Chem Int Ed 2005;44:4964–8.
[106] Johnson RM, Fraser CL. Metalloinitiation routes to biocompatible poly(lactic acid) and poly(acrylic acid) stars with luminescent ruthenium tris(bipyridine) cores. Biomacromolecules 2004;5:580–8.
[107] Kakwere H, Perrier S. Facile synthesis of star-shaped copolymers via combination of RAFT and ring opening polymerization. J Polym Sci Part A: Polym Chem 2009;47:6396–408.

Please cite this article in press as: Michalski A, et al. Star-shaped and branched polylactides: Synthesis, characterization, and properties. Prog Polym Sci (2018), https://doi.org/10.1016/j.progpolymsci.2018.10.004

[108] Coady DJ, Engler AC, Yang YY, Hedrick JL. Facile routes to star polymers via an organocatalytic approach. Polym Chem 2011;2:2619–26.
[109] Shaver MP, Cameron DJA. Tacticity control in the synthesis of poly(lactic acid) polymer stars with dipentaerythritol cores. Biomacromolecules 2010;11:3673–9.
[110] Stanford MJ, Dove AP. One-pot synthesis of α,ω-Chain end functional, stereoregular, star-shaped poly(lactide). Macromolecules 2009;42:141–7.
[111] Zhao W, Cui D, Liu X, Chen X. Facile synthesis of hydroxyl-ended, highly stereoregular, star-shaped poly(lactide) from immortal ROP of rac-lactide and kinetics study. Macromolecules 2010;43:6678–84.
[112] Hiemstra C, Zhong Z, Li L, Dijkstra PJ, Feijen J. In-situ formation of biodegradable hydrogels by stereocomplexation of PEG-(PLLA)8 and PEG-(PDLA)8 star block copolymers. Biomacromolecules 2006;7:2790–5.
[113] Hiemstra C, Zhou W, Zhong Z, Wouters M, Feijen J. Rapidly in situ forming biodegradable robust hydrogels by combining stereocomplexation and photopolymerization. J Am Chem Soc 2007;129:9918–26.
[114] Guerin W, Helou M, Carpentier JF, Slawinski M, Brusson JM, Guillaume SM. Macromolecular engineering via ring-opening polymerization (1): L-lactide/trimethylene carbonate block copolymers as thermoplastic elastomers. Polym Chem 2013;4:1095–106.
[115] Luo SH, Wang QF, Xiong JF, Wang ZY. Synthesis of biodegradable material poly(lactic acid-co-sorbitol) via direct melt polycondensation and its reaction mechanism. J Polym Res 2012;19, 9962/1-9.
[116] Kim SH, Kim YH. Direct condensation polymerization of lactic acid. Macromol Symp 1999;144:277–87.
[117] Tsuji H, Suzuki M. Hetero-Stereocomplex Crystallization between Star-Shaped 4-Arm Poly(L-2-hydroxybutanoic acid) and Poly(D-lactic acid) from the Melt. Macromol Chem Phys 2014;215:1879–88.
[118] Lin Y, Zhang A, Wang L. Synthesis and characterization of star-shaped poly(ethylene glycol)-block-poly(L-lactic acid) copolymers by melt polycondensation. J Appl Polym Sci 2012;124:4496–501.
[119] Xiong JF, Wang QF, Peng P, Shi J, Wang ZY, Yang Cl. Design, synthesis, and characterization of a potential flame retardant poly(lactic acid-co-pyrimidine-2,4,5,6-tetramine) via direct melt polycondensation. J Appl Polym Sci 2014;131, 40275/1-10.
[120] Abiko A, Sy Yano, Iguchi M. Star-shaped poly(lactic acid) with carboxylic acid terminal groups via poly-condensation. Polymer 2012;53:3842–8.
[121] Michalski A, Makowski T, Biedron T, Brzezinski M, Biela T. Controlling polylactide stereocomplex (sc-PLA) self-assembly: from microspheres to nanoparticles. Polymer 2016;90:242–8.
[122] Kulkarni A, Lele A, Sivaram S, Rajamohanan PR, Velankar S, Chatterji A. Star telechelic poly(L-lactide) ionomers. Macromolecules 2015;48:6580–8.
[123] Gu WX, Zhu MR, Song N, Du XX Yang YW, Gao H. Reverse micelles based on biocompatible beta-cyclodextrin conjugated polyethylene glycol block polylactide for protein delivery. J Mater Chem B Mater Biol Med 2015;3:316–22.
[124] George KA, Chirila TV, Wentrup-Byrne E. Carbodiimide-mediated synthesis of poly(L-lactide)-based networks. Polymer 2010;51:1670–8.
[125] Prabaharan M, Grailer JJ, Pilla S, Steeber DA, Gong S. Folate-conjugated amphiphilic hyperbranched block copolymers based on Boltorn H40, poly(L-lactide) and poly(ethylene glycol) for tumor-targeted drug delivery. Biomaterials 2009;30:3009–19.
[126] Cao W, Zhu L. Synthesis and unimolecular micelles of amphiphilic dendrimer-like star polymer with various functional surface groups. Macromolecules 2011;44:1500–12.
[127] Suneel, Buzza DMA, Groves DJ, McLeish TCB, Parker D, Keeney AJ, et al. Rheology and molecular weight distribution of hyperbranched polymers. Macromolecules 2002;35:9605–12.
[128] Tuominen J, Kylma J, Seppala J. Chain extending of lactic acid oligomers. 2. Increase of molecular weight with 1,6-hexamethylene diisocyanate and 2,2'-bis(2-oxazoline). Polymer 2001;43:3–10.
[129] Zhao Y, Shuai X, Chen C, Xi F. Synthesis of novel dendrimer-like star block copolymers with definite numbers of arms by combination of ROP and ATRP. Chem Commun (Camb) 2004:1608–9.
[130] Ni C, Zhu G, Zhu C, Yao B, Kumar DNT. Studies on core-shell structural nano-micelles based on star block copolymer of poly(lactide) and poly(2-(dimethylamino)ethyl methacrylate). Colloid Polym Sci 2010;288:1193–200.
[131] Zhao Y, Shuai X, Chen C, Xi F. Synthesis of star block copolymers from dendrimer initiators by combining ring-opening polymerization and atom transfer radical polymerization. Macromolecules 2004;37:8854–62.
[132] Yuan W, Yuan J, Zheng S, Hong X. Synthesis, characterization, and controllable drug release of dendritic star-block copolymer by ring-opening polymerization and atom transfer radical polymerization. Polymer 2007;48:2585–94.
[133] Qian XM, Long LX, Shi ZD, Liu CY, Qiu MZ, Sheng J, et al. Star-branched amphiphilic PLA-b-PDMAEMA copolymers for co-delivery of miR-21 inhibitor and doxorubicin to treat glioma. Biomaterials 2014;35:2322–35.
[134] Danko M, Libiszowski J, Biela T, Wolszczak M, Duda A. Molecular dynamics of star-shaped poly(l-lactide)s in tetrahydrofuran as solvent monitored by fluorescence spectroscopy. J Polym Sci Part A: Polym Chem 2005;43:4586–99.
[135] Concellon A, Asin L, Gonzalez-Lana S, de la Fuente JM, Sanchez-Somolinos C, Pinol M, et al. Photopolymers based on ethynyl-functionalized degradable polylactides by thiol-yne' Click Chemistry'. Polymer 2017;117:259–67.
[136] Nagahama K, Ouchi T, Ohya Y. Temperature-induced hydrogels through self-assembly of cholesterol-substituted star PEG-b-PLLA copolymers: an injectable scaffold for tissue engineering. Adv Funct Mater 2008;18:1220–31.
[137] Long LX, Zhao J, Li K, He LG, Qian XM, Liu CY, et al. Synthesis of star-branched PLA-b-PMPC copolymer micelles as long blood circulation vectors to enhance tumor-targeted delivery of hydrophobic drugs in vivo. Mater Chem Phys 2016;180:184–94.
[138] Karikari AS, Mather BD, Long TE. Association of star-shaped poly(D,L-lactide)s containing nucleobase multiple hydrogen bonding. Biomacromolecules 2007;8:302–8.
[139] Chang SK, Zeng C, Li J, Ren J. Synthesis of polylactide-based thermoset resin and its curing kinetics. Polym Int 2012;61:1492–502.
[140] Karikari AS, Edwards WF, Mecham JB, Long TE. Influence of peripheral hydrogen bonding on the mechanical properties of photo-cross-Linked star-shaped poly(D,L-lactide) networks. Biomacromolecules 2005;6:2866–74.
[141] Kusmierczuk M, Noechel U, Baudis S, Behl M, Kratz K, Lendlein A. Shape-memory polymer networks prepared from star-shaped poly[(L-lactide)-co-glycolide]. Macromol Symp 2014;345:98–104.
[142] Helminen AO, Korhonen H, Seppala JV. Crosslinked poly(ε-caprolactone/DL-lactide) copolymers with elastic properties. Macromol Chem Phys 2002;203:2630–9.
[143] Moeinzadeh S, Khorasani SN, Ma J, He X, Jabbari E. Synthesis and gelation characteristics of photo-crosslinkable star Poly(ethylene oxide-co-lactide-glycolide acrylate) macromonomers. Polymer 2011;52:3887–96.
[144] Buwalda SJ, Dijkstra PJ, Feijen J. In situ forming poly(ethylene glycol)- poly(L-lactide) hydrogels via Michael addition: mechanical properties, degradation, and protein release. Macromol Chem Phys 2012;213:766–75.
[145] Sakai R, John B, Okamoto M, Seppaelae JV, Vaithilingam J, Hussein H, et al. Fabrication of polylactide-based biodegradable thermoset scaffolds for tissue engineering applications. Macromol Mater Eng 2013;298:45–52.
[146] Goddard AR, Perez-Nieto S, Passos TM, Quilty B, Carmichael K, Irvine DJ, et al. Controlled polymerisation and purification of branched poly(lactic acid) surfactants in supercritical carbon dioxide. Green Chem 2016;18:4772–86.
[147] Karikari AS, Williams SR, Heisey CL, Rawlett AM, Long TE. Porous thin films based on photo-cross-Linked star-shaped poly(D,L-lactide)s. Langmuir 2006;22:9687–93.
[148] Amsden BG, Tse MY, Turner ND, Knight DK, Pang SC. In vivo degradation behavior of photo-cross-Linked star-poly(ε-caprolactone-co-D,L-lactide) elastomers. Biomacromolecules 2006;7:365–72.
[149] Chapanian R, Tse MY, Pang SC, Amsden BG. Long term in vivo degradation and tissue response to photo-cross-linked elastomers prepared from star-shaped prepolymers of poly(ε-caprolactone-co-D,L-lactide). J Biomed Mater Res Part B Appl Biomater 2010;92:830–42.
[150] Xie MH, Ge J, Xue YM, Du YZ Lei B, Ma PX. Photo-crosslinked fabrication of novel biocompatible and elastomeric star-shaped inositol-based polymer with highly tunable mechanical behavior and degradation. J Mech Behav Biomed Mater 2015;51:163–8.
[151] Aoyagi T, Miyata F, Nagase Y. Preparation of cross-linked aliphatic polyester and application to thermo-responsive material. J Control Release 1994;32:87–96.
[152] Jahandideh A, Muthukumarappan K. Synthesis, characterization and curing optimization of a biobased thermosetting resin from xylitol and lactic acid. Eur Polym J 2016;83:344–58.
[153] Aakesson D, Skrifvars M, Seppaelae J, Turunen M, Martinelli A, Matic A. Synthesis and characterization of a lactic acid-based thermoset resin suitable for structural composites and coatings. J Appl Polym Sci 2010;115:480–6.
[154] Helminen AO, Korhonen H, Seppala JV. Structure modification and crosslinking of methacrylated polylactide oligomers. J Appl Polym Sci 2002;86:3616–24.
[155] Aakesson D, Skrifvars M, Seppaelae J, Turunen M. Thermoset lactic acid-based resin as a matrix for flax fibers. J Appl Polym Sci 2011;119:3004–9.
[156] Inoue K, Yamashiro M, Iji M. Recyclable shape-memory polymer: poly(lactic acid) crosslinked by a thermoreversible Diels-Alder reaction. J Appl Polym Sci 2009;112:876–85.
[157] Ben-Shabat S, Kumar N, Domb AJ. PEG-PLA block copolymer as potential drug carrier: preparation and characterization. Macromol Biosci 2006;6:1019–25.
[158] Tao W, Zeng X, Liu T, Wang Z, Xiong Q, Ouyang C, et al. Docetaxel-loaded nanoparticles based on star-shaped mannitol-core PLGA-TPGS diblock copolymer for breast cancer therapy. Acta Biomater 2013;9:8910–20.
[159] Zeng X, Tao W, Mei L, Huang L, Tan C, Feng SS. Cholic acid-functionalized nanoparticles of star-shaped PLGA-vitamin E TPGS copolymer for docetaxel delivery to cervical cancer. Biomaterials 2013;34:6058–67.
[160] Wang T, Zhu DW, Liu G, Tao W, Cao W, Zhang LH, et al. DTX-loaded star-shaped TAPP-PLA-b-TPGS nanoparticles for cancer chemical and photodynamic combination therapy. RSC Adv 2015;5:50617–27.
[161] Tang X, Cai S, Zhang R, Liu P, Chen H, Zheng Y, et al. Paclitaxel-loaded nanoparticles of star-shaped cholic acid-core PLA-TPGS copolymer for breast cancer treatment. Nanoscale Res Lett 2013;8, 420/1-12.
[162] Wolf FK, Frey H. Inimer-promoted synthesis of branched and hyperbranched polylactide copolymers. Macromolecules 2009;42:9443–56.
[163] Bao J, Chang X, Xie Q, Yu C, Shan G, Bao Y, et al. Preferential formation of β-Form crystals and temperature-dependent polymorphic structure in supramolecular poly(L-lactic acid) bonded by multiple hydrogen bonds. Macromolecules 2017;50:8619–30.
[164] Socka M, Brzezinski M, Michalski A, Kacprzak A, Makowski T, Duda A. Self-assembly of triblock copolymers from cyclic esters as a tool for tuning their particle morphology. Langmuir 2018;34:3701–10.
[165] Bao J, Chang R, Shan G, Bao Y, Pan P. Promoted stereocomplex crystallization in supramolecular stereoblock copolymers of enantiomeric poly(Lactic acid)s. Cryst Growth Des 2016;16:1502–11.

Please cite this article in press as: Michalski A, et al. Star-shaped and branched polylactides: Synthesis, characterization, and properties. Prog Polym Sci (2018), https://doi.org/10.1016/j.progpolymsci.2018.10.004

[166] Inkinen S, Nobes GA, Soedergard A. Telechelic poly(L-lactic acid) for dilactide production and prepolymer applications. J Appl Polym Sci 2011;119:2602–10.
[167] Cheng S, Yang L, Gong F. Novel branched poly(L-lactide) with poly(glycerol-co-sebacate) core. Polym Bull (Berl) 2010;65:643–55.
[168] Dai XH, Wang ZM, Liu W, Dong CM, Pan JM, Yuan SS, et al. Biomimetic star-shaped porphyrin-cored poly(L-lactide)-b-glycopolymer block copolymers for targeted photodynamic therapy. Colloid Polym Sci 2014;292:2111–22.
[169] Ahn NY, Seo M. Heteroarm core cross-linked star polymers via RAFT copolymerization of styrene and bismaleimide. RSC Adv 2016;6:47715–22.
[170] Dai XH, Jin H, Cai MH, Wang H, Zhou ZP, Pan JM, et al. Fabrication of thermosensitive, star-shaped poly(L-lactide)-block-poly(N-isopropylacrylamide) copolymers with porphyrin core for photodynamic therapy. React Funct Polym 2015;89:9–17.
[171] Leng X, Ren Y, Wei Z, Bian Y, Li Y. Synthesis of star-comb double crystalline diblock copolymer of poly(ε-caprolactone)-block-poly(L-lactide): effect of chain topology on crystallization behavior. Macromol Chem Phys 2017;218, 1700178/1-9.
[172] Yao N, Lin WJ, Zhang XF, Gu HW, Zhang LJ. Amphiphilic beta-cyclodextrin-Based star-like block copolymer unimolecular micelles for facile in situ preparation of gold nanoparticles. J Polym Sci Part A: Polym Chem 2016;54:186–96.
[173] Zhang XF, Lin WJ, Wen LY, Yao N, Nie SY, Zhang LJ. Systematic design and application of unimolecular star-like block copolymer micelles: a coarsegrained simulation study. Phys Chem Chem Phys 2016;18:26519–29.
[174] Hadjichristidis N. Synthesis of Miktoarm star (μ-star) polymers. J Polym Sci Part A: Polym Chem 1999;37:857–71.
[175] Pitsikalis M, Pispas S, Mays JW, Hadjichristidis N. Nonlinear block copolymer architectures. Adv Polym Sci 1998;135:1–137.
[176] Hadjichristidis N, Pispas S, Pitsikalis M, Iatrou H, Vlahos C. Asymmetric star polymers: synthesis and properties. Adv Polym Sci 1999;142:71–127.
[177] Hadjichristidis N, Pitsikalis M, Pispas S, Iatrou H. Polymers with complex architecture by living anionic polymerization. Chem Rev 2001;101:3747–92.
[178] Gorczynski JL, Chen J, Fraser CL. Iron tris(dibenzoylmethane)-centered polylactide stars: multiple roles for the metal complex in lactide ring-opening polymerization. J Am Chem Soc 2005;127:14956–7.
[179] Bender JL, Corbin PS, Fraser CL, Metcalf DH, Richardson FS, Thomas EL, et al. Site-isolated luminescent europium complexes with polyester macroligands: metal-centered heteroarm stars and nanoscale assemblies with labile block junctions. J Am Chem Soc 2002;124:8526–7.
[180] Chen J, Gorczynski JL, Zhang G, Fraser CL. Iron Tris(dibenzoylmethane-polylactide). Macromolecules 2010;43:4909–20.
[181] Smith AP, Fraser CL. Ruthenium-centered heteroarm stars by a modular coordination approach: effect of polymer composition on rates of chelation. Macromolecules 2003;36:5520–5.
[182] Fiore GL, Klinkenberg JL, Fraser CL. Iron tris(bipyridine)-Centered poly(ethylene glycol)-Poly(lactic acid) star block copolymers. Macromolecules 2008;41:9397–405.
[183] Corbin PS, Webb MP, McAlvin JE, Fraser CL. Biocompatible polyester macroligands: new subunits for the assembly of star-shaped polymers with luminescent and cleavable metal cores. Biomacromolecules 2001;2:223–32.
[184] Froehling P, Brackman J. Properties and applications of poly(propylene imine) dendrimers and poly(esteramide) hyperbranched polymers. Macromol Symp 2000;151:581–9.
[185] Klajnert B, Bryszewska M. Dendrimers: properties and applications. Acta Biochim Pol 2001;48:199–208.
[186] Malkoch M, Malmstrom E, Nystrom AM. Dendrimers: properties and applications. In: Matyjaszewski K, Moller M, editors. Polymer science: a comprehensive reference. Amsterdam: Elsevier Ltd; 2012. p. 113–76.
[187] Zhang W, Zheng S. Synthesis and characterization of dendritic star poly(L-Lactide)s. Polym Bull (Berl) 2007;58:767–75.
[188] Yuan W, Yuan J, Zhou M, Sui X. Synthesis, characterization, and thermal properties of dendrimer-star, block-comb copolymers by ring-opening polymerization and atom transfer radical polymerization. J Polym Sci Part A: Polym Chem 2006;44:6575–86.
[189] Biela T, Polanczyk I. One-pot synthesis of star-shaped aliphatic polyesters with hyperbranched cores and their characterization with size exclusion chromatography. J Polym Sci Part A: Polym Chem 2006;44:4214–21.
[190] Park S, Cho D, Im K, Chang T, Uhrig D, Mays JW. Utility of interaction chromatography for probing structural purity of model branched copolymers: 4-Miktoarm star copolymer. Macromolecules 2003;36:5834–8.
[191] Nederberg F, Appel E, Tan JPK, Kim SH, Fukushima K, Sly J, et al. Simple approach to stabilized micelles employing miktoarm terpolymers and stereocomplexes with application in paclitaxel delivery. Biomacromolecules 2009;10:1460–8.
[192] Voit BI, Lederer A. Hyperbranched and highly branched polymer architectures-synthetic strategies and major characterization aspects. Chem Rev 2009;109:5924–73.
[193] Arvanitoyannis I, Nakayama A, Kawasaki N, Yamamoto N. Novel star-shaped polylactide with glycerol using stannous octoate or tetraphenyl tin as catalyst: 1. Synthesis, characterization and study of their biodegradability. Polymer 1995;36:2947–56.
[194] Arvanitoyannis I, Nakayama A, Kawasaki N, Yamamoto N. Novel polylactides with aminopropanediol or aminohydroxymethylpropanediol using stannous octoate as catalyst; synthesis, characterization and study of their biodegradability. 2. Polymer 1995;36:2271–9.
[195] Helminen A, Korhonen H, Seppala JV. Biodegradable crosslinked polymers based on triethoxysilane terminated polylactide oligomers. Polymer 2001;42:3345–53.
[196] Grijpma DW, Joziasse CAP, Pennings AJ. Star-shaped polylactide-containing block copolymers. Makromol Chem Rapid Commun 1993;14:155–61.
[197] Zhao YL, Cai Q, Jiang J, Shuai XT, Bei JZ, Chen CF, et al. Synthesis and thermal properties of novel star-shaped poly(L-lactide)s with starburst PAMAM-OH dendrimer macroinitiator. Polymer 2002;43:5819–25.
[198] Arvanitoyannis I, Nakayama A, Psomiadou E, Kawasaki N, Yamamoto N. Synthesis and degradability of a novel aliphatic polyester based on L-lactide and sorbitol: 3. Polymer 1996;37:651–60.
[199] Joziasse CAP, Grablowitz H, Pennings AJ. Star-shaped poly[(trimethylene carbonate)-co-(ε-caprolactone)] and its block copolymers with lactide/glycolide. Synthesis, characterization, and properties. Macromol Chem Phys 2000;201:107–12.
[200] Bai H, Huang C, Xiu H, Zhang Q, Fu Q. Enhancing mechanical performance of polylactide by tailoring crystal morphology and lamellae orientation with the aid of nucleating agent. Polymer 2014;55:6924–34.
[201] Kratochvil P. Characterization of branched polymers. Macromol Symp 2000;152:279–87.
[202] Szymanski R. On the reshuffling of polymer segments in star polymer systems. Macromolecules 2002;35:8239–42.
[203] Franta E, Reibel L, Lehmann J, Penczek S. Use of mono- and multifunctional oxocarbenium salts in the polymerization of tetrahydrofuran. J Polym Sci Polym Symp 1976;56:139–48.
[204] Ji H, Sakellariou G, Advincula RC, Smith GD, Kilbey IISM, Dadmun MD, et al. Synthesis and characterization of well-defined [polystyrene-b-poly(2-vinylpyridine)]n star-block copolymers with poly(2-vinylpyridine) corona blocks. J Polym Sci Part A: Polym Chem 2007;45:3949–55.
[205] Wiltshire JT, Qiao GG. Selectively degradable core cross-linked star polymers. Macromolecules 2006;39:9018–27.
[206] Kilz P, Radke W. Application of two-dimensional chromatography to the characterization of macromolecules and biomacromolecules. Anal Bioanal Chem 2015;407:193–215.
[207] Kilz P. Two-dimensional chromatography as an essential means for understanding macromolecular structure. Chromatographia 2004;59:3–14.
[208] Pasch H, Adler M, Rittig F, Becker S. New developments in multidimensional chromatography of complex polymers. Macromol Rapid Commun 2005;26:438–44.
[209] Baumgaertel A, Altuntas E, Schubert US. Recent developments in the detailed characterization of polymers by multidimensional chromatography. J Chromatogr A 2012;1240:1–20.
[210] Skvortsov AM, Belen'kii BG, Gankina ES, Tennikov MB. Conformity between the behavior of a real macromolecule and the Gaussian chain during adsorption in pores. Vysokomol Soedin Ser A 1978;20:678–86.
[211] Entelis SG, Evreinov VV, Gorshkov AV. Functionality and molecular weight distribution of Telechelic polymers. Adv Polym Sci 1986;76:129–75.
[212] Biela T, Duda A, Pasch H, Rode K. Star-shaped poly(L-lactide)s with variable numbers of hydroxyl groups at polyester arms chain-ends and directly attached to the star-shaped core - controlled synthesis and characterization. J Polym Sci Part A: Polym Chem 2005;43:6116–33.
[213] Radke W, Rode K, Gorshkov AV, Biela T. Chromatographic behavior of functionalized star-shaped poly(lactide)s under critical conditions of adsorption. Comparison of theory and experiment. Polymer 2005;46:5456–65.
[214] Biela T, Duda A, Rode K, Pasch H. Characterization of star-shaped poly(L-lactide)s by liquid chromatography at critical conditions. Polymer 2003;44:1851–60.
[215] Biela T, Duda A, Penczek S, Rode K, Pasch H. Well-defined star polylactides and their behavior in two-dimensional chromatography. J Polym Sci Part A: Polym Chem 2002;40:2884–7.
[216] Jikei M, Suzuki M, Itoh K, Matsumoto K, Saito Y, Kawaguchi S. Synthesis of hyperbranched poly(L-lactide)s by self-polycondensation of AB2 macromonomers and their structural characterization by light scattering measurements. Macromolecules 2012;45:8237–44.
[217] Konkolewicz D, Monteiro MJ, Perrier S. Dendritic and hyperbranched polymers from macromolecular units: elegant approaches to the synthesis of functional polymers. Macromolecules 2011;44:7067–87.
[218] Corre YM, Duchet J, Reignier J, Maazouz A. Melt strengthening of poly (lactic acid) through reactive extrusion with epoxy-functionalized chains. Rheol Acta 2011;50:613–29.
[219] Pitet LM, Hait SB, Lanyk TJ, Knauss DM. Linear and branched architectures from the polymerization of Lactide with glycidol. Macromolecules 2007;40:2327–34.
[220] Dorgan JR, Williams JS, Lewis DN. Melt rheology of poly(lactic acid): entanglement and chain architecture effects. J Rheol (N Y N Y) 1999;43:1141–55.
[221] Izzo L, Pappalardo D. Tree-shapedčopolymers based on poly(ethylene glycol) and atactic or isotactic polylactides: synthesis and characterization. Macromol Chem Phys 2010;211:2171–8.
[222] Ikada Y, Jamshidi K, Tsuji H, Hyon SH. Stereocomplex formation between enantiomeric poly(lactides). Macromolecules 1987;20:904–6.
[223] Nouri S, Dubois C, Lafleur PG. Effect of chemical and physical branching on rheological behavior of polylactide. J Rheol (N Y N Y) 2015;59:1045–63.
[224] Magnusson H, Malmstrom E, Hult A, Johansson M. The effect of degree of branching on the rheological and thermal properties of hyperbranched aliphatic polyethers. Polymer 2001;43:301–6.

Please cite this article in press as: Michalski A, et al. Star-shaped and branched polylactides: Synthesis, characterization, and properties. Prog Polym Sci (2018), https://doi.org/10.1016/j.progpolymsci.2018.10.004

[225] Mannion AM, Bates FS, Macosko CW. Synthesis and rheology of branched multiblock polymers based on polylactide. Macromolecules 2016;49:4587–98.
[226] Carlson D, Dubois P, Nie L, Narayan R. Free radical branching of polylactide by reactive extrusion. Polym Eng Sci 1998;38:311–21.
[227] Liu J, Lou L, Yu W, Liao R, Li R, Zhou C. Long chain branching polylactide: structures and properties. Polymer 2010;51:5186–97.
[228] Deenadayalan E, Lele AK, Balasubramanian M. Reactive extrusion of poly(L-lactic acid) with glycidol. J Appl Polym Sci 2009;112:1391–8.
[229] Wang L, Jing X, Cheng H, Hu X, Yang L, Huang Y. Blends of linear and long-chain branched poly(l-lactide)s with high melt strength and fast crystallization rate. Ind Eng Chem Res 2012;51:10088–99.
[230] Dorgan JR, Janzen J, Clayton MP, Hait SB, Knauss DM. Melt rheology of variable L-content poly(lactic acid). J Rheol (N Y N Y) 2005;49:607–19.
[231] Ouchi T, Ichimura S, Ohya Y. Synthesis of branched poly(lactide) using polyglycidol and thermal, mechanical properties of its solution-cast film. Polymer 2006;47:429–34.
[232] Nouri S, Dubois C, Lafleur PG. Synthesis and characterization of polylactides with different branched architectures. J Polym Sci Part B: Polym Phys 2015;53:522–31.
[233] Basko M, Bednarek M, Kubisa P. Cationic copolymerization of L,L-lactide with hydroxyl substituted cyclic ethers. Polym Adv Technol 2015;26:804–13.
[234] Mena M, Lopez-Luna A, Shirai K, Tecante A, Gimeno M, Barzana E. Lipase-catalyzed synthesis of hyperbranched poly-L-lactide in an ionic liquid. Bioprocess Biosyst Eng 2013;36:383–7.
[235] Liu JY, Zhang SJ, Zhang LY, Bai YQ. Preparation and rheological characterization of long chain branching polylactide. Polymer 2014;55:2472–80.
[236] You J, Lou L, Yu W, Zhou C. The preparation and crystallization of long chain branching polylactide made by melt radicals reaction. J Appl Polym Sci 2013;129:1959–70.
[237] Li ZQ, Zhao XW, Ye L, Coates P, Caton-Rose F, Martyn M. Fibrillation of chain branched poly (lactic acid) with improved blood compatibility and bionic structure. Chem Eng J 2015;279:767–76.
[238] Zhao RX, Li L, Wang B, Yang WW, Chen Y, He XH, et al. Aliphatic tertiary amine mediated synthesis of highly branched polylactide copolymers. Polymer 2012;53:719–27.
[239] Fischer AM, Wolf FK, Frey H. Long-chain branched poly(Lactide)s based on polycondensation of AB2-type macromonomers. Macromol Chem Phys 2012;213:1349–58.
[240] Cooper TR, Storey RF. Poly(lactic acid) and chain-extended poly(lactic acid)-Polyurethane functionalized with pendent carboxylic acid groups. Macromolecules 2008;41:655–62.
[241] Liu MJ, Chen SC, Yang KK, Wang YZ. Biodegradable polylactide based materials with improved crystallinity, mechanical properties and rheological behaviour by introducing a long-chain branched copolymer. RSC Adv 2015;5:42162–73.
[242] Wang ZY, Zhao HJ, Wang QF, Ye RR, Finlow DE. Synthesis of poly(D,L-lactic acid) modified by cholic acid via direct melt copolycondensation and its characterization. J Appl Polym Sci 2010;117:1405–15.
[243] Carrasco F, Cailloux J, Sanchez-Jimenez PE, Maspoch ML. Improvement of the thermal stability of branched poly(lactic acid) obtained by reactive extrusion. Polym Degrad Stab 2014;104:40–9.
[244] Li H, Huneault MA. Effect of chain extension on the properties of PLA/TPS blends. J Appl Polym Sci 2011;122:134–41.
[245] Najafi N, Heuzey MC, Carreau PJ, Therriault D, Park CB. Rheological and foaming behavior of linear and branched polylactides. Rheol Acta 2014;53:779–90.
[246] Najafi N, Heuzey MC, Carreau P, Therriault D. Quiescent and shear-induced crystallization of linear and branched polylactides. Rheol Acta 2015;54:831–45.
[247] Najafi N, Heuzey MC, Carreau PJ, Wood-Adams PM. Control of thermal degradation of polylactide (PLA)-clay nanocomposites using chain extenders. Polym Degrad Stab 2012;97:554–65.
[248] Al-Itry R, Lamnawar K, Maazouz A. Reactive extrusion of PLA, PBAT with a multi-functional epoxide: physico-chemical and rheological properties. Eur Polym J 2014;58:90–102.
[249] Pilla S, Kim SG, Auer GK, Gong S, Park CB. Microcellular extrusion-foaming of polylactide with chain-extender. Polym Eng Sci 2009;49:1653–60.
[250] Mihai M, Huneault MA, Favis BD. Rheology and extrusion foaming of chain-branched poly(lactic acid). Polym Eng Sci 2010;50:629–42.
[251] Cailloux J, Santana OO, Franco-Urquiza E, Bou JJ, Carrasco F, Gamez-Perez J, et al. Sheets of branched poly(lactic acid) obtained by one step reactive extrusion calendering process: melt rheology analysis. Express Polym Lett 2013;7:304–18.
[252] Gu SY, Yang M, Yu T, Ren TB, Ren J. Synthesis and characterization of biodegradable lactic acid-based polymers by chain extension. Polym Int 2008;57:982–6.
[253] Zhou M, Zhou P, Xiong P, Qian X, Zheng HH. Crystallization, rheology and foam morphology of branched PLA prepared by novel type of chain extender. Macromol Res 2015;23:231–6.
[254] Dean KM, Petinakis E, Meure S, Yu L, Chryss A. Melt strength and rheological properties of biodegradable poly(Lactic acid) modified via alkyl radical-based reactive extrusion processes. J Polym Environ 2012;20:741–7.
[255] Takamura M, Sugimoto M, Kawaguchi S, Takahashi T, Koyama K. Influence of extrusion temperature on molecular architecture and crystallization behavior of peroxide-induced slightly crosslinked poly(L-lactide) by reactive extrusion. J Appl Polym Sci 2012;123:1468–78.
[256] Xu HJ, Fang HG, Bai J, Zhang YQ, Wang ZG. Preparation and characterization of high-melt-Strength polylactide with long-chain branched structure through gamma-radiation-Induced chemical reactions. Ind Eng Chem Res 2014;53:1150–9.
[257] Shin BY, Han DH, Narayan R. Rheological and thermal properties of the PLA modified by electron beam irradiation in the presence of functional monomer. J Polym Environ 2010;18:558–66.
[258] Wang Y, Yang L, Niu Y, Wang Z, Zhang J, Yu F, et al. Rheological and topological characterizations of electron beam irradiation prepared long-chain branched polylactic acid. J Appl Polym Sci 2011;122:1857–65.
[259] Di Y, Iannace S, Di Maio E, Nicolais L. Reactively modified poly(lactic acid): properties and foam processing. Macromol Mater Eng 2005;290:1083–90.
[260] Lehermeier HJ, Dorgan JR. Melt rheology of poly(lactic acid): consequences of blending chain architectures. Polym Eng Sci 2001;41:2172–84.
[261] Zhang CX, Wang B, Chen Y, Cheng F, Jiang SC. Amphiphilic multiarm star polylactide with hyperbranched polyethylenimine as core: a systematic reinvestigation. Polymer 2012;53:3900–9.
[262] Cailloux J, Santana OO, Franco-Urquiza E, Bou JJ, Carrasco F, Maspoch ML. Sheets of branched poly(lactic acid) obtained by one-step reactive extrusion-calendering process: physical aging and fracture behavior. J Mater Sci 2014;49:4093–107.
[263] Wang L, Jing X, Cheng H, Hu X, Yang L, Huang Y. Rheology and crystallization of long-chain branched poly(l-lactide)s with controlled branch length. Ind Eng Chem Res 2012;51:10731–41.
[264] Chen CQ, Ke DM, Zheng TT, He GJ, Cao XW, Liao X. An ultraviolet-induced reactive extrusion to control chain scission and long-chain branching reactions of polylactide. Ind Eng Chem Res 2016;55:597–605.
[265] Fang H, Zhang Y, Bai J, Wang Z. Shear-induced nucleation and morphological evolution for bimodal long chain branched polylactide. Macromolecules 2013;46:6555–65.
[266] Fang H, Zhang Y, Bai J, Wang Z, Wang Z. Bimodal architecture and rheological and foaming properties for gamma-irradiated long-chain branched polylactides. RSC Adv 2013;3:8783–95.
[267] Li ZQ, Ye L, Zhao XW, Coates P, Caton-Rose F, Martyn M. High orientation of long chain branched poly (lactic acid) with enhanced blood compatibility and bionic structure. J Biomed Mater Res Part B Appl Biomater 2016;104:1082–9.
[268] McLeish TCB, Allgaier J, Bick DK, Bishko G, Biswas P, Blackwell R, et al. Dynamics of entangled H-polymers: theory, rheology, and neutron-scattering. Macromolecules 1999;32:6734–58.
[269] Han DH, Pan CY. Simple route for synthesis of H-shaped copolymers. J Polym Sci Part A: Polym Chem 2006;44:2794–801.
[270] Yuan W, Zhang J, Zou H, Ren J. Synthesis, crystalline morphologies, self-assembly, and properties of H-shaped amphiphilic dually responsive terpolymers. J Polym Sci Part A: Polym Chem 2012;50:2541–52.
[271] Pitet LM, Chamberlain BM, Hauser AW, Hillmyer MA. Synthesis of linear, H-Shaped, and arachnearm block copolymers by tandem ring-opening polymerizations. Macromolecules 2010;43:8018–25.
[272] Lu DD, Yuan JC, Li H, Lei ZQ. Synthesis and characterization of a series of biodegradable and biocompatible PEG-supported poly(lactic-ran-glycolic acid) amphiphilic barbell-like copolymers. J Polym Sci Part A: Polym Chem 2008;46:3802–12.
[273] Han DH, Pan CY. Preparation and characterization of heteroarm H-shaped terpolymers by combination of reversible addition-fragmentation transfer polymerization and ring-opening polymerization. J Polym Sci Part A: Polym Chem 2007;45:789–99.
[274] Liu H, Li S, Zhang M, Shao W, Zhao Y. Facile synthesis of ABCDE-type H-shaped quintopolymers by combination of ATRP, ROP, and click chemistry and their potential applications as drug carriers. J Polym Sci Part A: Polym Chem 2012;50:4705–16.
[275] Li A, Li Z, Zhang S, Sun G, Wooley KL, Policarpio DM. Synthesis and direct visualization of dumbbell-shaped molecular brushes. ACS Macro Lett 2012;1:241–5.
[276] Tsuji H. Poly(lactic acid) stereocomplexes: a decade of progress. Adv Drug Deliv Rev 2016;107:97–135.
[277] Edens RE. Polysaccharides: structural diversity and functional versatility. J Am Chem Soc 2005;127:10118–22.
[278] Stephen AM, Churms SC. Food polysaccharides and their applications. 2nd ed. New York: CRC Press; 2006. p. 1–17.
[279] Luscombe NM, Austin SE, Berman HM, Thornton JM. An overview of the structures of protein-DNA complexes. Genome Biol 2000;1(001):1–37.
[280] Alberts B, Alexander J, Lewis J, Raff M, Roberts K, Walter P. Molecular biology of the cell. 4th edition New York: Garland Science Publ; 2002. p. 1065–126.
[281] Bekturov EA, Bimendina LA. Interpolymer complexes. Adv Polym Sci 1981;41:99–147.
[282] Papisov IM, Litmanovich AA. Molecular recognition in interpolymer interactions and matrix polymerization. Adv Polym Sci 1989;90:139–79.
[283] Kondepudi D, Hall J. The origins of order. J Am Chem Soc 1995;117:3317–8.
[284] Lehn JM. Supramolecular chemistry. Proc Chem Sci Indian Acad Sci 1994;106:915–22.
[285] Lehn JM. Supramolecular polymer chemistry-scope and perspectives. Polym Int 2002;51:825–39.
[286] Han MJ, Chang JY. Polynucleotide analogues. Adv Polym Sci 2000;153:1–36.
[287] Ungar G, Liu Y, Zeng X, Percec V, Cho WD. Giant Supramolecular Liquid Crystal Lattice. Science 2003;299:1208–11.

Please cite this article in press as: Michalski A, et al. Star-shaped and branched polylactides: Synthesis, characterization, and properties. Prog Polym Sci (2018), https://doi.org/10.1016/j.progpolymsci.2018.10.004

[288] Kabanov VA. From synthetic polyelectrolytes to polymer-subunit vaccines. Pure Appl Chem 2004;76:1659–77.
[289] Cameron DJA, Shaver MP. Control of thermal properties and hydrolytic degradation in poly(lactic acid) polymer stars through control of isospecificity of polymer arms. J Polym Sci Part A: Polym Chem 2012;50:1477–84.
[290] Brzezinski M, Biela T. Micro- and nanostructures of polylactide stereocomplexes and their biomedical applications. Polym Int 2015;64:1667–75.
[291] Brzezinski M, Biela T. Stereocomplexed polylactides. In: Kobayashi S, Müllen K, editors. Encyclopedia of polymeric nanomaterials. Berlin: Springer; 2015. p. 2274–81.
[292] Brizzolara D, Cantow HJ, Diederichs K, Keller E, Domb AJ. Mechanism of the stereocomplex formation between enantiomeric poly(lactide)s. Macromolecules 1996;29:191–7.
[293] Sarasua JR, Lopez Rodriguez N, Lopez Arraiza A, Meaurio E. Stereoselective crystallization and specific interactions in Polylactides. Macromolecules 2005;38:8362–71.
[294] Zhang J, Sato H, Tsuji H, Noda I, Ozaki Y. Infrared spectroscopic study of CH3···O=C interaction during poly(L-lactide)/Poly(D-lactide) stereocomplex formation. Macromolecules 2005;38:1822–8.
[295] Fujiwara T, Mukose T, Yamaoka T, Yamane H, Sakurai S, Kimura Y. Novel thermo-responsive formation of a hydrogel by stereo-complexation between PLLA-PEG-PLLA and PDLA-PEG-PDLA block copolymers. Macromol Biosci 2001;1:204–8.
[296] Tsuji H. Poly(lactide) stereocomplexes: formation, structure, properties, degradation, and applications. Macromol Biosci 2005;5:569–97.
[297] Biela T, Duda A, Penczek S. Enhanced Melt Stability of Star-Shaped Stereocomplexes As Compared with Linear Stereocomplexes. Macromolecules 2006;39:3710–3.
[298] Biela T. Stereocomplexes of star-shaped poly[(R)-lactide]s and poly[(S)-lactide]s bearing various number of arms. Synthesis and thermal properties. Polimery 2007;52:106–16.
[299] Jing ZX, Shi XT, Zhang GC. Rheology and crystallization behavior of asymmetric PLLA/PDLA blends based on linear PLLA and PDLA with different structures. Polym Adv Technol 2016;27:1108–20.
[300] Nagahama K, Nishimura Y, Ohya Y, Ouchi T. Impacts of stereoregularity and stereocomplex formation on physicochemical, protein adsorption and cell adhesion behaviors of star-shaped 8-arms poly(ethylene glycol)-poly(lactide) block copolymer films. Polymer 2007;48:2649–58.
[301] Isono T, Kondo Y, Otsuka I, Nishiyama Y, Borsali R, Kakuchi T, et al. Synthesis and Stereocomplex Formation of Star-Shaped Stereoblock Polylactides Consisting of Poly(L-lactide) and Poly(D-lactide) Arms. Macromolecules 2013;46:8509–18.
[302] Andersson SR, Hakkarainen M, Inkinen S, Sodergard A, Albertsson A-C. Customizing the hydrolytic degradation rate of stereocomplex PLA through different PDLA architectures. Biomacromolecules 2012;13:1212–22.
[303] Shao J, Sun J, Bian X, Cui Y, Zhou Y, Li G, et al. Modified PLA. Homochiral Crystallites Facilitated by the Confinement of PLA Stereocomplexes. Macromolecules 2013;46:6963–71.
[304] Inkinen S, Stolt M, Soedergard A. Effect of blending ratio and oligomer structure on the thermal transitions of stereocomplexes consisting of a D-lactic acid oligomer and poly(L-lactide). Polym Adv Technol 2011;22:1658–64.
[305] Shao J, Sun J, Bian X, Cui Y, Li G, Chen X. Investigation of Poly(lactide) Stereocomplexes: 3-Armed Poly(l-lactide) Blended with Linear and 3-Armed Enantiomers. J Phys Chem B 2012;116:9983–91.
[306] Tsuji H, Ozawa R, Arakawa Y. Stereocomplex Crystallization of Star-Shaped Four-Armed Stereo Diblock Poly(lactide) from the Melt: Effects of Incorporated Linear One-Armed Poly(L-lactide) or Poly(D-lactide). J Phys Chem B 2017;121:9936–46.
[307] Tsuji H, Matsumura N, Arakawa Y. Stereocomplex Crystallization and Homocrystallization of Star-Shaped Four-Armed Stereo Diblock Poly(lactide)s with Different L-Lactyl Unit Contents: Isothermal Crystallization from the Melt. J Phys Chem B 2016;120:1183–93.
[308] Han L, Shan G, Bao Y, Pan P. Exclusive Stereocomplex Crystallization of Linear and Multiarm Star-Shaped High-Molecular-Weight Stereo Diblock Poly(lactic acid)s. J Phys Chem B 2015;119:14270–9.
[309] Nijenhuis AJ, Grijpma DW, Pennings AJ. Crosslinked poly(L-lactide) and poly(ε-caprolactone). Polymer 1996;37:2783–91.
[310] Kaplan DL. Introduction to Biopolymers from Renewable Resources In: Kaplan DL, editor. Biopolymers from Renewable Resources.Heidelberg: Springer 1998:1–29.
[311] Esmaeili N, Jahandideh A, Muthukumarappan K, Aakesson D, Skrifvars M. Synthesis and characterization of methacrylated star-shaped poly(lactic acid) employing core molecules with different hydroxyl groups. J Appl Polym Sci 2017;134, 45341/1-13.
[312] Bakare FO, Skrifvars M, Aakesson D, Wang Y, Afshar SJ, Esmaeili N. Synthesis and characterization of bio-based thermosetting resins from lactic acid and glycerol. J Appl Polym Sci 2014;131, 40488/1-9.
[313] Esmaeili N, Bakare FO, Skrifvars M, Javanshir Afshar S, Aakesson D. Mechanical properties for bio-based thermoset composites made from lactic acid, glycerol and viscose fibers. Cellulose 2015;22:603–13.
[314] Melchels FPW, Feijen J, Grijpma DW. A poly(D,L-lactide) resin for the preparation of tissue engineering scaffolds by stereolithography. Biomaterials 2009;30:3801–9.
[315] Amsden B, Wang S, Wyss U. Synthesis and Characterization of Thermoset Biodegradable Elastomers Based on Star-Poly(ε-caprolactone-co-D,L-lactide). Biomacromolecules 2004;5:1399–404.
[316] George KA, Chirila TV, Wentrup-Byrne E. Effects of crosslink density on hydrolytic degradation of poly(L-lactide)-based networks. Polym Degrad Stab 2012;97:964–71.
[317] Takase H, Morita K, Shibita A, Shibata M. Polymer networks prepared from 4-arm star-shaped L-lactide oligomers with different arm lengths and their semi-interpenetrating polymer networks containing poly (L-lactide). J Polym Res 2014;21, 592/1-10.
[318] Amsden BG, Misra G, Gu F, Younes HM. Synthesis and characterization of a photo-cross-linked biodegradable elastomer. Biomacromolecules 2004;5:2479–86.
[319] Storey RF, Warren SC, Allison CJ, Puckett AD. Methacrylate-endcapped poly(d,l-lactide-co-trimethylene carbonate) oligomers: Network formation by thermal free-radical curing. Polymer 1997;38:6295–301.
[320] Nerkar M, Ramsay JA, Ramsay BA, Kontopoulou M. Dramatic Improvements in Strain Hardening and Crystallization Kinetics of PLA by Simple Reactive Modification in the Melt State. Macromol Mater Eng 2014;299:1419–24.
[321] Zhang S, Feng Y, Zhang L, Sun J, Xu X, Xu Y. Novel interpenetrating networks with shape-memory properties. J Polym Sci Part A Polym Chem 2007;45:768–75.
[322] Sugane K, Kumai N, Yoshioka Y, Shibita A, Shibata M. Thermo-responsive alternating conetworks by the Diels-Alder reaction of furan-terminated 4-armed star-shaped ε-caprolactone oligomers and maleimide-terminated 4-armed star-shaped L-lactide oligomers. Polymer 2017;124:20–9.
[323] Basu A, Kunduru KR, Doppalapudi S, Domb AJ, Khan W. Poly(lactic acid) based hydrogels. Adv Drug Deliv Rev 2016;107:192–205.
[324] Buwalda SJ, Calucci L, Forte C, Dijkstra PJ, Feijen J. Stereocomplexed 8-armed poly(ethylene glycol)-poly(lactide) star block copolymer hydrogels: Gelation mechanism, mechanical properties and degradation behavior. Polymer 2012;53:2809–17.
[325] Wei H, Zhang A-Y, Qian L, Yu H, Hou D, Qiu R, et al. Supramolecular structured hydrogel preparation based on self-assemblies of photocurable star-shaped macromers with α-cyclodextrins. J Polym Sci Part A Polym Chem 2005;43:2941–9.
[326] Buwalda SJ, Dijkstra PJ, Calucci L, Forte C, Feijen J. Influence of Amide versus Ester Linkages on the Properties of Eight-Armed PEG-PLA Star Block Copolymer Hydrogels. Biomacromolecules 2010;11:224–32.
[327] Calucci L, Forte C, Buwalda SJ, Dijkstra PJ, Feijen J. Self-Aggregation of Gel Forming PEG-PLA Star Block Copolymers in Water. Langmuir 2010;26:12890–6.
[328] Hiemstra C, Zhong Z, Dijkstra PJ, Feijen J. Stereocomplex mediated gelation of PEG-(PLA)2 and PEG-(PLA)8 block copolymers. Macromol Symp 2005;224:119–31.
[329] Buwalda SJ, Dijkstra PJ, Feijen J. Poly(ethylene glycol)-poly(L-lactide) star block copolymer hydrogels crosslinked by metal-ligand coordination. J Polym Sci Part A Polym Chem 2012;50:1783–91.
[330] Velthoen IW, Tijsma EJ, Dijkstra PJ, Feijen J. Thermo-responsive hydrogels based on branched poly(L-lactide)-poly(ethylene glycol) copolymers. Macromol Symp 2008;272:13–27.
[331] Nagahama K, Fujiura K, Enami S, Ouchi T, Ohya Y. Irreversible temperature-responsive formation of high-strength hydrogel from an enantiomeric mixture of starburst triblock copolymers consisting of 8-arm PEG and PLLA or PDLA. J Polym Sci Part A Polym Chem 2008;46:6317–32.
[332] Calucci L, Forte C, Buwalda SJ, Dijkstra PJ. Solid-State NMR Study of Stereocomplexes Formed by Enantiomeric Star-Shaped PEG-PLA Copolymers in Water. Macromolecules 2011;44:7288–95.
[333] Klok H-A, Becker S, Schuch F, Pakula T, Muellen K. Synthesis and solid state properties of novel fluorescent polyester star polymers. Macromol Biosci 2003;3:729–41.
[334] Cai Q, Zhao Y, Bei J, Xi F, Wang S. Synthesis and Properties of Star-Shaped Polylactide Attached to Poly(Amidoamine) Dendrimer. Biomacromolecules 2003;4:828–34.
[335] Sodergard A, Stolt M. Properties of lactic acid based polymers and their correlation with composition. Prog Polym Sci 2002;27:1123–63.
[336] Thi TH, Matsusaki M, Akashi M. Development of Photoreactive Degradable Branched Polyesters with High Thermal and Mechanical Properties. Biomacromolecules 2009;10:766–72.
[337] Tasaka F, Ohya Y, Ouchi T. Synthesis of Novel Comb-Type Polylactide and Its Biodegradability. Macromolecules 2001;34:5494–500.
[338] Nofar M, Zhu W, Park CB, Randall J. Crystallization Kinetics of Linear and Long-Chain-Branched Polylactide. Ind Eng Chem Res 2011;50:13789–98.
[339] Nagahama K, Mori Y, Ohya Y, Ouchi T. Biodegradable Nanogel Formation of Polylactide-Grafted Dextran Copolymer in Dilute Aqueous Solution and Enhancement of Its Stability by Stereocomplexation. Biomacromolecules 2007;8:2135–41.
[340] Wang L, Cai C, Dong C-M. Synthesis, characterization and nanoparticle formation of star-shaped poly(L-lactide) with six arms. Chin J Polym Sci 2008;26:161–9.
[341] Tsuji H, Hayashi T. Hydrolytic degradation of linear 2-arm and branched 4-arm poly(dl-lactide)s: Effects of branching and terminal hydroxyl groups. Polym Degrad Stab 2014;102:59–66.
[342] Perry MR, Shaver MP. Flexible and rigid core molecules in the synthesis of poly(lactic acid) star polymers. Can J Chem 2011;89:499–505.
[343] Wang C, Li H, Zhao X. Ring opening polymerization of L-lactide initiated by creatinine. Biomaterials 2004;25:5797–801.

Please cite this article in press as: Michalski A, et al. Star-shaped and branched polylactides: Synthesis, characterization, and properties. Prog Polym Sci (2018), https://doi.org/10.1016/j.progpolymsci.2018.10.004

[344] Fan Y, Nishida H, Shirai Y, Endo T. Racemization on thermal degradation of poly(l-lactide) with calcium salt end structure. Polym Degrad Stab 2003;80:503–11.
[345] Middleton JC, Tipton AJ. Synthetic biodegradable polymers as orthopedic devices. Biomaterials 2000;21:2335–46.
[346] Zuideveld M, Gottschalk C, Kropfinger H, Thomann R, Rusu M, Frey H. Miscibility and properties of linear poly(L-lactide)/branched poly(L-lactide) copolyester blends. Polymer 2006;47:3740–6.
[347] Jamshidi K, Hyon SH, Ikada Y. Thermal characterization of polylactides. Polymer 1988;29:2229–34.
[348] Yuan W, Liu X, Zou H, Li J, Yuan H, Ren J. Synthesis, Self-Assembly, and Properties of Homoarm and Heteroarm Star-Shaped Inorganic-Organic Hybrid Polymers with a POSS Core. Macromol Chem Phys 2013;214:1580–9.
[349] Teng L, Xu X, Nie W, Zhou Y, Song L, Chen P. Synthesis and degradability of a star-shaped polylactide based on L-lactide and xylitol. J Polym Res 2015;22, 83/1-7.
[350] Torres L, McMahan C, Ramadan L, Holtman KM, Tonoli GHD, Flynn A, et al. Effect of multi-branched PDLA additives on the mechanical and thermo-mechanical properties of blends with PLLA. J Appl Polym Sci 2016;133, 42858/1-10.
[351] Phuphuak Y, Chirachanchai S. Simple preparation of multi-branched poly(l-lactic acid) and its role as nucleating agent for poly(lactic acid). Polymer 2013;54:572–82.
[352] Bai J, Fang HG, Zhang YQ, Wang ZG. Studies on crystallization kinetics of bimodal long chain branched polylactides. CrystEngComm 2014;16:2452–61.
[353] Saeidlou S, Huneault MA, Li H, Park CB. Poly(lactic acid) crystallization. Prog Polym Sci 2012;37:1657–77.
[354] Fischer EW, Sterzel HJ, Wegner G. Investigation of the structure of solution grown crystals of lactide copolymers by means of chemicals reactions. Kolloid Z 1973;251:980–90.
[355] Choochottiros C. Effect of polycaprolactone-co-polylactide copolyesters' arms in enhancing optical transparent PLA toughness. Macromol Res 2016;24:838–46.
[356] Wang J-L, Dong C-M. Synthesis, sequential crystallization and morphological evolution of well-defined star-shaped poly(ε-caprolactone)-b-poly(L-lactide) block copolymer. Macromol Chem Phys 2006;207:554–62.
[357] Zhao C, Wu D, Huang N, Zhao H. Crystallization and thermal properties of PLLA comb polymer. J Polym Sci Part B Polym Phys 2008;46:589–98.
[358] Liu J, Zhang S, Zhang L, Bai Y. Crystallization Behavior of Long-Chain Branching Polylactide. Ind Eng Chem Res 2012;51:13670–9.
[359] Mitomo H, Kaneda A, Quynh TM, Nagasawa N, Yoshii F. Improvement of heat stability of poly(L-lactic acid) by radiation-induced crosslinking. Polymer 2005;46:4695–703.
[360] Perego G, Cella GD, Bastioli C. Effect of molecular weight and crystallinity on poly(lactic acid) mechanical properties. J Appl Polym Sci 1996;59:37–43.
[361] Vainionpaa S, Rokkanen P, Tormala P. Surgical applications of biodegradable polymers in human tissues. Prog Polym Sci 1989;14:679–716.
[362] Numata K, Finne-Wistrand A, Albertsson A-C, Doi Y, Abe H. Enzymatic Degradation of Monolayer for Poly(lactide) Revealed by Real-Time Atomic Force Microscopy: Effects of Stereochemical Structure, Molecular Weight, and Molecular Branches on Hydrolysis Rates. Biomacromolecules 2008;9:2180–5.
[363] Breitenbach A, Pistel KF, Kissel T. Biodegradable comb polyesters. Part II. Erosion and release properties of poly(vinyl alcohol)-g-poly(lactic-co-glycolic acid). Polymer 2000;41:4781–92.
[364] Li Y, Volland C, Kissel T. Biodegradable brush-like graft polymers from poly(D,L-lactide) or poly(D,L-lactide-coglycolide) and charge-modified, hydrophilic dextrans as backbone – in-vitro degradation and controlled releases of hydrophilic macromolecules. Polymer 1998;39:3087–97.
[365] Tsuji H, Hayashi T. Hydrolytic degradation and crystallization behavior of linear 2-armed and star-shaped 4-armed poly(L-lactide)s: Effects of branching architecture and crystallinity. J Appl Polym Sci 2015;132, 41983/1-13.
[366] Atkinson JL, Vyazovkin S. Thermal Properties and Degradation Behavior of Linear and Branched Poly(L-lactide)s and Poly(L-lactide-co-glycolide)s. Macromol Chem Phys 2012;213:924–36.
[367] Zhao M, Liu J, Lei Z. PLA-PEG grafted hollow magnetic silica microspheres as the carrier of iodinated contrast media. J Appl Polym Sci 2017;134, 44914/1-7.
[368] Li Y, Nothnagel J, Kissel T. Biodegradable brush-like graft polymers from poly(D,L-lactide) or poly(D,L-lactide-co-glycolide) and charge-modified, hydrophilic dextrans as backbone – synthesis, characterization and in vitro degradation properties. Polymer 1997;38:6197–206.
[369] Salaam LE, Dean D, Bray TL. In vitro degradation behavior of biodegradable 4-star micelles. Polymer 2006;47:310–8.
[370] Kong JF, Lipik V, Abadie MJM, Deen RG, Venkatraman SS. Characterization and degradation of elastomeric four-armed star copolymers based on caprolactone and L-lactide. J Biomed Mater Res Part A 2012;100:3436–45.
[371] Lee JS, Choo D-J, Kim SH, Kim YH. Synthesis and degradation property of star-shaped polylactide. Polymer 1998;22:880–9.
[372] Yuan W, Yuan J, Huang X, Tang X. Synthesis, characterization, and in vitro degradation of star-shaped p(ε-caprolactone)-b-poly(L-lactide)-b-poly(D, L-lactide-co-glycolide) from hexakis [p-(hydroxymethyl)phenoxy]cyclotriphosphazene initiator. J Appl Polym Sci 2007;104:2310–7.
[373] Prabaharan M, Grailer JJ, Pilla S, Steeber DA, Gong S. Amphiphilic multi-arm block copolymer based on hyperbranched polyester, poly(L-lactide) and poly(ethylene glycol) as a drug delivery carrier. Macromol Biosci 2009;9:515–24.
[374] Park SY, Han BR, Na KM, Han DK, Kim SC. Micellization and Gelation of Aqueous Solutions of Star-Shaped PLLA-PEO Block Copolymers. Macromolecules 2003;36:4115–24.
[375] Park SY, Han DK, Kim SC. Synthesis and Characterization of Star-Shaped PLLA-PEO Block Copolymers with Temperature-Sensitive Sol-Gel Transition Behavior. Macromolecules 2001;34:8821–4.
[376] Stepanek M, Uchman M, Prochazka K. Self-assemblies formed by four-arm star copolymers with amphiphilic diblock arms in aqueous solutions. Polymer 2009;50:3638–44.
[377] Jie P, Venkatraman SS, Min F, Freddy BYC, Huat GL. Micelle-like nanoparticles of star-branched PEO-PLA copolymers as chemotherapeutic carrier. J Controlled Release 2005;110:20–33.
[378] Yin H, Kang S-W, Bae YH. Polymersome Formation from AB2 Type 3-Miktoarm Star Copolymers. Macromolecules 2009;42:7456–64.
[379] Ma G, Zhang C, Zhang L, Sun H, Song C, Wang C, et al. Doxorubicin-loaded micelles based on multiarm star-shaped PLGA-PEG block copolymers: influence of arm numbers on drug delivery. J Mater Sci Mater Med 2016;27, 17/1-15.
[380] Lee SJ, Han BR, Park SY, Han DK, Kim SC. Sol-gel transition behavior of biodegradable three-arm and four-arm star-shaped PLGA-PEG block copolymer aqueous solution. J Polym Sci Part A Polym Chem 2005;44:888–99.
[381] Yu X, Tang X, Pan C. Synthesis, characterization and self-assembly behavior of six-armed star block copolymers with triphenylene core. Polymer 2005;46:11149–56.
[382] Li J, Ren J, Cao Y, Yuan W. Synthesis of biodegradable pentaarmed star-block copolymers via an asymmetric BIS-TRIS core by combination of ROP and RAFT: From star architectures to double responsive micelles. Polymer 2010;51:1301–10.
[383] Wei H, Zhang X-Z, Chen W-Q, Cheng S-X, Zhuo R-X. Self-assembled thermosensitive micelles based on poly(L-lactide-star block-N-isopropylacrylamide) for drug delivery. J Biomed Mater Res Part A 2007;83:980–9.
[384] Sun MM, Yin WY, Dong XH, Yang WT, Zhao YL, Yin MZ. Fluorescent supramolecular micelles for imaging-guided cancer therapy. Nanoscale 2016;8:5302–12.
[385] Liu X, Jin X, Ma PX. Nanofibrous hollow microspheres self-assembled from star-shaped polymers as injectable cell carriers for knee repair. Nat Mater 2011;10:398–406.
[386] Yuan W, Zhang J, Wei J, Zhang C, Ren J. Synthesis and self-assembly of pH-responsive amphiphilic dendritic star-block terpolymer by the combination of ROP, ATRP and click chemistry. Eur Polym J 2011;47: 949–58.
[387] Akbarzadeh R. Yousefi A-M. Effects of processing parameters in thermally induced phase separation technique on porous architecture of scaffolds for bone tissue engineering. J Biomed Mater Res Part B 2014;102:1304–15.
[388] Murariu M, Dubois P. PLA composites: From production to properties. Adv Drug Deliv Rev 2016;107:17–46.
[389] Tyler B, Gullotti D, Mangraviti A, Utsuki T, Brem H. Polylactic acid (PLA) controlled delivery carriers for biomedical applications. Adv Drug Deliv Rev 2016;107:163–75.
[390] Narayanan G, Vernekar VN, Kuyinu EL, Laurencin CT. Poly (lactic acid)-based biomaterials for orthopaedic regenerative engineering. Adv Drug Deliv Rev 2016;107:247–76.
[391] Farah S, Anderson DG, Langer R. Physical and mechanical properties of PLA, and their functions in widespread applications – A comprehensive review. Adv Drug Deliv Rev 2016;107:367–92.
[392] James R, Manoukian OS, Kumbar SG. Poly(lactic acid) for delivery of bioactive macromolecules. Adv Drug Deliv Rev 2016;107:277–88.
[393] Santoro M, Shah SR, Walker JL. Mikos AG. Poly(lactic acid) nanofibrous scaffolds for tissue engineering. Adv Drug Deliv Rev 2016;107:206–12.
[394] Ramot Y, Zada MH, Domb AJ, Nyska A. Biocompatibility and safety of PLA and its copolymers. Adv Drug Deliv Rev 2016;107:153–62.
[395] Lee BK, Yun Y, Park K. PLA micro- and nano-particles. Adv Drug Deliv Rev 2016;107:176–91.
[396] Saini P, Arora M, Kumar MVNR. Poly(lactic acid) blends in biomedical applications. Adv Drug Deliv Rev 2016;107:47–59.
[397] Pistel KF, Bittner B, Koll H, Winter G, Kissel T. Biodegradable recombinant human erythropoietin loaded microspheres prepared from linear and star-branched block copolymers: Influence of encapsulation technique and polymer composition on particle characteristics. J Controlled Release 1999;59:309–25.
[398] Joung YK, Lee JS, Park KD, Lee S-J. 6-Arm PLLA-PEG block copolymers for micelle formation and controlled drug release. Macromol Res 2008;16:66–9.
[399] Guo B, Finne-Wistrand A, Albertsson A-C. Molecular Architecture of Electroactive and Biodegradable Copolymers Composed of Polylactide and Carboxyl-Capped Aniline Trimer. Biomacromolecules 2010;11:855–63.
[400] Nagahama K, Ohya Y, Ouchi T. Suppression of cell and platelet adhesion to star-shaped 8-armed poly(ethylene glycol)-poly(L-lactide) block copolymer films. Macromol Biosci 2006;6:412–9.
[401] Kong L-Z, Pan C-Y. Preparation of dendrimer-like copolymers based on polystyrene and poly(L-lactide) and formation of hollow microspheres. Polymer 2008;49:200–10.
[402] Shi W, Tateishi Y, Li W, Hawker CJ, Fredrickson GH, Kramer EJ. Producing Small Domain Features Using Miktoarm Block Copolymers with Large Interaction Parameters. ACS Macro Lett 2015;4:1287–92.

Please cite this article in press as: Michalski A, et al. Star-shaped and branched polylactides: Synthesis, characterization, and properties. Prog Polym Sci (2018), https://doi.org/10.1016/j.progpolymsci.2018.10.004

[403] Wang F, Bronich TK, Kabanov AV, Rauh RD, Roovers J. Synthesis and Characterization of Star Poly(ϵ-caprolactone)-b-Poly(ethylene glycol) and Poly(L-lactide)-b-Poly(ethylene glycol) Copolymers: Evaluation as Drug Delivery Carriers. Bioconjugate Chem 2008;19:1423–9.
[404] Wei H, Chen W-Q, Chang C, Cheng C, Cheng S-X, Zhang X-Z, et al. Synthesis of Star Block, Thermosensitive Poly(L-lactide)-star block-poly(N-isopropylacrylamide-co-N-hydroxymethylacrylamide) Copolymers and Their Self-Assembled Micelles for Controlled Release. J Phys Chem C 2008;112:2888–94.
[405] Hira SK, Ramesh K, Gupta U, Mitra K, Misra N, Ray B, et al. Methotrexate-loaded four-arm star amphiphilic block copolymer elicits CD8+ T cell response against a highly aggressive and metastatic experimental lymphoma. ACS Appl Mater Interfaces 2015;7:20021–33.
[406] Kang N, Leroux J-C. Triblock and star-block copolymers of N-(2-hydroxypropyl)methacrylamide or N- vinyl-2-pyrrolidone and D,L-lactide: synthesis and self-assembling properties in water. Polymer 2004;45:8967–80.
[407] He Q, Wu W, Xiu KM, Zhang Q, Xu FJ, Li JS. Controlled drug release system based on cyclodextrin-conjugated poly(lactic acid)-b-poly(ethylene glycol) micelles. Int J. Pharm 2013;443:110–9.
[408] Atkinson JL, Vyazovkin S. Dynamic Mechanical Analysis and Hydrolytic Degradation Behavior of Linear and Branched Poly(L-lactide)s and Poly(L-lactide-co-glycolide)s. Macromol Chem Phys 2013;214:835–43.
[409] Teng LJ, Nie WY, Zhou YF, Chen PP. Synthesis and characterization of star-shaped poly(L-lactide)s with an erythritol core and evaluation of their rifampicin-loaded microspheres for controlled drug delivery. Polym Bull 2016;73:97–112.
[410] Zhang Z, Feng S-S. In Vitro Investigation on Poly(lactide)-Tween 80 Copolymer Nanoparticles Fabricated by Dialysis Method for Chemotherapy. Biomacromolecules 2006;7:1139–46.
[411] Zhang XD, Yang Y, Liang X, Zeng XW, Liu ZG, Tao W, et al. Enhancing Therapeutic Effects of Docetaxel-Loaded Dendritic Copolymer Nanoparticles by Co-Treatment with Autophagy Inhibitor on Breast Cancer. Theranostics 2014;4:1085–95.
[412] Ouyang C-P, Liu Q, Zhao S-X, Ma G, Zhang Z-P, Song C-X. Synthesis and characterization of star-shaped poly (lactide-co-glycolide) and its drug-loaded microspheres. Polym Bull 2012;68:27–36.
[413] Adeli M, Zarnegar Z, Kabiri R. Amphiphilic star copolymers containing cyclodextrin core and their application as nanocarrier. Eur Polym J 2008;44:1921–30.
[414] Hu MY, Shen YR, Zhang L, Qiu LY. Polymersomes via Self-Assembly of Amphiphilic beta-Cyclodextrin-Centered Triarm Star Polymers for Enhanced Oral Bioavailability of Water-Soluble Chemotherapeutics. Biomacromolecules 2016;17:1026–39.
[415] Qiu LY, Bae YH. Polymer Architecture and Drug Delivery. Pharm Res 2006;23:1–30.
[416] Li WL, Zhang WJ, Yang XY, Xie ZG, Jing XB. Biodegradable Polymersomes from Four-Arm PEG-b-PDLLA for Encapsulating Hemoglobin. J Appl Polym Sci 2014;131, 40433/1-5.
[417] Zou T, Li S-L, Cheng S-X, Zhang X-Z, Zhuo R-X. Fabrication and in vitro drug release of drug-loaded star oligo/poly(DL-lactide) microspheres made by novel ultrasonic-dispersion method. J Biomed Mater Res Part A 2007;83:696–702.
[418] Tao W, Zeng XW, Zhang JX, Zhu HJ, Chang DF, Zhang XD, et al. Synthesis of cholic acid-core poly(epsilon-caprolactone-ran-lactide)-b-poly(ethylene glycol) 1000 random copolymer as a chemotherapeutic nanocarrier for liver cancer treatment. Biomater Sci 2014;2:1262–74.
[419] Zeng X, Tao W, Wang Z, Zhang X, Zhu H, Wu Y, et al. Docetaxel-Loaded Nanoparticles of Dendritic Amphiphilic Block Copolymer H40-PLA-b-TPGS for Cancer Treatment. Part Part Syst Charact 2015;32:112–22.
[420] Adeli M, Haag R. Multiarm star nanocarriers containing a poly(ethylene imine) core and polylactide arms. J Polym Sci Part A. Polym Chem 2006;44:5740–9.
[421] Wang J, Shen K, Xu W, Ding J, Wang X, Liu T, et al. Stereocomplex micelle from nonlinear enantiomeric copolymers efficiently transports antineoplastic drug. Nanoscale Res Lett 2015;10:1–11.
[422] Wu W, Wang W, Li J. Star polymers: Advances in biomedical applications. Prog Polym Sci 2015;46:55–85.
[423] Zhao Y, Pan D, Wang Z. Comparison of four-arm and six-arm star-shaped mPEG-PLA block copolymer micelles for drug delivery. J Controlled Release 2013;172, 84-84.
[424] Lin Y-L, Zhang A-Q. Synthesis and characterization of star-shaped poly(D, L-lactide)-block-poly(ethylene glycol) copolymers. Polym Bull 2010;65:883–92.
[425] Fan XS, Wang Z, He CB. Breathing unimolecular micelles based on a novel star-like amphiphilic hybrid copolymer. J Mater Chem B 2015;3:4715–22.
[426] Fu H-L, Zou T, Cheng S-X, Zhang X-Z, Zhuo R-X. Cholic acid functionalized star poly(DL-lactide) for promoting cell adhesion and proliferation. J Tissue Eng Regener Med 2007;1:368–76.
[427] Dong PW, Wang XH, Gu YC, Wang YJ, Wang YJ, Gong CY, et al. Self-assembled biodegradable micelles based on star-shaped PCL-b-PEG copolymers for chemotherapeutic drug delivery. Colloids Surf A 2010;358:128–34.
[428] Miao Y, Rousseau C, Mortreux A, Martin P, Zinck P. Access to new carbohydrate-functionalized polylactides via organocatalyzed ring-opening polymerization. Polymer 2011;52:5018–26.
[429] Lopes MS, Jardini AL, Filho RM. Poly (lactic acid) production for tissue engineering applications. Procedia Eng 2012;42:1530–42.
[430] Benicewicz BC, Hopper PK. Polymers for absorbable surgical sutures – part II. J Bioact Compat Polym 1991;6:64–94.
[431] John G, Morita M. Synthesis and characterization of photo-cross-linked networks based on L-lactide/serine copolymers. Macromolecules 1999;32:1853–8.
[432] Albertsson A-C, Varma IK. Recent Developments in Ring Opening Polymerization of Lactones for Biomedical Applications. Biomacromolecules 2003;4:1466–86.
[433] Rozga-Wijas K, Stanczyk WA, Kurjata J, Kazmierski S. Star-Shaped and Linear POSS-Polylactide Hybrid Copolymers. Materials 2015;8:4400–20.
[434] Nagahama K, Ohya Y, Ouchi T. Synthesis of star-shaped 8 arms poly(ethylene glycol)-poly(L-lactide) block copolymer and physicochemical properties of its solution cast film as soft biomaterial. Polym J 2006;38:852–60.
[435] Sosnik A, Leung BM, Sefton MV. Lactoyl-poloxamine/collagen matrix for cell-containing tissue engineering modules. J Biomed Mater Res Part A 2008;86:339–53.
[436] Xie MH, Wang L, Ge J, Guo BL, Ma PX. Strong Electroactive Biodegradable Shape Memory Polymer Networks Based on Star-Shaped Polylactide and Aniline Trimer for Bone Tissue Engineering. ACS Appl Mater Interfaces 2015;7:6772–81.
[437] Zhao L, Zhang X, Yao Y, Yu C, Yang J. Synthesis of Y-shaped copolymers containing phenylborate ester and biodegradable poly(lactic acid) blocks and their glucose-sensitive behavior for controlled insulin release. Macromol Chem Phys 2014;215:1609–19.
[438] Go DH, Joung YK, Park SY, Park YD, Park KD. Heparin-conjugated star-shaped PLA for improved biocompatibility. J Biomed Mater Res Part A 2008;86:842–8.
[439] Zou P, Suo J, Nie L, Feng S. Temperature-responsive biodegradable star-shaped block copolymers for vaginal gels. J Mater Chem 2012;22:6316–26.
[440] Teng L, Nie W, Zhou Y, Song L, Chen P. Synthesis and characterization of star-shaped PLLA with sorbitol as core and its microspheres application in controlled drug release. J Appl Polym Sci 2015;132, 42213/1-7.
[441] Nie L, Zou P, Feng S, Suo J. Temperature-sensitive star-shaped block copolymers hydrogels for an injection application: phase transition behavior and biocompatibility. J Mater Sci Mater Med 2013;24:689–700.
[442] Gu SY, Gao XF. Improved shape memory performance of star-shaped POSS-polylactide based polyurethanes (POSS-PLAUs). RSC Adv 2015;5:90209–16.
[443] Wang TQ, Ding J, Li JM, Liu Y, Hao JY. Blends of Poly(d, l-lactide) with Polyhedral Oligomeric Silsesquioxanes-Based Biodegradable Polyester: Synthesis, Morphology, Miscibility, and Mechanical Property. J Appl Polym Sci 2014;131, 40776/1-8.
[444] Zhang W, Wang S, Li X, Yuan J, Wang S. Organic/inorganic hybrid star-shaped block copolymers of poly(l-lactide) and poly(N-isopropylacrylamide) with a polyhedral oligomeric silsesquioxane core: Synthesis and self-assembly. Eur Polym J 2012;48:720–9.
[445] Xu J, Song J. High performance shape memory polymer networks based on rigid nanoparticle cores. Proc Natl Acad Sci USA 2010;107:7652–7.
[446] Sun Y, He C. Biodegradable Core-Shell Rubber Nanoparticles and Their Toughening of Poly(lactides). Macromolecules 2013;46:9625–33.
[447] Petchsuk A, Buchatip S, Supmak W, Opaprakasit M, Opaprakasit P. Preparation and properties of multi-branched poly(D-lactide) derived from polyglycidol and its stereocomplex blends. eXPRESS Polym Lett 2014;8:779–89.
[448] Baimark Y, Srisuwan Y. Biodegradable linear/star-shaped poly(L-lactide) blends prepared by single step ring-opening polymerization. J Appl Sci 2012;12:1364–70.
[449] Deokar MD, Idage SB, Idage BB, Sivaram S. Synthesis and characterization of well-defined random and block copolymers of epsilon-caprolactone with l-lactide as an additive for toughening polylactide: Influence of the molecular architecture. J Appl Polym Sci 2016;133, 43267/1-12.
[450] Xu H, Hua G, Odelius K, Hakkarainen M. Stereocontrolled Entanglement-Directed Self-Alignment of Poly(lactic acid) Cylindrites. Macromol Chem Phys 2016;217:2567–75.
[451] Bian X, Zhang B, Sun Z, Xiang S, Li G, Chen X. Synthesis of multi-arm poly(L-lactide) and its modification on linear polylactide. Polym Bull 2017;74:245–62.
[452] Konwar DB, Jacob J, Satapathy BK. A comparative study of poly(L-lactide)-block-poly((-caprolactone) six-armed star diblock copolymers and polylactide/poly(ε-caprolactone) blends. Polym Int 2016;65:1107–17.
[453] Qin YY, Liu SQ, Zhang YJ, Yuan MW, Li HL, Yuan ML. Effect of poly(epsilon-caprolactone-co-L-lactide) on thermal and functional properties of poly(L-lactide). Int J Biol Macromol 2014;70:327–33.
[454] Najafi N, Heuzey MC, Carreau PJ, Therriault D, Park CB. Mechanical and morphological properties of injection molded linear and branched-polylactide (PLA) nanocomposite foams. Eur Polym J 2015;73:455–65.
[455] Li JZ, Song ZW, Gao LB, Shan H. Preparation of carbon nanotubes/polylactic acid nanocomposites using a non-covalent method. Polym Bull 2016;73:2121–8.
[456] Brzezinski M, Boguslawska M, Ilcikova M, Mosnacek J, Biela T. Unusual Thermal Properties of Polylactides and Polylactide Stereocomplexes Containing Polylactide-Functionalized Multi-Walled Carbon Nanotubes. Macromolecules 2012;45:8714–21.
[457] Purnama P, Kim SH. Synergism of cellulosic nanowhiskers and graft structure in stereocomplex-based materials: formation in solution and a stereocomplex memory study. Cellulose 2014;21:2539–48.
[458] Xia H, Kan S, Li Z, Chen J, Cui S, Wu W, et al. N-heterocyclic carbenes as organocatalysts in controlled/living ring-opening polymerization of O-

Please cite this article in press as: Michalski A, et al. Star-shaped and branched polylactides: Synthesis, characterization, and properties. Prog Polym Sci (2018), https://doi.org/10.1016/j.progpolymsci.2018.10.004

carboxyanhydrides derived from L-lactic acid and L-mandelic acid. J Polym Sci Part A Polym Chem 2014;52:2306–15.
[459] Han DK, Hubbell JA. Lactide-based poly(ethylene glycol) polymer networks for scaffolds in tissue engineering. Macromolecules 1996;29:5233–5.
[460] Csihony S, Culkin DA, Sentman AC, Dove AP, Waymouth RM, Hedrick JL. Single-component catalyst/initiators for the organocatalytic ring-opening polymerization of lactide. J Am Chem Soc 2005;127:9079–84.
[461] Mauck SC, Wang S, Ding WY, Rohde BJ, Fortune CK, Yang GZ, et al. Biorenewable Tough Blends of Polylactide and Acrylated Epoxidized Soybean Oil Compatibilized by a Polylactide Star Polymer. Macromolecules 2016;49:1605–15.
[462] Kim SH, Han YK, Ahn KD, Kim YH, Chang T. Preparation of star-shaped polylactide with pentaerythritol and stannous octoate. Makromol Chem 1993;194:3229–36.
[463] Shibita A, Shimasaki T, Teramoto N, Shibata M. Conetworks composed of 4-armed star-shaped L-lactide oligomer and 4-armed star-shaped ε-caprolactone oligomer. Polymer 2015;74:54–62.
[464] Nederberg F, Connor EF, Glausser T, Hedrick JL. Organocatalytic chain scission of poly(lactides): a general route to controlled molecular weight, functionality and macromolecular architecture. Chem Commun 2001:2066–7.
[465] Lai PS. Star-Shaped Porphyrin-polylactide Formed Nanoparticles for Chemo-Photodynamic Dual Therapies. In: Lim CT, Goh JCH, editors. 13th International Conference on Biomedical Engineering. IFMBE Proceedings, 23. Berlin, Heidelberg: Springer; 2009.
[466] Jing Z, Shi X, Zhang G, Li J, Li J, Zhou L, et al. Formation, structure and promoting crystallization capacity of stereocomplex crystallite network in the poly(lactide) blends based on linear PLLA and PDLA with different structures. Polymer 2016;92:210–1.
[467] Fu H-L, Cheng S-X, Zhang X-Z, Zhuo R-X. Dendrimer/DNA complexes encapsulated in a water soluble polymer and supported on fast degrading star poly(DL-lactide) for localized gene delivery. J Controlled Release 2007;124:181–8.
[468] Zhang Q, Zhao D, Zhang X-Z, Cheng S-X, Zhuo R-X. Calcium phosphate/DNA co-precipitates encapsulated fast-degrading polymer films for substrate-mediated gene delivery. J Biomed Mater Res Part B 2009;91:172–80.
[469] Zhang Q, Cheng S-X, Zhang X-Z, Zhuo R-X. Water Soluble Polymer Protected Lipofectamine 2000/DNA Complexes for Solid-Phase Transfection. Macromol Biosci 2009;9:1262–71.
[470] Li Y-Q, Li F, Zhang X-Z, Cheng S-X, Zhuo R-X. Three-dimensional fast-degrading polymer films for delivery of calcium phosphate/DNA co-precipitates in solid-phase transfection. J Mater Chem 2009;19:6733–9.
[471] Burke J, Donno R, d'Arcy R, Cartmell S, Tirelli N. The Effect of Branching (Star Architecture) on Poly(D, L-lactide) (PDLLA) Degradation and Drug Delivery. Biomacromolecules 2017;18:728–39.
[472] Zhao W, Li CY, Liu B, Wang X, Li P, Wang Y, et al. A New Strategy To Access Polymers with Aggregation-Induced Emission Characteristics. Macromolecules 2014;47:5586–94.
[473] Li J, Jiang F, Wan X. Preparation and characterization of four armed star polylactic acid with porphyrin core. Acta Polym Sin 2012;11:1314–8.
[474] Tian D, Dubois P, Jerome R, Teyssie P. Macromolecular engineering of polylactones and polylactides. 18. Synthesis of star-branched aliphatic polyesters bearing various functional end groups. Macromolecules 1994;27:4134–44.
[475] Minehara H, Pitet LM, Kim S, Zha RH, Meijer EW, Hawker CJ. Branched Block Copolymers for Tuning of Morphology and Feature Size in Thin Film Nanolithography. Macromolecules 2016;49:2318–26.
[476] Yang D, Lu Q, Fan Z, Li S, Tu J, Wang W. Synthesis and characterization of degradable triarm low unsaturated poly(propylene oxide)-block-polylactide copolymers. J Appl Polym Sci 2010;118:2304–13.
[477] Yu I, Ebrahimi T, Hatzikiriakos SG, Mehrkhodavandi P. Star-shaped PHB-PLA block copolymers: immortal polymerization with dinuclear indium catalysts. Dalton T 2015;44:14248–54.
[478] Alteheld A, Feng Y, Kelch S, Lendlein A. Biodegradable, amorphous copolyester-urethane networks having shape-memory properties. Angew Chem Int Ed 2005;44:1188–92.
[479] Dong CM, Qiu KY, Gu ZW, Feng XD. Synthesis of star-shaped poly(D, L-lactic acid-alt-glycolic acid) with multifunctional initiator and SnOct2 catalyst. Polymer 2001;42:6891–6.
[480] Kessler M, Groll J, Tessmar J. Application of Linear and Branched Poly(Ethylene Glycol)-Poly(Lactide) Block Copolymers for the Preparation of Films and Solution Electrospun Meshes. Macromol Biosci 2016;16:441–50.
[481] Tsuji H, Matsumura N. Stereocomplex Crystallization of Star-Shaped 4-Armed Equimolar Stereo Diblock Poly(lactide)s with Different Molecular Weights: Isothermal Crystallization from the Melt. Macromol Chem Phys 2016;217:1547–57.
[482] Satoh T, Nishikawa N, Kawato D, Suemasa D, Jung S, Kim YY, et al. Precise synthesis of a rod-coil type miktoarm star copolymer containing poly(n-hexyl isocyanate) and aliphatic polyester. Polym Chem 2014;5:588–99.
[483] Wischke C, Neffe AT, Steuer S, Lendlein A. Evaluation of a degradable shape-memory polymer network as matrix for controlled drug release. J Controlled Release 2009;138:243–50.
[484] Leroy A, Pinese C, Bony C, Garric X, Noel D, Nottelet B, et al. Investigation on the properties of linear PLA-poloxamer and star PLA-poloxamine copolymers for temporary biomedical applications. Mater Sci Eng C 2013;33:4133–9.
[485] Cui Y, Tang X, Huang X, Chen Y. Synthesis of the Star-Shaped Copolymer of ε-Caprolactone and L-Lactide from a Cyclotriphosphazene Core. Biomacromolecules 2003;4:1491–4.
[486] Lukaszczyk J, Jelonek P, Trzebicka B, Domb AJ. Stereocomplexes formation from enantiomeric star-shaped block copolymers of ε-caprolactone and lactide. e-Polymers 2010;10, 073/1-15.
[487] Ren J, Zhang Z, Feng Y, Li J, Yuan W. Synthesis of star-shaped poly(ε-caprolactone)-b-poly(L-lactide) copolymers: from star architectures to crystalline morphologies. J Appl Polym Sci 2010;118:2650–8.
[488] Yuan W, Tang X, Huang X, Zheng S. Synthesis, characterization and thermal properties of hexaarmed star-shaped poly(ε-caprolactone)-b-poly(D, L-lactide-co-glycolide) initiated with hydroxyl-terminated cyclotriphosphazene. Polymer 2005;46:1701–7.
[489] Saito K, Isono T, Sun H-S, Kakuchi T, Chen W-C, Satoh T. Rod-coil type miktoarm star copolymers consisting of polyfluorene and polylactide: precise synthesis and structure-morphology relationship. Polym Chem 2015;6:6959–72.
[490] Vora A, Singh K, Webster DC. A new approach to 3-miktoarm star polymers using a combination of reversible addition-fragmentation chain transfer (RAFT) and ring opening polymerization (ROP) via Click chemistry. Polymer 2009;50:2768–74.
[491] Robin MP, Mabire AB, Damborsky JC, Thom ES, Winzer-Serhan UH, Raymond JE, et al. New Functional Handle for Use as a Self-Reporting Contrast and Delivery Agent in Nanomedicine. J Am Chem Soc 2013;135:9518–24.
[492] Mabire AB, Robin MP, Willcock H, Pitto-Barry A, Kirby N, O'Reilly RK. Dual effect of thiol addition on fluorescent polymeric micelles: ON-to-OFF emissive switch and morphology transition. Chem Commun 2014;50:11492–5.
[493] Oyama HT, Tanishima D, Ogawa R. Biologically Safe Poly(L-lactic acid) Blends with Tunable Degradation Rate: Microstructure, Degradation Mechanism, and Mechanical Properties. Biomacromolecules 2017;18:1281–92.
[494] Shinoda H, Asou Y, Suetsugu A, Zhang X-Z, Tanaka K. Synthesis and characterization of amphiphilic biodegradable copolymer poly(aspartic acid-co-lactic acid). Macromol Biosci 2003;3:34–43.
[495] Deng F, Bisht KS, Gross RA, Kaplan DL. Chemoenzymatic Synthesis of a Multiarm Poly(lactide-co-ε-caprolactone). Macromolecules 1999;32:5159–61.
[496] Uyar Z, Durgun M, Yavuz MS, Abaci MB, Arslan U, Degirmenci M. Two-arm PCL. and PLLA macrophotoinitiators with benzoin end-functional groups by combination of ROP and click chemistry and their use in the synthesis of A2B2 type miktoarm star copolymers. Polymer 2017;123:153–68.
[497] Shi P-J, Li Y-G, Pan C-Y. Block and star block copolymers by mechanism transformation X. Eur Polym J 2004;40:1283–90.
[498] Ozlem S, Iskin B, Yilmaz G, Kukut M, Hacaloglu J. Yagci Y. Synthesis and pyrolysis of ABC type miktoarm star copolymers with polystyrene, poly(lactic acid) and poly(ethylene glycol) arms. Eur Polym J 2012;48:1755–67.
[499] Lambert O, Reutenauer S, Hurtrez G, Dumas P. Synthesis of three-arm star block copolymers. Macromol Symp 2000;161:97–102.
[500] Lambert O, Reutenauer S, Hurtrez G, Riess G, Dumas P. Synthesis of amphiphilic triarm star block copolymers. Polym Bull 1998;40:143–9.
[501] Trollsas M, Claesson H, Atthoff B, Hedrick JL, Pople JA, Gast AP. Conformational and structural properties of high functionality dendrimer-like star polymers synthesized from living polymerization techniques. Macromol Symp 2000;153:87–108.
[502] Zhang W, Zheng S, Guo Q. Synthesis and characterization of dendritic star-shaped poly((-caprolactone)-block-poly(L-lactide) block copolymers. J Appl Polym Sci 2007;106:417–24.
[503] Fischer AM, Thiermann R, Maskos M, Frey H. One-pot synthesis of poly(l-lactide) multi-arm star copolymers based on a polyester polyol macroinitiator. Polymer 2013;54:1993–2000.
[504] Fischer AM, Frey H. Multi-arm polylactide stars with hyperbranched poly(glycolide) core. Polym Prepr Am Chem Soc Div Polym Chem 2011;52(1):45.
[505] Khamsarn T, Supthanyakul R, Matsumoto M. Chirachanchai S. PLA with high elongation induced by multi-branched poly(ethylene imine) (mPEI) containing poly(L-lactic acid) (PLLA) terminals. Polymer 2017;112:87–91.
[506] Hyun J, Lee CW. Kimura Y. Synthesis of Novel Hyper-Branched Polymers From Trimethoxysilyl-Terminated Polylactides and Their Utilization for Modification of Poly(L-Lactide) Materials. Macromol Mater Eng 2015;300:650–60.
[507] Lee S, Lee K, Jang J, Choung JS, Choi WJ, Kim G-J, et al. Sustainable poly(ε-decalactone)-poly(L-lactide) multiarm star copolymer architectures for thermoplastic elastomers with fixed molar mass and block ratio. Polymer 2017;112:306–17.

Please cite this article in press as: Michalski A, et al. Star-shaped and branched polylactides: Synthesis, characterization, and properties. Prog Polym Sci (2018), https://doi.org/10.1016/j.progpolymsci.2018.10.004